UTS UNIVERSITY OF TECHNOLOGY SYDNEY

Development of electrically conductive membrane distillation for zero liquid discharge by mitigating inorganic scaling

by Junghyun Kim

Thesis submitted in fulfilment of the requirements for the degree of

Doctor of Philosophy

under the supervision of Professor Ho Kyong Shon and Professor Leonard Tijing

University of Technology Sydney
Faculty of Engineering and Information Technology

December 2023

CERTIFICATE OF ORIGINAL AUTHORSHIP

I, **Junghyun Kim** declare that this thesis, is submitted in fulfilment of the requirements for the award of Doctor of Philosophy, in the School of Civil and Environmental Engineering, Faculty of Engineering and Information Technology at the University of Technology Sydney.

This thesis is wholly my own work unless otherwise referenced or acknowledged. In addition, I certify that all information sources and literature used are indicated in the thesis.

I certify that the work in this thesis has not previously been submitted for a degree nor has it been submitted as part of the requirements for a degree at any other academic institution except as fully acknowledged within the text. This thesis is the result of a Collaborative Doctoral Research Degree program with Korea University. This research is supported by the Australian Government Research Training Program.

Production Note:
Signature: Signature removed prior to publication.

Date: 5th Dec 2023

LIST OF PUBLICATIONS

1. **Junghyun Kim**, Leonard D. Tijing, Ho Kyong Shon, Seungkwan Hong, "Electrically conductive membrane distillation via an alternating current operation for zero liquid discharge", *Water Research* Vol 244 (2023), 120510
2. Seonkyu Lee, Jungbin Kim, **Junghyun Kim***, Seungkwan Hong*, "Application of electrically conductive membrane contactor in the carbon dioxide stripping process for mitigation of fouling induced by flue gas", *Chemical Engineering Journal* Vol 473 (2023), 145425,
3. Taekgeun Yun, **Junghyun Kim**, Seockheon Lee, Seungkwan Hong, "Application of vacuum membrane distillation process for lithium recovery in spent lithium ion batteries (LIBs) recycling process", *Desalination* Vol 565 (2023),
4. **Junghyun Kim**[#], Eun-Tae Yun[#], Leonard D. Tijing, Ho Kyong Shon, Seungkwan Hong, "Mitigation of fouling and wetting in membrane distillation by electrical repulsion using a multi-layered single-wall carbon nanotube/polyvinylidene fluoride membrane", *Journal of Membrane Science* Vol 653 (2022), 120519
5. **Junghyun Kim**, Hye-Won Kim, Leonard D. Tijing, Ho Kyong Shon, Seungkwan Hong, "Elucidation of physicochemical scaling mechanisms in membrane distillation (MD): Implication to the control of inorganic fouling", *Desalination* 527 (2022), 115573 **(Chapter 4)**
6. Yonguk Shin[#], Eun-Tae Yun[#], **Junghyun Kim**, Hongshin Lee, Seungkwan Hong, and Jaesang Lee "An Electrochemical Oxidation-Membrane Distillation Hybrid Process: Utilizing Electric Resistance Heating for Distillation and Membrane Defouling through Thermal Activation of Anodically Formed Persulfate", *Environmental science & technology* Vol 54 (2020), 1867
7. **Junghyun Kim**, Jungwon Kim, Jihun Lim, Sangheon Lee, Cheoljin Lee, and Seungkwan Hong, "Cold-cathode X-ray irradiation pre-treatment for fouling control of reverse osmosis (RO) in shale gas produced water (SGPW) treatment", *Chemical Engineering Journal* Vol 374 (2019), 49-58
8. Jungwon Kim, **Junghyun Kim**, Jihun Lim, and Seungkwan Hong, "Evaluation of ethanol as draw solute for forward

osmosis (FO) process of highly saline (waste)water", *Desalination* Vol 456 (2019), 23-31

9. Jungwon Kim, Jungbin Kim, **Junghyun Kim**, and Seungkwan Hong, "Osmotically enhanced dewatering – reverse osmosis (OED – RO) hybrid system: implication for shale gas produced water treatment", *Journal of Membrane Science* Vol 554 (2018), 282-290
10. **Junghyun Kim**, Jungwon Kim, and Seungkwan Hong, "Recovery of water and minerals from shale gas produced water by membrane distillation crystallization", *Water Research* Vol 129 (2018), 447-459
11. **Junghyun Kim**, Heejung Kwon, Seockheon Lee, Sangho Lee, and Seungkwan Hong, "Membrane distillation (MD) integrated with crystallization (MDC) for shale gas produced water (SGPW) treatment", *Desalination* Vol 403 (2017), 172-178

LIST OF ABBREVIATIONS

AC	Alternating current
AFM	Atomic force microscope
AGMD	Air gap membrane distillation
AL	Active layer
AMP	2-amino-2-methyl-1-propanol
AOP	Advanced oxidation process
BSA	Bovine serum albumin
CCS	Carbon capture and storage
CF	Concentration factor
CGMD	Conductive gap membrane distillation
CNT	Carbon nanotube
CP	Concentration polarization
CR	Congo red
CV	Cyclic voltammetry
DC	Direct current
DCA	Direct contact angle
DCMD	Direct contact membrane distillation
DEA	Diethanolamine
DI	Deionized
DMF	Dimethylformamide
DS	Draw solution
EC	Electrochemical cleaning
ECM	Electrically conductive membrane
ECMCO	Electrically conductive membrane contactor ozonation
ECMD	Electrically conductive membrane distillation
EDL	Electrical double layer
EI	Electrostatic interaction
EIS	Electrochemical impedance spectroscopy
EL	Electrostatic
EO	Electrochemical oxidation
EPS	Extracellular polymeric substances
FDR	Flux decline rate
FE-SEM	Field emission scanning electron microscopy
FO	Forward osmosis
FS	Feed solution
FTIR	Fourier transform infrared
HA	Humic acid
HFP	Hexafluoropropylene
IAP	Ion activity product

IBU	Ibuprofen
ICP	Internal concentration polarization
IMD	Ion moving distance
IPA	Isopropyl alcohol
LEP	Liquid entry pressure
LW	Lifshitz-van der Waals
MB	Methylene blue
MC	Membrane contactor
MCO	Membrane contactor ozonation
MD	Membrane distillation
MEA	Monoethanolamine
MF	Microfiltration
MGMD	Material gap membrane distillation
MMT	Montmorillonite
MO	Methylene orange
MWCNT	Multi-wall carbon nanotube
NB	Nitrobenzene
NC	Networked cellulose
NF	Nanofiltration
NOM	Natural organic matter
PANI	Polyaniline
PDS	Peroxydisulfate
PE	Polyethylene
PEI	Polyetherimide
PGMD	Permeate gap membrane distillation
PMS	Peroxomonosulfate
PP	Polypropylene
PTFE	Polytetrafluoroethylene
PVA	Polyvinyl alcohol
PVDF	Polvinylidene fluoride
RB	Rhodamine B
RCS	Reactive chlorine species
RO	Reverse osmosis
ROS	Reactive oxygen species
SA	Sodium alginate
SDS	Sodium dodecyl sulfate
SEEC	Specific electrical energy consumption
SGMD	Sweep gas membrane distillation
SI	Saturation index
SMM	Surface modifying macromolecule
SWNT	Single-wall carbon nanotube

TEA	Triethanolamine
UF	Ultrafiltration
UPW	Ultrapure water
VCF	Volume concentration factor
VMD	Vacuum membrane distillation
VOCs	Volatile organic compounds
XPS	X-ray photoelectron spectroscopy
ZLD	Zero liquid discharge

LIST OF SYMBOLS

a_c	Radius of the spherical organic matter
C_i	Initial concentration of the solution
$\{Ca^{2+}\}_e$	Activity of Ca^{2+}
$\{CO_3^{2-}\}_e$	Activity of CO_3^{2-}
d_p	The largest pore size of the membrane
$E°$	Electric potential
$ECM(OH\cdot)$	ECM with Hydroxyl radicals
G_{LW}	Free energy of adhesion per unit area between the membrane and organic matter
h	Operation time
I	Applied current
J	Water flux at time t
J_0	Initial water flux
K_{sp}	Solubility in equilibrium state
$OH\cdot$	Hydroxyl radicals
$Organics_{ads}$	Organic foulant adsorbed
$Organics_{oxidized}$	Organic foulant oxidized
$P_{breakthrough}$	Breakthrough pressure
R	System recovery rate
R_{ct}	Charge transfer resistance
S	Supersaturation
$tan\theta_{t=0}$	Slope of the flux behavior at t=0
U_{DLVO}	Total interaction energy
U_{EL}	Repulsion force between membrane and organic matter
U_{LW}	Attraction force between membrane and organic matter
V_{ECMD}	Applied voltage
V_{water}	Increased yield compared to the pristine PVDF experiment
y_0	Minimum equilibrium cut-off distance
Z'	Real component of impedance
$-Z''$	Fictitious component of impedance
β	Geometric factor
γ	Surface tension
ε_0	relative dielectric permittivity
ε_r	vacuum dielectric permittivity
θ	Contact angle
κ	Inverse Debye screening length

ξ_m	Zeta potentials of membrane
ξ_o	Zeta potentials of organic matter

CONTENTS

LIST OF TABLES

LIST OF FIGURES

ABSTRACT

Membrane distillation (MD) is a promising technique in water treatment, known for perfect removal efficiency, low energy use, and low sensitivity to feed salinity. However, high recovery rates lead to challenges like foulant concentration and scaling. Electrically conductive membrane (ECM) technology has been applied to address this challenge. Unlike conventional physical and chemical fouling control techniques, the ECM utilizes electrochemical mechanisms in conjunction, providing excellent fouling mitigation performance and synergistic effects with conventional fouling control techniques, which can lead to further performance improvement. ECM can mitigate fouling through mechanisms such as preventing contact with the membrane or transforming contaminants into a state with low fouling potential by leveraging the electrical properties of pollutants. ECM technology was applied to MD for electrically conductive membrane distillation (ECMD) operation, and scaling inhibition during operation overcame the concentration limit of the conventional process, resulting in a dramatic improvement in final water recovery. Another concept of ECM, electrochemical cleaning (EC), has been proposed by applying it to membrane scaling cleaning, showing excellent performance without

efficiency degradation even after repeated cleaning cycles at scaling stage 3.

An extensive review of ECM cases currently used for fouling control was performed in this study. New challenges were identified for the practical application of ECM technology in fouling control, such as a new understanding of foulant characteristics from an ECM perspective, optimal membrane material selection, and customized ECM operation conditions optimization (Chapter 3). Furthermore, fundamental research on MD scaling mechanisms was conducted for accurate understanding prior to applying ECM technology to MD scaling control, resulting in identifying a new scaling stage (Chapter 4). Subsequently, an evaluation of the applicability of ECM technology for actual MD scaling control was performed (Chapters 5, 6).

This study demonstrated the feasibility and development of ECMD AC operation and EC application for MD scaling control. The transition to ECM technology overcomes the limitations of conventional physical and chemical approaches and increases water productivity and energy efficiency in MD operation by more than two times using new electrochemical mechanisms. As a result, the excellent potential of ECM technology for MD scaling control has been sufficiently confirmed. However, as ECM technology is in its early stages of research and

development, additional studies, such as optimization of operating conditions and modules, are necessary for practical application.

Chapter 1. Introduction

1.1. Motivations

Water scarcity is one of the biggest challenges of modern times. With population growth, economic development, and climate change, the demand for freshwater is increasing worldwide. As water is a major requirement for human survival, new technologies are needed to meet the growing demand for freshwater (Cosgrove & Loucks, 2015; Gude, 2017). It is essential to evaluate the potential of new water resources beyond surface water, which is the traditional and typical source. Alternative water resources such as seawater and industrial wastewater can be considered (Abdulbaki et al., 2017; X. Liu et al., 2019). However, additional measures are required to deal with the high salinity in seawater and toxic substances in industrial wastewater (Ahmad & Baddour, 2014; Panagopoulos, 2021; Younker & Walsh, 2015). Moreover, environmental and safety regulations on water resources are becoming more stringent to ensure sustainable solutions. Therefore, there is an urgent need to develop new freshwater technologies based on a new paradigm for water diversification.

To meet the rapidly increasing demand for freshwater, it is necessary to increase the recovery rate from existing water sources or ensure the perfect treatment of alternative water sources. Membrane processes are widely used in the water treatment field due to their unique

cost-effectiveness, compactness, and superior water quality production (Adam et al., 2022; Goh et al., 2016). The water industry is shifting its technological trends to desalination processes, and membrane processes provide the ability to produce fresh water from the world's major alternative seawater sources. Currently, reverse osmosis (RO), the most energy-efficient desalination technology, accounts for over 60% of the world's desalination capacity. Basically, RO operations are set up as large centralized desalination plants due to the energy recovery capabilities of large power plants. Therefore, RO units are suitable for high-density population areas. However, many low-density population areas located inland or rural areas require small-scale independent desalination devices due to the need for fresh water. In addition, there is challenging to address the limitations of RO application in treating high-salinity water due to the pressure drop limit and high energy demand (Chen & Yip, 2018; Schantz et al., 2018; Shah et al., 2022).

The membrane distillation (MD) process is a promising technology that can meet the increasing demand for fresh water. The MD process is a membrane separation process that utilizes a porous hydrophobic membrane to induce molecular-scale transport (i.e., water vapor) from the feed side to the permeate side, driven by the temperature (i.e., vapor pressure) difference across the membrane (Alkhudhiri et al., 2012;

Onsekizoglu, 2012). In particular, MD can be operated at relatively low temperatures compared to conventional distillation processes and does not rely on pressure like RO processes, allowing fresh water production at lower costs. Furthermore, MD theoretically shows very high salt rejection rates, meaning it can only allow pure water vapor to pass through (Cai & Guo, 2017; Hong et al., 2022). Additionally, MD has the advantage of having larger pore sizes than separation membranes used in RO processes, which minimizes membrane fouling. Moreover, it can be easily combined with other processes such as microfiltration (MF) and ultrafiltration (UF) and can be operated using renewable energy sources such as solar energy (Ahmed et al., 2019b; Ali et al., 2018; Gude, 2015). MD can be very effective in desalinating seawater and brackish water, as well as for removing organic matter and heavy metals present in wastewater or for the safe treatment of radioactive waste.

Recent research has focused on the application of MD in wastewater treatment and reuse. MD is particularly promising for the treatment of high-salinity wastewater in emerging industries where conventional membrane-based desalination processes, such as RO, are not feasible (Deshmukh et al., 2018; Swaminathan et al., 2018). Additionally, MD has gained interest as a promising technology for producing high-quality freshwater from wastewater through the use of available waste heat or

low-grade solar or geothermal energy sources (Kim et al., 2018a; Kim et al., 2017a; Warsinger et al., 2015). By improving the design of MD systems, developing new or modified membrane materials, and integrating MD with other processes, the energy and process efficiency of MD systems can be continuously improved while recovering freshwater from wastewater and providing excellent modularity for scalability. Although primarily used for water recovery from high-salinity water sources, MD has shown potential for the reuse of high-strength wastewater in small-scale decentralized systems with available waste/alternative heat sources.

However, the MD process still faces challenges in dealing with fouling from concentrated foulants and scaling caused by salt precipitation under high recovery conditions (Abdel-Karim et al., 2021; Lee et al., 2020). Various studies have attempted to overcome these issues, such as enhanced pretreatment, hybrid processes, and membrane modification, but they still need to fully meet the needs of the industry (Alkhatib et al., 2021; Castillo et al., 2019; Kim, Yun, et al., 2022; Shin et al., 2020). The electrically conductive membrane (ECM) technology has recently gained attention as a new and promising option for increasing MD recovery rates due to its unique mechanism (Anvari, Yancheshme, et al., 2020; Rao et al., 2020). The ECM utilizes an

electrochemical mechanism rather than the physical and chemical approaches used to address fouling and scaling issues in conventional methods, resulting in excellent performance efficiency in increasing recovery rates and potential synergistic effects with existing processes. However, as it is still in the early stages of research, further studies are needed to determine the precise application methods, optimal operating conditions, energy consumption evaluations, and detailed mechanisms of ECM. Given the abundant potential of ECM for securing water resources, various studies should be conducted to optimize it and find scientifically based evidence to apply it practically in the industry. Additionally, moving beyond simple MD scaling mitigation, further research should be conducted for applications in high-value-added fields that require control of ion behavior in solutions, such as batteries, hydrogen production, carbon capture, and conversion.

1.2. Objectives and scope of the thesis

Therefore, with the current level of MD fouling control technology, the ultimate goal of ZLD through high recovery rates may be limited. It is urgent to develop a cost-effective and feasible ECM technology that incorporates a new concept of electrochemical mechanisms, rather than relying solely on physical and chemical fouling control. Furthermore, it is necessary to optimize operating conditions based on a precise understanding of the fouling control mechanism of ECM technology to maximize its applicability. Therefore, the doctoral thesis is mainly focused on the following goals;

1. Deriving future research directions through a review of the current status and evaluation analysis of ECM's fouling control application
2. Identification of the fundamental mechanism of MD scaling for practical application of ECM
3. Development and application of ECMD scaling mitigation with alternating current operation
4. Identification and evaluation of the mechanisms and efficiency of EC for sustainable ECMD operation

1.3. Thesis organization

The thesis begins with a general introduction, which presents the motivation and necessity of this study as well as the objectives and scope. In Chapter 2, a literature review briefly presented the fundamental mechanisms of MD processes and their limitations due to fouling. Chapter 3 extensively reviewed the application and mechanisms of ECM technology for fouling control, and provided future directions based on the review. In Chapter 4, as a preparatory stage for the practical application of ECM technology to MD, scaling stages were identified through fundamental and experimental analysis of inorganic scaling in MD. Chapter 5 evaluated the practical applicability of ECM technology for fouling control, and demonstrated the superior performance of a new alternating current (AC) operation. In Chapter 6, EC was evaluated as another application of ECM technology, and an increase in cleaning efficiency compared to existing technologies was confirmed. Finally, Chapter 7 consisted of an analysis of the application of ECM technology to MD fouling control and suggestions for future research directions based on the results of the previous chapters. Consequently, through this study, by understanding the mechanism for MD scaling mitigation in ECM technology, we can take one step closer to applying it to high-

value-added fields that necessitate the control of ion behavior in solutions.

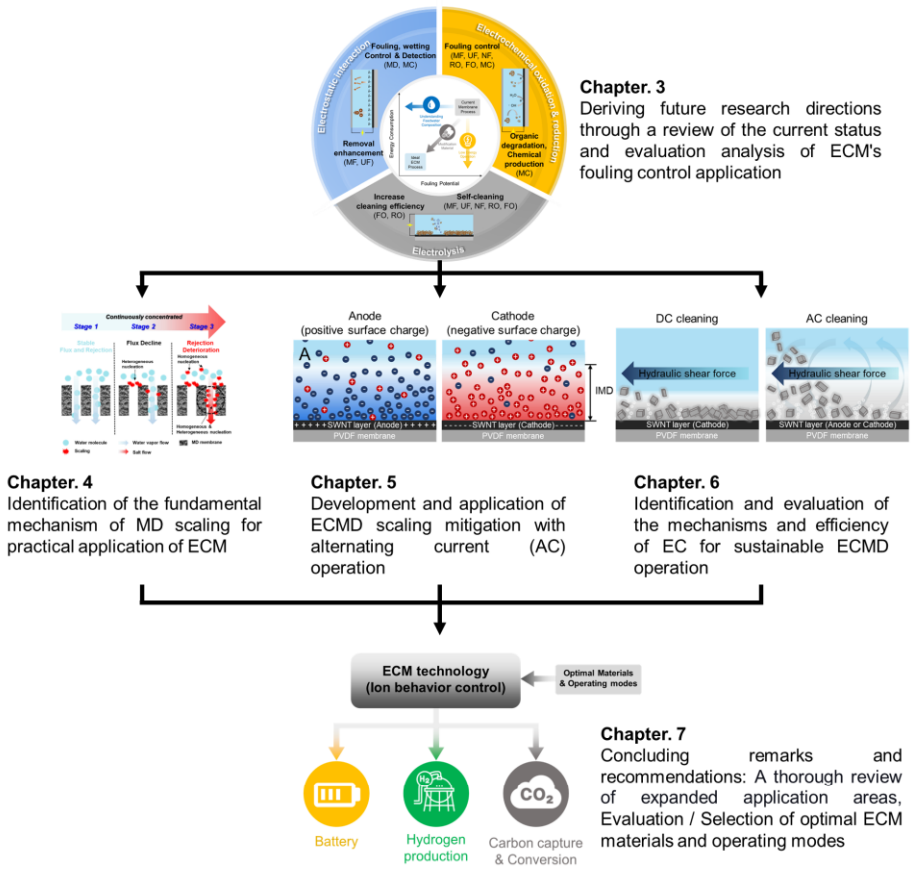

Figure 1-1 The structure of the current thesis

Chapter 2. Literature review

2.1. Membrane distillation (MD)

The MD process is a process that selectively separates specific components in a mixture by inducing mass transfer through a partial vapor pressure difference between the feed and permeate sides driven by the temperature difference between the two channels in the membrane. More specifically, the process involves supplying a liquid mixture to the feed side of a porous and hydrophobic membrane and maintaining a higher operating temperature on the feed side relative to the permeate side, thereby increasing the vapor pressure of the component to be permeated. At the same time, a vacuum, sweep gas, or low-temperature liquid is supplied to the opposite side (permeate side) of the membrane to maintain low pressure. In this case, the material transfer occurs through the pores in the membrane due to the pressure difference, allowing for selective separation of the mixture.

In MD, there are several advantages including (a) theoretically 100% salt removal, (b) lower operating temperatures compared to conventional distillation processes, (c) lower energy consumption when using waste heat or alternative energy sources, and (d) reduced membrane mechanical property requirements compared to conventional pressure-driven processes (González et al., 2017; Zhong et al., 2021).

As a result, MD is distinct from other membrane processes in that its driving force is the vapor pressure across the entire membrane. MD can operate in places where RO and thermal distillation technologies are difficult to apply because it is not limited by the salinity of the feed and operates at low-temperature requirements. Due to these advantages, MD can be applied in various fields such as freshwater production, organic removal, wastewater treatment, recovery of valuable components, and radioactive waste treatment. However, despite many pilot systems being operated in recent years, MD has not yet discovered large-scale industrial applications due to issues such as performance degradation caused by fouling under high recovery conditions, and challenges such as module optimization development (Eykens et al., 2016; Soukane & Ghaffour, 2021; Yang et al., 2022).

2.1.1. MD configurations

The MD process can be configured in various forms depending on the application, and can be classified into four types based on the method used to induce the vapor pressure difference that acts as the driving force (Dong et al., 2021; Hardikar et al., 2020). In all four types of MD configurations, the feed solution comes into direct contact with the feed

side membrane. The hydrophobic nature of the membrane creates a surface tension that prevents the liquid solution from entering the membrane pores, thus forming a liquid/vapor interface at the pore entrance. Therefore, the membrane pores must be kept dry throughout the MD operation.

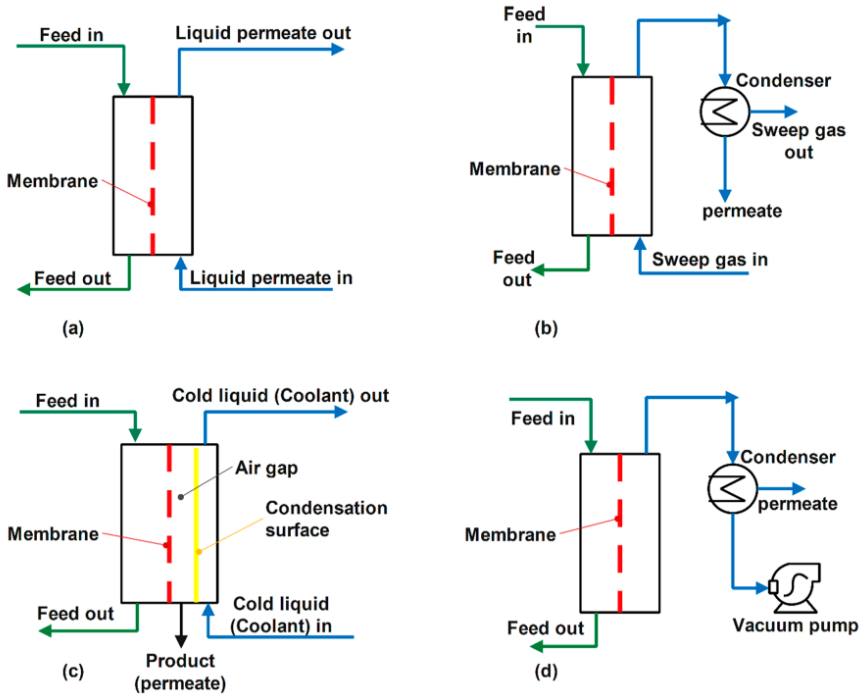

Figure 2-1 Schematic diagram of conventional membrane configurations (a) direct contact membrane distillation (DCMD); (b) sweeping gas membrane distillation (SGMD); (c) air gap membrane distillation (AGMD); (d) vacuum membrane distillation (VMD) (Biniaz et al., 2019).

2.1.1.1. Direct Contact Membrane Distillation (DCMD)

DCMD is a process in which high-temperature feed solution and low-temperature permeate are brought into direct contact with a membrane, which is a simple and easy-to-operate device widely used for desalination and concentration of aqueous solutions, and the production of acids in the food industry. Due to the hydrophobic nature of the membrane, liquid feed solution cannot pass through the membrane directly, but water vapor in the feed solution evaporates due to the vapor pressure difference caused by the temperature difference and passes through the membrane pores to mix with the permeate. Although the permeation rate of DCMD is higher than that of other membrane distillation processes, it has the disadvantage of the high cost to maintain the temperature of the feed and permeate solutions due to the significant heat loss occurring at both sides of the membrane compared to other processes.

2.1.1.2. Air gap membrane distillation (AGMD)

AGMD operates similarly to DCMD in that the hot feed solution comes into direct contact with the membrane, while the permeate side flows between the membrane and a low-temperature heat transfer medium on the condensing plate surface through a fixed air gap. This

process has the advantage of minimizing heat loss, but introduces a new mass transfer resistance in the air layer. As a result, AGMD reduces heat loss by conduction, but has a lower flux than other MD configurations due to the enhanced resistance to mass transport caused by inflow in the air gap. The AGMD process is used for the desalination and removal of volatile organic compounds (VOCs) in aqueous solutions.

2.1.1.3. Sweep gas membrane distillation (SGMD)

SGMD employs the same MD approach as previously described for both configurations and feed-side setup, where hot feed solution comes into direct contact with the membrane and non-reactive gas is passed through the permeate side to transport the resulting vapor through the membrane module to the outside, maintaining the vapor pressure difference. The exiting vapor and non-reactive gas from the module are then condensed in a condenser, with the non-reactive gas being reused. This process is useful for the removal of volatile components from aqueous solutions, but requires a relatively large condenser due to the significant amount of non-reactive gas used compared to the amount of permeating water vapor. In SGMD, condensation occurs outside the membrane module on the distillate side. Thus, an external condenser is necessary to collect the vapor. Low-temperature non-reactive gas is

typically used to create a sweeping flow and collect vapor from the permeate side. Due to the sweeping flow, SGMD exhibits low heat loss with high mass transport compared to AGMD. The feed temperature and sweeping gas flow rate in SGMD are important operating parameters that control the distillate flux.

2.1.1.4. Vacuum membrane distillation (VMD)

VMD is a vacuum-based MD process with almost no heat loss, which is very similar to SGMD except that vacuum is introduced on the permeate side to collect the permeated water vapor outside the membrane module and recover it through a condenser, instead of using an inert gas. The biggest advantage of this configuration is that heat loss can be almost ignored. Since there is no air inside the membrane cell, gas diffusion through pores can be considered without the influence of air. In this case, the permeated water vapor through the membrane is condensed outside the module like SGMD and can be very effective for removing VOCs from the solution. Although it has a high permeation rate, the disadvantage is that the entire system must maintain a vacuum.

2.1.1.5. Novel MD configuration

Recently, several new variations on the existing AGMD and VMD configurations have been developed to improve process energy efficiency and vapor flux through the membrane. Among the new configurations with altered gaps are permeate gap MD (PGMD), material gap MD (MGMD), and conductive gap MD (CGMD) (Cai et al., 2020; Francis et al., 2022; L. Gao et al., 2019; Swaminathan et al., 2016). PGMD, also known as liquid-gap MD, is a mixture of AGMD and DCMD configurations, and is used to fill the gap between the membrane and the cold condensation surface with water or liquid. The MGMD configuration uses additional materials, such as sand, in the gap between the membrane and the condensation plate. Lastly, the CGMD configuration enhances the conductivity of the gap in the thickness direction by using a high thermal conductivity spacer (e.g., metal mesh) in the permeation gap.

2.1.2. MD operating parameters

The operating temperature has a significant impact on the permeate flux of MD, and as the temperature increases, the vapor pressure increases dramatically (Lian et al., 2016; Shalaby et al., 2022). In particular, the operating temperature has a greater influence on the

permeate flux than the temperature of the low-temperature condensate on the permeate side. This leads to an increase in the diffusion coefficient. In addition, an increase in operating temperature can reduce temperature polarization. The presence or concentration of solutes in the feed solution directly affects the permeate flux (Alkhudhiri & Hilal, 2017; Kiss & Kattan Readi, 2018).

This is because the concentration of solutes reduces the vapor pressure of the solution and increases concentration polarization, resulting in a decrease in the permeate flux. There are three main reasons for this: firstly, the activity of water, which is expressed as a function of temperature, decreases as the concentration of solutes increases. Secondly, an increase in concentration polarization at the membrane surface increases mass transfer resistance. Finally, an increase in solute concentration in the feed solution reduces the heat transfer coefficient at the boundary layer due to a decrease in partial pressure.

An increase in the viscosity of the feed solution directly affects the Reynolds number, leading to an increase in the heat transfer coefficient. In addition, it is affected by the density of the feed solution. An increase in the circulation flow rate can reduce the thickness of the boundary layer, leading to an increase in permeate flux through a decrease in mass transfer resistance and temperature polarization (Anvari, Yancheshme,

et al., 2020; Politano et al., 2019). When spacers were introduced on the feed side, a decrease in permeate flux was observed. Generally, a decrease in the gap of spacers can increase the temperature gradient and result in a high permeate flux. The permeate flux through the membrane is proportional to the porosity of the polymer membrane and inversely proportional to the tortuosity. As the pore size increases, the permeate flux increases, and it is also affected by the presence of the support layer of the membrane. Finally, it is important that the membrane material itself has a low thermal conductivity (J.-W. Wang et al., 2016; Yang et al., 2019). However, a long-term operation depends on the characteristics of the water, and stable operation can be achieved by maintaining appropriate operating conditions.

As a result, the performance of MD is most significantly influenced by vapor pressure, and vapor pressure is most affected by the temperature of the solution. Therefore, controlling the hydrodynamic conditions that influence the solution's temperature is essential.

2.2. MD fouling

The fouling issue in the MD has yet to be well understood, but it is believed to be less prone than pressure-driven membrane processes such as RO and NF. However, fouling is time-dependent, and its long-term

effects are not easily predictable. Due to differences in membrane structure and operating conditions, which are different from conventional pressure-driven membrane processes, the fouling mechanisms and tendencies in MD are expected to be different (Tijing et al., 2015). In particular, the thermal integrated membrane characteristic of the MD process exhibits unique scaling and fouling phenomena compared to conventional membrane processes. Therefore, it is essential to focus on fouling and scaling development and evaluate the feasibility of MD as a water treatment process.

Despite significant advantages such as low concentration polarization, high removal of non-volatile components, and low-temperature requirements, the industrial application of MD has been minimal due to some operational/functional challenges such as temperature polarization and membrane fouling (Laqbaqbi et al., 2019). Like other membrane-based processes, fouling is a significant challenge that reduces membrane permeability and efficiency. As fouling is important, the formation mechanism and other effective parameters for this challenge should be studied to improve the performance of the MD process.

Wetting and fouling are two interrelated phenomena in MD, which have a significant impact and pose major challenges to its application

(AbdulKadir et al., 2020; Yang et al., 2022). Membrane wetting is an inherent challenge in MD, related to the direct infiltration of the feed solution through the membrane pores, leading to reduced salt removal and overall process failure. Wetting can occur even in short-term MD operations due to unacceptable operating conditions of the system (e.g., pore size, membrane hydrophobicity, and liquid entry pressure (LEP)). On the other hand, membrane fouling, like in other membrane-based processes, is a significant drawback of MD, where undesirable substances accumulate on the membrane surface and pores, reducing the permeate flux. Both fouling and wetting are time-dependent phenomena, and their long-term effects are difficult to be predicted.

Fouling in MD is broadly classified as (a) inorganic fouling, (b) organic fouling, and (c) biological fouling, causing partial or complete blockage of pores and surface fouling (Tijing et al., 2015). Inorganic fouling refers to scaling, which is composed of precipitates of hardness salts such as calcium carbonate, calcium sulfate, silica, sodium chloride, and calcium phosphate. Water evaporation and temperature changes result in supersaturation leading to nucleation and crystallization of inorganic contaminants on the feed side and membrane surface. Colloidal organic matter (e.g., humic substances, proteins, extracellular polymeric substances (EPS)) is responsible for organic fouling in MD

processes. Finally, biological fouling or biofouling refers to the accumulation and evolution of microorganisms on the membrane surface, leading to reduced permeate flux. However, most MD studies on membrane fouling have focused on inorganic scaling and organic fouling. Microbial proliferation has been deemed insignificant in its impact on MD operation, owing to the high salt concentration and thermal conditions used in MD (Bogler & Bar-Zeev, 2018; Costa et al., 2021).

As shown in Fig. 2-2, fouling can be divided into two parts: external (surface fouling) and internal (pore blocking) (Tijing et al., 2015). External surface fouling is related to the deposition of foulants on the feed side external surface of the membrane. The occurrence of pore blocking results from partial blocking or gradual narrowing of pores, leading to the formation of foulants inside the membrane pores. External surface fouling is often a reversible phenomenon and cleaning processes are chemical, whereas pore blocking is an irreversible phenomenon that can be justified by fouling layer compression/membrane compaction (Abdel-Karim et al., 2021; Chiao et al., 2022).

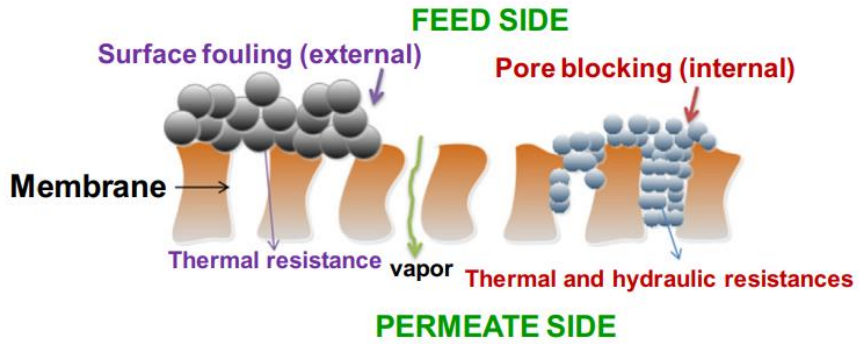

Figure 2-2 The fouling sites on a membrane can be divided into surface fouling (external) or pore blocking (internal) (Tijing et al., 2015).

2.2.1. Membrane wetting

Membrane wetting, as well as fouling, is another issue (Chamani et al., 2021; Chang et al., 2020). Membrane wetting is generally defined as the contact of liquid with the solid membrane surface through intermolecular interactions between the liquid and the solid, gas, liquid, and solid states. Specifically, wetting of a porous membrane can be observed when liquid penetrates the membrane pores. As a result, salt removal drops sharply while flux decreases (due to partial pore wetting) or increases abruptly (due to complete wetting for liquid transport). In MD, membrane wetting is facilitated by organic fouling/scaling, amphiphilic molecules (e.g., surfactants and proteins), low surface tension liquids (e.g., alcohols), the use of anti-scalants, and membrane

chemical degradation. Wetting can also occur when the feed side pressure exceeds the membrane's LEP (Rácz et al., 2015).

Fig. 2-3 illustrates the wetting potential of MD membranes (partial or complete) (Yao et al., 2020). This phenomenon is unique to MD because it requires a phase change (vapor formation) rather than liquid water passing through the membrane. The various stages of MD membrane wetting are (a) non-wetting (a state where the maximum flux and maximum salt removal are achieved by through the pores), (b) surface/partial wetting (transition state where partial wetting of the feed occurs), and (c) pore penetration/complete wetting (a state where some pores are completely penetrated and salt from the feed stream can move freely through the wetted pores). Operating parameters of MD, such as pressure, temperature, and flow rate, can affect membrane wetting behavior and salt rejection rate.

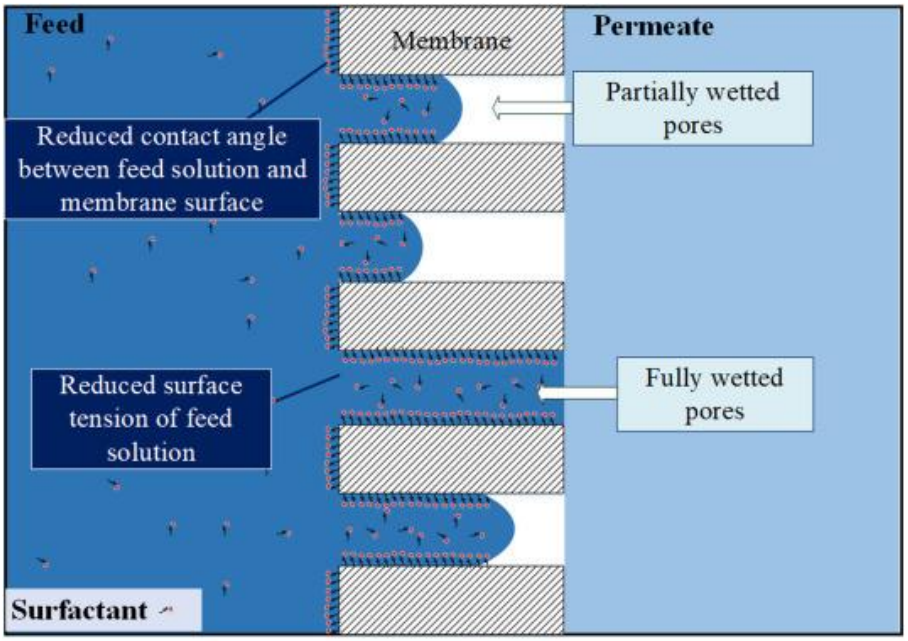

Figure 2-3 Illustration of the occurrence of pore wetting (partially or fully-wetted) of a hydrophobic membrane when in contact with wastewater containing surfactants; the surfactants have hydrophobic tails and hydrophilic heads (Yao et al., 2020).

2.2.2. Membrane fouling

Fig. 2-4 shows the fouling mechanisms in MD (Choudhury et al., 2019). Fouling in membrane separation technologies can generally be classified into three categories: inorganic fouling, organic fouling, and biological fouling, depending on the nature of the feed solution. In MD, inorganic fouling is caused by inorganic colloidal particles and salt deposition. The deposition of organic matter such as humic acid and proteins induces organic fouling. Ultimately, the generation of biological fouling can be attributed to the concentration of microorganisms,

including bacteria and fungi. Comprehensive consideration of each fouling mechanism is essential for practical application. In other words, fouling control becomes more complex in MD systems as a combination of different fouling substances and mechanisms can occur.

2.2.2.1. Inorganic scaling

Inorganic scaling is the phenomenon of crystallized substances separated from the concentrated feed solution being deposited on the membrane surface. In MD, the supersaturation of the feed solution occurs due to the concentration increase and temperature changes caused by continued evaporation. This can lead to the formation and growth of crystalline nuclei on the feed side and membrane surface (Karanikola et al., 2018; Rolf et al., 2022). Typically, the growth of nuclei begins with larger pores because wetting acceleration is faster in smaller pores. Ions, precipitated particles, and external substances can generate secondary nucleation in the bulk phase in supersaturation conditions, which then move to the membrane surface by gravity-induced settling or particle transport. These scaling layers increase thermal resistance and temperature polarization, ultimately causing a decrease in the driving force of MD. The degree of supersaturation, flow conditions, temperature, water properties, and membrane surface roughness all

greatly affect the scaling. Typical inorganic scaling substances include multivalent ions such as calcium and magnesium, and heavy metals with a valence of 3 or higher, and silica is also a common inorganic scale (Chang et al., 2021; Presson et al., 2023; Yan et al., 2022).

2.2.2.2. Organic fouling

Organic fouling is where many substances such as humic acid, polysaccharides, carboxylic acids, and microbial excreta are adsorbed/deposited on the membrane surface. Generally, the main substances of organic fouling originate from natural organic matter (NOM) (Alkhatib et al., 2021; Ji et al., 2023; Naidu et al., 2014). NOM contains humic substances, which are abundant in most natural rivers and freshwater bodies. They are mainly composed of aromatic and aliphatic compounds containing carboxylic and phenolic functional groups. NOM can be adsorbed on the surface by different mechanisms based on chemical affinity. Deposition of such organic matter can partially or completely block the pores in the membrane due to adsorption or deposition within the pores, thus reducing the membrane permeability. Organic fouling poses a significant problem in MD in particular. If organic matter exists in the feed, the solution's surface tension decreases, and the membrane's wetting can occur due to the high affinity of

hydrophobic species such as oils to the hydrophobic membrane surface at a critical surface tension (free energy of the membrane surface).

2.2.2.3. Biological fouling

Biological fouling refers to the accumulation and growth of organisms on the membrane surface, which can affect the permeability of the membrane and result in loss of productivity and other operational issues. Specifically, in membrane processes, biofilm and biological fouling growth can lead to a decrease in the permeate flux due to a reduction in the transport mechanism, particularly during long-term operation, which can affect membrane performance (Costa et al., 2021; Mpala et al., 2023). Microorganisms are the primary cause of biological fouling. However, biological fouling in MD processes is limited by high feed water salinity, which restricts microbial growth, and high operating temperatures, which are higher than the growth temperatures of most bacteria. Therefore, the formation of a biological fouling layer in MD is expected to be lower than in other membrane processes such as MF, UF, and RO. However, bacteria that can survive and grow in extreme environments also exist so that biological fouling can occur in MD, and in full-scale MD modules, the feed temperature varies from the module inlet to the outlet. Ultimately, biological fouling in MD is greatly

influenced by operational conditions such as feed water temperature, concentration, flow rate, membrane properties, microbial cell characteristics, and module length.

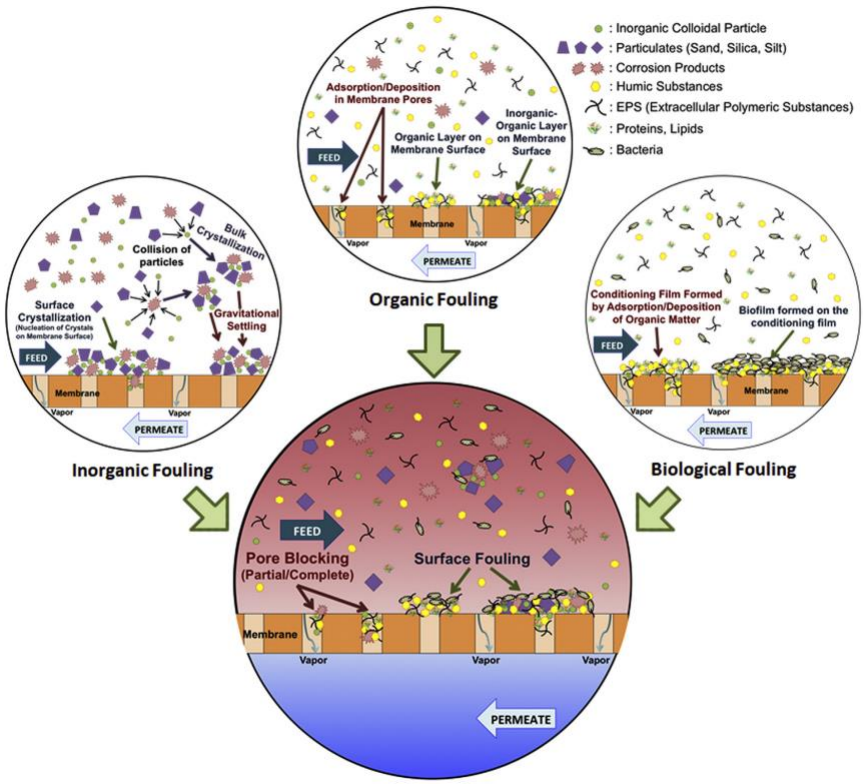

Figure 2-4 Combined effect of different fouling mechanisms (i.e., inorganic fouling, organic fouling, and biological fouling) leading to partial or complete pore blocking (internal fouling) and surface fouling (external fouling) in membrane distillation process (Choudhury et al., 2019).

2.3. Fouling mitigation Strategies

2.3.1. Optimal operation (pre-treatment, membrane cleaning, and anti-scalant)

The success of a process utilizing membrane-based technologies is greatly influenced by the efficiency of feed water pre-treatment (Cho et al., 2018; Ji et al., 2023). Pre-treatment should effectively reduce the potential for membrane fouling reliably and consistently. The development of an appropriate pre-treatment process emphasizes removing as many contaminants as possible from the feed water before the membrane process. Specifically, pre-treatment techniques such as coagulation/precipitation, multi-layer filtration, ultrasonication, and microfiltration can be employed for pre-treatment in desalination or purification processes (Kalla, 2021; C. Liu et al., 2022). The performance of such pre-treatment methods depends on factors such as additives and temperature conditions. While MD processes are less sensitive to pressure than general pressure-driven membrane separation processes, the importance of pre-treatment cannot be underestimated. The removal of large particles and microbes must be prioritized through pre-treatment. The concentration of contaminants in the feed solution can be reduced using established physical and chemical pre-treatment methods. Coagulation/precipitation is a cost-effective approach that forms flocs that incorporate contaminants and can be removed from the

feed using methods such as sedimentation, porous media filtration, or MF. Ultimately, the selection of pre-treatment for contaminant mitigation is heavily influenced by the characteristics of the feed water rather than the membrane process.

In addition to the concept of pre-treatment that reduces the fouling potential of feed water in the pre-MD operation stage, there are effective additional chemical and physical strategies for removing contaminants already attached to the membrane surface, namely membrane cleaning. Standard membrane cleaning methods, including the use of cleaning agents based on alkalinity, acidity, surfactants, and chelating agents, are effective in removing fouling layers. However, most cleaning methods use powerful oxidants (such as hydrochloric acid, oxalic acid, and sulfuric acid solutions), which can decrease membrane performance after prolonged exposure to the oxidants. In the case of MD, however, since hydrophobic membranes containing fluoropolymers are used, membrane damage caused by cleaning is smaller than in conventional membrane processes, but this damage cannot be ignored due to the nature of long-term membrane operation (McGaughey et al., 2017; P. Zhang et al., 2015).

The use of anti-scalants in MD processes is the most common strategy to prevent inorganic scaling (Qu et al., 2020; D. Xu et al., 2022;

Yin et al., 2021). Anti-scalants hinder scaling formation by delaying nucleation initiation and growth of formed crystals, thus preventing crystal deposition. However, additional evaluation is required to perform anti-scalants in MD for scaling control. For instance, polyphosphate-based anti-scalants have been reported to hinder crystal formation in MD, but also result in the formation of amorphous, non-porous scaling layers on the membrane surface that decrease water flux (Xiao et al., 2019). Therefore, it is desirable to develop improved resistance and new MD scaling technologies to enhance the sustainability of the MD process (Liao et al., 2023; Zhong et al., 2022).

2.3.2. Fouling-resistant membranes modifications

The evolution of membrane modification has emerged as a challenge in new MD applications beyond desalination. This technology has enabled water recovery from industrial wastewater containing organic solutes, pollutants, various salts, and low-surface-tension substances due to improved removal rates, permeability quality, and low energy requirements.

In recent years, many studies have been conducted on membrane surface modification to enhance the hydrophobicity and fouling prevention properties of MD membranes (Beauregard et al., 2020;

Hamad et al., 2022; J. Liu et al., 2019). Different superhydrophobic coatings have been applied to various substrates, leading to increased fouling resistance of the membranes. Currently, efforts to prepare MD membranes for fouling prevention are relatively limited. In addition to preventing membrane destruction by wetting, optimizing surface hydrophobicity, which significantly affects the fouling propensity of MD membranes, is currently the primary goal of membrane modification.

Coating and electrospinning methods have been used for membrane modification in MD, and membrane hydrophobicity can be enhanced by inducing new cross-linking through membrane coating, ensuring high fouling (Lee et al., 2016; Madalosso et al., 2021; Shaulsky et al., 2017; Yan et al., 2018). When using electrospinning, control of membrane porosity and thickness can be increased during spinning by controlling the deposition time and dope solution, which can reduce fouling. In addition, research is being conducted using plasma treatment and other methods to reduce fouling by targeting chemical reactions on the membrane surface (Madalosso et al., 2021).

Consequently, the development of anti-fouling membranes has resulted in the stable performance of MD desalination for low-surface-tension feedwater including industrial wastewater (Boo et al., 2016; Kharraz et al., 2020; Lu et al., 2019). Recently, hydrophilic, or water-

loving, coatings have been integrated into the MD membrane surface to reduce fouling caused by hydrophobic contaminants such as oil. However, there has been no significant progress in designing MD membranes with resistance to mineral scaling. An improved understanding of the fundamental relationship between membrane surface chemistry and scaling is essential for the further development of anti-scaling MD membranes.

Chapter 3. Electrically conductive membrane for fouling control: Its mechanisms and applications

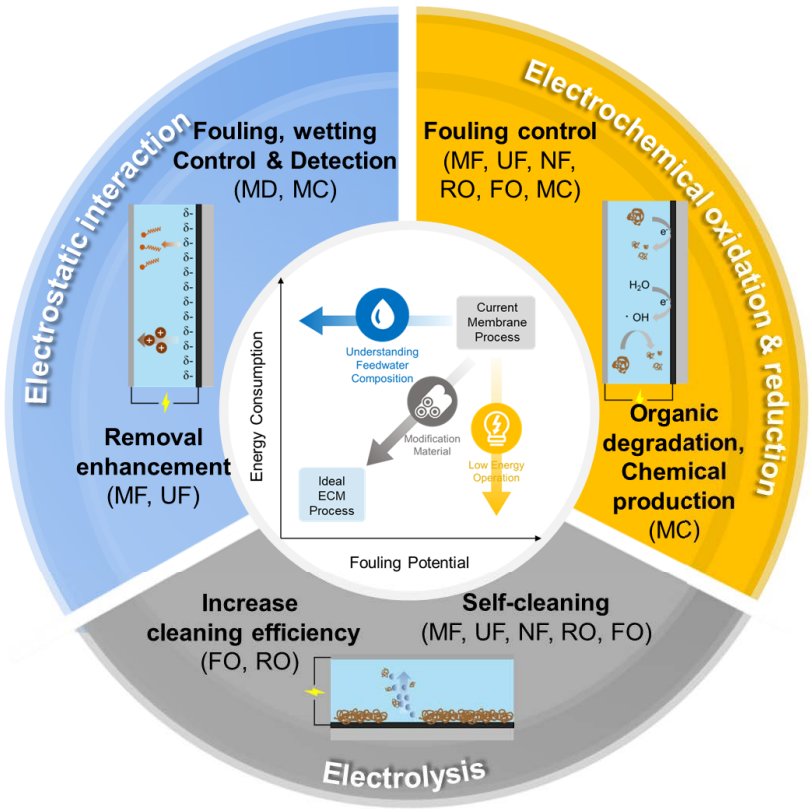

This chapter is based on:
Kim, J., Lee, J., Lee, S., Tijing, L., Shon, H.K. and Hong, S. Electrically conductive membrane for fouling control: Its mechanisms and application.

3.1. Introduction

Since the global interest in water resources has increased due to rapid population growth and climate change, the membrane process has received much attention, studied, and applied in various ways due to its high removal rate, compactness, ease of operation and management, and low energy consumption (X. Li et al., 2019; Rodriguez-Narvaez et al., 2017). However, the main challenge remains fouling, which could cause performance degradation (Y. Gao et al., 2019; Lee et al., 2020; Li et al., 2017; Liao et al., 2018; Meng et al., 2017).

Conventional fouling control methods include pre-treatment to lower the fouling potential at the previous process, an optimization operation that reduces fouling, and effectively cleaning the membrane to prolong the use cycle when fouling occurs (Gao et al., 2011; Jin et al., 2017; Mohammad et al., 2012). However, each has its own limitations. In the case of pre-treatment, the foulant is removed from the previous process. Although it is advantageous in terms of total energy and cost, it reduces foulant loading at only this process, so it could not be a fundamental solution to fouling control from the overall process control point of view. In the case of optimization operation, there is a limit to the removal of micro-pollutants, and pharmaceuticals, which have recently emerged as an environmental issue, because the conventional methods

are mainly based on physical mechanisms by controlling hydraulic conditions or membrane materials. Lastly, most of the membrane cleaning is concentrated in chemical cleaning. However, the use of chemicals not only entails a high regular operation cost, but there is also a risk of permanent damage to the membrane, which can eventually lead to a reduction in the life expectancy of the membrane process (G. Liu et al., 2018; Rabuni et al., 2015; H. Sun et al., 2018).

Electrically conductive membrane (ECM) technology is recently emerging as a new technology to overcome these weaknesses due to its future value in electro-driven processes (Barbhuiya et al., 2021; M. Sun et al., 2021; Z. Zhang et al., 2022; Zhu & Jassby, 2019). ECM is a membrane in which electrically conductive material is modified on a conventional polymer membrane, and its synergy could be expected by using the electrochemical phenomena along with the physicochemical removal mechanism of the conventional membrane processes. ECM could increase the removal rate for toxic contaminants that are difficult to be removed with conventional physical methods due to their small molecular weight and size, and degrade or decompose the foulant itself through electrochemical oxidation, thereby reducing the fouling potential of the feed water rather than simply dividing the foulant loading (M. Sun et al., 2021). Even during operation, by controlling the

movement path and direction of foulant through electrostatic interaction, it is possible to additionally control contaminants that are difficult to control through hydraulic conditions. A synergistic effect could be expected by electric and physical interaction. As a result, ECM could extend the role of the membrane process beyond pure separation as well as solute separation, the traditional function of the membrane process by using various electrochemical-based phenomena, including electrochemical oxidation and reduction, electrostatic interaction, and electrolysis (M. Sun et al., 2021).

However, ECM technology has been actively researched for only a few years, so the maturity of the technology is low, and most of the research is in the early application stage. In order to improve ECM technology with excellent potential for fouling control, it is necessary to study demand-tailored applications based on a more accurate understanding of the fundamental mechanisms. Therefore, in this paper, a comprehensive review of current ECM studies was performed. The level of current ECM technology and its application cases were evaluated. In detail, the fouling control mechanism was elucidated and categorized, and ECM characteristic analysis for each application process was performed. Additionally, , the development direction, future research topic, and potential application fields of ECM technology were proposed.

3.2. Identification of fouling control mechanisms of ECM

Membrane fouling is a major obstacle and challenge in membrane-based separation processes, which deteriorates membrane performance such as water flux, and rejection rate. ECM can mitigate or prevent such fouling by using various electrochemical phenomena. The method is, first, electrochemical oxidation and reduction that degrades the foulant itself. Second, is the electrostatic interaction that inhibits the generation of the fouling layer itself by blocking the movement and access of the foulant to the membrane surface. Finally, the self-cleaning method detaches the already generated fouling layer from the membrane surface through a microbubble generated by electrolysis. In this section, electrochemical oxidation and reduction, electrostatic interaction, and microbubble by electrolysis, which are the fouling control mechanisms of ECM, are reviewed, described, and categorized from a foulant point of view.

3.2.1. Electrochemical oxidation and reduction

The most typical foulants that induce membrane fouling are organic foulants such as natural organic matter (NOM), protein, and polysaccharides (Guo et al., 2012; Tian et al., 2013). These organic

foulants accumulate on the membrane surface either by rejection during membrane operation or by depositing under hydraulic flow. Accumulated foulants are gradually developed to form a cake layer forming a fouling layer (Lee et al., 2010a; Y. Sun et al., 2018; Wang et al., 2013). This fouling layer blocks the flow of water to the membrane, resulting in a decrease in water flux, which is a primary performance indicator of the basic membrane process. Electrochemical oxidation and reduction could lower the fouling potential by degrading the foulant itself and decomposing it into small substances or completely oxidizing it. Two pathways (including direct and indirect oxidations) exist for this electrochemical oxidation and reduction (Barbhuiya et al., 2021; M. Sun et al., 2021; Z. Zhang et al., 2022).

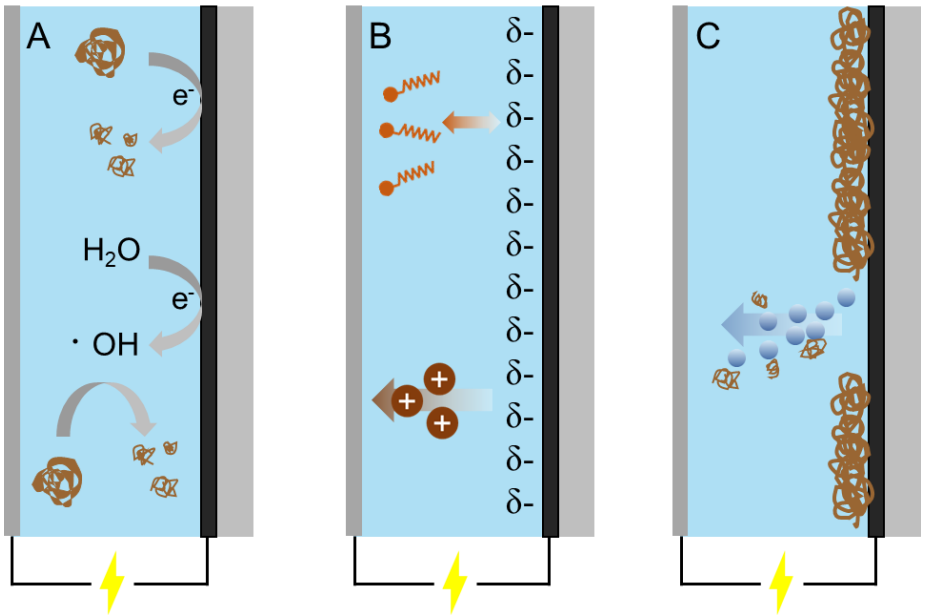

Figure 3-1 Fouling control mechanisms of ECM. (A: electrochemical oxidation and reduction, B: electrostatic interaction, and C: microbubble by electrolysis)

3.2.1.1. Direct oxidation and reduction

Direct oxidation occurs when an organic substance acting as a foulant comes into direct contact with the surface of the ECM that exhibits anodic potential by the series of actions mentioned above. At this time, the ECM acts as an anode (**Fig. 3-1A**). The detailed reaction is as follows (Karkooti et al., 2020; Rastgar et al., 2019):

$$Organics_{ads} - ne^{-} \rightarrow Organics_{oxidized} \quad \textbf{(3-1)}$$

Where $organics_{ads}$ refers to organic foulant adsorbed in direct contact with the ECM surface;. Once the organic foulant directly contacts with the ECM of anodic potential, direct electron transfer from the organic foulant to the ECM occurs, and the organic foulant is transformed into an oxidized form. Through this oxidation process, the organic foulant is decomposed and the MW and size are decreased, thereby lowering the fouling potential. Direct oxidation occurs only at a relatively low anodic potential where oxygen evolution cannot occur (Jing et al., 2016; Trellu et al., 2018; Zaky & Chaplin, 2013). Therefore, the fate of oxidation of organic foulant by direct oxidation is relatively slow, and the oxidizing power is also weak, so the typical organic foulant in the membrane process is limited to complete oxidation and usually remains in an intermediate state. On the other hand, by using a material with selectivity for target foulant for ECM modification, it could be advantageous for specific water resources (food industry wastewater, oil-field produced water, and semiconductor industry wastewater) for customized fouling control. As a result, since these oxidation intermediates can also form a fouling layer, an accurate understanding of direct oxidation of target

organic matter is essentially required when ECM is applied for fouling control.

3.2.1.2. Indirect oxidation and reduction

Indirect oxidation utilizes reactive oxygen species (ROS) in the oxidation process of organic foulants, unlike direct oxidation in which direct electron transfer occurs. In ECM for fouling control case, intermediate hydroxyl radicals (•OH) are used as ROS. •OH is generated by the oxidation of water molecules on the ECM surface (M. Sun et al., 2021). This process occurs only when the anodic potential of the ECM is high enough to generate oxygen evolution. Consequently, the generated •OH oxidizes or degrades the organic foulant (**Eqs. (3-2)** and **(3-3)**) (Karkooti et al., 2020; Rastgar et al., 2019).

$$ECM + H_2O \rightarrow ECM(OH\cdot) + H^+ + e^- \quad \textbf{(3-2)}$$

$$ECM(OH\cdot) + Organics \rightarrow ECM + Organics_{Oxidized} + H^+ + e^- \quad \textbf{(3-3)}$$

Since the oxidizing power of intermediate hydroxyl radicals is stronger than that of direct oxidation of ECM, the degradation rate of organic foulants is relatively higher (Pan et al., 2020; Wei et al., 2020; J.

Xie et al., 2022). Therefore, the amount and size of intermediate organic foulant are small, so the risk of additional fouling due to the intermediate is low. However, the energy consumption of the entire process is increased due to the high required potential used in ECM (Pan et al., 2020; Wei et al., 2020). To overcome the energy issue, studies are active to reduce energy consumption through modifications such as carbon-based materials, which could lower the potential value generated by oxygen evolution (Lin et al., 2014; Suen et al., 2017; Yi et al., 2015).

3.2.2. Electrostatic interaction

3.2.2.1. Electrostatic attraction and repulsion

As a fouling control method of ECM, the approach is though blocking or blocking access of the foulant to the membrane surface by employing electrostatic interaction forces via attraction and repulsion. According to the applied potential of the ECM, the surface charge is changed to negative or positive, which is influenced by one of the attractive or repulsive forces depending on the surface charge of the foulant. This electrostatic interaction force could be determined by The Derjaguin-Landau-Verwey-Overbeek (DLVO) theory.

The DLVO theory presents the total interaction energy which is combined with the Lifshitz-van der Waals (LW) and electrostatic (EL) forces, and LW and EL forces represent the attraction and repulsion forces between the membrane and organic matter. The DLVO theory expresses the dominant force between organic matter and membrane, as shown in **Eqs. (3-4)** to **(3-6)** (Ahmad et al., 2013; Kim, Yun, et al., 2022; Tanudjaja & Chew, 2018).

$$U_{DLVO} = U_{LW} + U_{EL} \quad \textbf{(3-4)}$$

$$U_{LW}(h) = 2\pi \cdot \Delta G_{LW} \cdot \frac{y_0^2 a_c}{h} \quad \textbf{(3-5)}$$

$$U_{EL}(h) = \pi \cdot \varepsilon_o \varepsilon_r a_c [2\xi_o \xi_m \, ln\left(\frac{1+e^{-\kappa h}}{1-e^{-\kappa h}}\right) + (\xi_o^2 + \xi_m^2) \, ln(1 - e^{-2\kappa h})] \quad \textbf{(3-6)}$$

Where U_{DLVO}, U_{LW}, and U_{EL} are the interaction energy, LW, and EL between the membrane and organic matter, respectively; h is the distance between the membrane and organic matter; ΔG_{LW} is the free energy of adhesion per unit area between the membrane and organic matter; y_0 is the minimum equilibrium cut-off distance; a_c is the radius of the

spherical organic matter; ε_0 and ε_r are the relative dielectric permittivity and vacuum dielectric permittivity, respectively; ξ_o and ξ_m are the zeta potentials of organic matter and membrane, respectively; and κ is the inverse Debye screening length.

As a result, it is possible to control fouling by inducing an electrostatic interaction between the foulant and the membrane surface through surface modification to block direct contact between them (**Fig. 3-1B**). In the case of typical organic foulants in the water treatment field, most of them have a negative surface charge, so in the case of fouling control using electrostatic interaction using ECM, most of the cathodic potential are employed to negatively charge the surface of ECM to induce repulsion with the foulant (Kim, Yun, et al., 2022). On the other hand, in the case when the specific target foulant has a positive surface charge, the same effect could be obtained by using the anodic potential. In addition, this approach has recently been used to improve the rejection of heavy metal or dye using this interaction (Li et al., 2022; L. Liu et al., 2019). Those interaction forces are deeply associated with the zeta potentials of the membrane and foulant. Hence, for effective fouling control by electrostatic interaction, it is important to select a modification material suitable for the characteristics of the target foulant.

3.2.2.2. Electrophoresis

Electrophoresis is a phenomenon in which ionic species present in the electric field move toward the counter electrode according to their surface charge, respectively, and is one of the electrostatic interaction mechanisms used in ECM. The movement of the ionic species is faster as the electric field is stronger and the charge of the ion species is greater, and is inversely proportional to the molecular weight and size of the ionic species. In ECM, it is mainly used to control multi-valent ions that cause inorganic fouling. Multi-valent ions move toward the counter electrode rather than to the membrane surface by electrophoresis, and local crystallization on the membrane surface is hindered by this movement (**Fig. 3-1B**) (Rao et al., 2020). However, if the effect of electrophoresis is too high, the concentration polarization and mixing effect happen wherein the concentration of the multi-valent ionic species at the counter electrode side becomes relatively high, and the risk of inorganic fouling may rather increase. Therefore, it is essential to consider the ionic composition of feed water and electrostatic interaction force in ECM applications.

3.2.3. Electrolysis

Electrolysis generates hydrogen and oxygen gas bubbles by electron transfer between water molecules and the ECM surface. It occurs only when the ECM applied potential is higher than the value that can cause oxygen evolution similar to indirect oxidation (**Eqs. (3-7)** and **(3-8)**) (Karkooti et al., 2020; Rastgar et al., 2019).

$$2H_2O(l) \rightarrow O_2(g) + 4H^+(aq) + 4e^- \quad \textbf{(3-7)}$$

$$H_2O(l) + 4e^- \rightarrow (\tfrac{1}{2})H_2(g) + OH^- \quad \textbf{(3-8)}$$

The generation of hydrogen and oxygen gas by water electrolysis in ECM application could provide fouling control advantages (**Fig. 3-1C**). First, the movement of the foulant to the ECM surface is limited basically by the generated microbubbles. Because microbubbles are generated on the ECM surface, when the foulant tries to move to the ECM surface, it physically blocks the path of the foulant. Second, when a fouling layer has already been created on the ECM surface, the generated microbubbles rise from the bottom of the fouling layer, thereby rising up while breaking or removing the fouling layer. The self-cleaning effect of ECM could be expected by this process (Barbhuiya et al., 2021; M. Sun

et al., 2021; Z. Zhang et al., 2022). The microbubbles by electrolysis could be an in-situ cleaning method that does not damage the membrane itself, unlike chemical cleaning used for conventional membrane cleaning, and offer a promising option for fouling mitigation as well as membrane cleaning (Anis et al., 2022; Anis et al., 2021; Hashaikeh et al., 2014; Ye et al., 2019; W. Zhang et al., 2022).

3.3. Applications of ECM

3.3.1. Hydrophilic membrane process

3.3.1.1. Porous membrane process (MF, UF)

Porous microfiltration (MF) and ultrafiltration (UF) technology, with pore size ranging from 0.1 to 10 μm for MF membranes and 2–100 nm for UF membranes are one of the most promising and attractive techniques for water treatment process (ElHadidy et al., 2013). Typically, the MF membrane is for removing macromolecules, colloids, and suspended particles from solution and the UF membrane acts as an effective barrier to suspended particles, colloids, viruses, and the high-molecular fraction of NOM in broad applications such as food processing and production, drinking water, and wastewater treatment (Kumar & Ismail, 2015). However, fouling is one of the most significant technical

issues for the practical application and operation of MF/UF, causing severe performance degradation through pores blocking, adsorption, and gel formation (Howe & Clark, 2002; Y. Zhang et al., 2021). Therefore, the ECM process could be one of the great options for mitigating MF/UF fouling by electrochemical oxidation and reduction, electrostatic attraction and repulsion.

3.3.1.1.1. Fouling control

Especially, NOM is the most critical foulant for MF/UF membrane since NOM could adsorb to the membrane surface and cause pore blocking, leading to severe membrane fouling. Furthermore, membrane fouling by NOM is significantly influenced by solution properties such as pH, ionic strength, and calcium concentration (Hong & Elimelech, 1997). To prevent NOM fouling, ECM is used as an anodic or cathodic electrode for electrochemical reactions, which could partially or completely degrade the chemical structure of NOM or repulse NOM from the membrane surface (Karkooti et al., 2020). To elaborate on the effect of different NOM fouling control performance, three typical organic model foulants, humic acid (HA), sodium alginate (SA) and bovine serum albumin (BSA) were analyzed for electrically conductive MF/UF membranes in previous cases.

Fig. 3-2 shows the normalized water flux decline of ECMs for NOM fouling control by applying continuous voltages. The decrease of normalized flux was mitigated as the applied voltage was increased for all types of NOM, but fouling was more effectively controlled by applying a cathodic potential to ECM. Due to the negatively charged surface of NOM, the ECM can repel the NOM molecules through electrostatic repulsive forces between the membrane surface and the charged foulants (Dudchenko et al., 2014), and higher applied voltages increase the efficiency of electrostatic repulsion in cathodic potential. Furthermore, gas bubbling phenomena (hydrogen gas production from cathode) through water electrolysis (**Eqs. (3-7)** and **(3-8)**) can effectively decrease the membrane fouling rate by preventing the absorption of NOM on the membrane surface (Kim, Yun, et al., 2022). Unlike the conventional gas scouring process where there is a parallel flow of gas and water, the perpendicular generation of micro-nano bubbles on the ECM surface by electrolysis, leads to the foulant being readily removed and prevented from attaching to the ECM surface, as mentioned above. Increasing electric potential increases the amount of produced gas on the ECM surface, which can effectively reduce the fouling rate. The two-electron reduction reaction of dissolved oxygen could occur on ECMs as a cathodic electrode by generating hydrogen peroxide via

electrochemical reactions. Oxygen reduction produces hydroperoxide ions (HO_2^-), a conjugated form of H_2O_2 (Liu et al., 2015b). These oxidants reduce hydrophobic interaction between NOM compounds and membrane surfaces by minimizing the molecular size of organics or completely breaking down their chemical structures. Furthermore, the production of hydroxyl radicals by H_2O_2 can be accelerated by existing ferric ions (Karkooti et al., 2020; L. Xu et al., 2020), which is the Fenton process. The reaction equation is as follows:

$$Fe^{2+} + H_2O_2 + H^+ \rightarrow Fe^{3+} + H_2O + OH\cdot \quad \textbf{(3-9)}$$

A cathodic potential of ECM could also activate sulfate radical-based oxidants, such as peroxomonosulfate (PMS) and peroxydisulfate (PDS), which continuously provides electrons to activate PMS and generate sulfate radicals and hydroxyl radicals (J. Sun et al., 2021). Therefore, ECM can perform as a catalyst to activate oxidants in cathodic potentials. In addition, the rejection of NOM would be improved by cathodic potential due to strong electrostatic repulsive forces between NOM and the membrane surface (Du et al., 2020; Mantel et al., 2021).

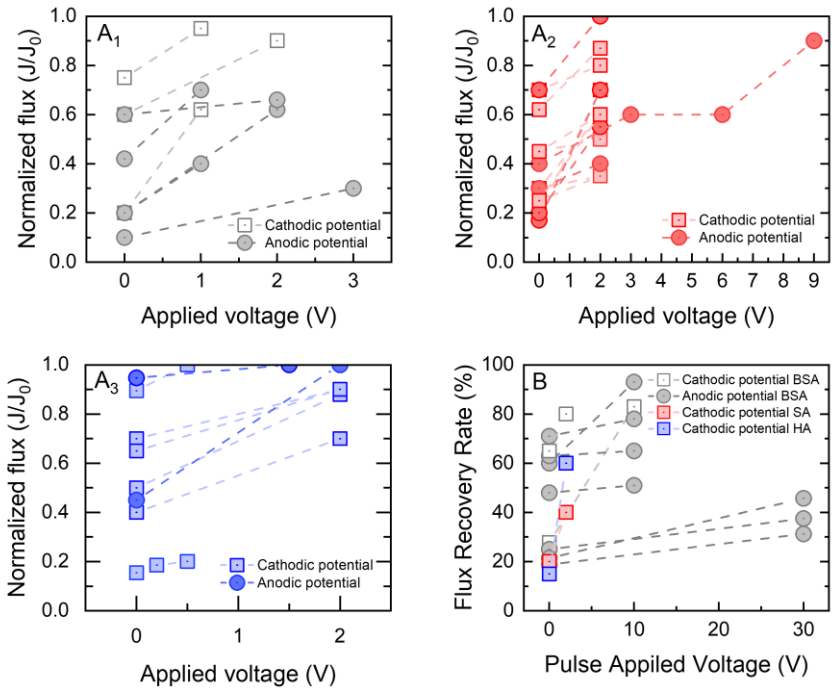

Figure 3-2 Normalized flux as function of applied voltage in continuous applied voltage operation for mitigating NOM fouling: (A_1) BSA, (A_2) SA, and (A_3) HA, and (B) Flux recovery rate as a function of applied voltage in pulse applied voltage operation. All data in the figure are from (Anis et al., 2022; Duan et al., 2016; Dudchenko et al., 2014; Karkooti et al., 2020; Li et al., 2022; Liu et al., 2015a; R. Liu et al., 2019; Mantel et al., 2021; Mantel et al., 2018; Mao et al., 2019; J. Sun et al., 2021; L. L. Xu et al., 2019; Zhang & Vecitis, 2014; Y. Zhang et al., 2021).

The oxidation reaction by ECM is the primary fouling control mechanism in anodic potential. Direct oxidation occurs on the membrane surface by direct transfer of electrons to organic species and subsequently oxidized (Karkooti et al., 2020). In the direct oxidation process, the oxygen should not be involved on the electrode ECM surface

with low potentials (Sirés et al., 2014). In contrast, indirect oxidation uses a reactive intermediate that is produced from the oxidation of water or ions to the degradation of organic compounds (Sirés et al., 2014). The most common indirect oxidation reaction in ECM is water oxidation, producing hydroxyl radicals or ozone species (Duan et al., 2016; Karkooti et al., 2020; R. Liu et al., 2019; Mantel et al., 2021; Mantel et al., 2018; L. L. Xu et al., 2019). However, if the oxidation rate of organic compounds by the anodic potential of ECM is not enough to completely degrade the compounds, the positive charge of the ECM membrane (induced by anodic potential) attracts negatively charged NOM, reducing the fouling control effect. Particularly the slight decrease in the normalized flux of BSA is owing to the difficulty of degrading the main chain of BSA than other NOM organic compounds (Cheng et al., 2016). Furthermore, the rejection of NOM would be deteriorated in anodic potential due to electrostatic attraction (Du et al., 2020; Mantel et al., 2021).

The self-cleaning process of ECM with pulse applied voltage operation was further studied to overcome the high energy consumption of ECM with continuous applied voltage operation. As shown in **Fig. 3-2B**, the BSA, SA, and HA fouling was alleviated by a pulse applied potential of 3 V. Since the fouling rate was not severe (~about 15%

decrease to initial flux) for BSA fouling, the cathodic potential of 3 V has efficiently removed fouling layer of BSA on the membrane surface, which was 8% higher compared with that of non-applied voltage cleaning process (Y. Zhang et al., 2021). Although SA and HA fouling was reduced by around 80% from the initial flux, the pulse applied voltage of 3V for cleaning shows higher efficiency of 15% and 27% than the non-electricity cleaning process, respectively (Y. Zhang et al., 2021). On the other hand, a high concentration of BSA of 1 g/L led to a severe flux decline of less than 30% of the initial flux (Yu et al., 2019). After the interval voltage operation within 10 V for 1 min, the flux recovered to 94% of the initial flux even there was severe flux decline before applying the electricity. The in-situ aeration by electrolysis could produce the bubbles on the membrane surface through a perpendicular direction, detaching the BSA fouling layer from the membrane surface and subsequently removed by high turbulence flow (Yu et al., 2019).

In the case of anodic potential during self-cleaning, electrolysis is also important, similar to a cathodic potential, but the oxidation ability of ECM should be considered. For example, ECM shows excellent anti-fouling capacities with flux recovering 65%, 78%, and 93%, after applying 10 V of anodic potential, respectively (Li et al., 2022). This difference in cleaning efficiency is attributed to the coating materials in

ECM. The oxidation process in rGO/ZnO/PSF ECMs was improved since the excited ZnO on the membrane surface formed hole/electrons. Subsequently, rGO promoted electron transfer between O_2 and ZnO with excellent electrocatalytic activity (Li et al., 2022). These electrocatalytic processes produce hydroxyl radicals, which decompose the organic fouling layer on the membrane pore or surface by oxidation (Wang et al., 2019). However, the low cleaning efficiency was shown after severe BSA fouling in polyaniline membrane incorporated with exfoliated graphite and dopant dodecylbenzene sulfonic acid (L. L. Xu et al., 2019). Even though applying a high potential of 30 V, the self-cleaning efficiency observed less than 40% of flux recovery (L. L. Xu et al., 2019). Therefore, it could be concluded that the coating material is a key option to reduce electrochemical reaction resistance to ensure oxidation capacity.

Biofouling, caused by biofilm deposition on the membrane surface, is also a limiting factor of membrane technologies, decreasing water permeability, increasing energy consumption, and shortening membrane replacing cycles (Baker, 2012; Li et al., 2018). Carbon nanotube (CNT) is the disinfection material in that the needlelike structure destroys microorganism and induces lysis (Omi, Choudhury, Anwar, Bakr, & Rahaman, 2017). In one study, a CNT-coated ECM membrane without

any potential shows 31% of disinfection capacity for *E. Coli*, but the inactivation rate increased up to 100% at the applied anodic potential of 3 V. (Omi, Choudhury, Anwar, Bakr, Rahaman, et al., 2017). In another study, a laser-induced GO shows a great inactivation rate for microorganisms, achieving >6 log removal when ECM was used at applied voltage of 2.5 V (Thakur, Singh, Kleinberg, et al., 2019) and 2 V of anodic potential (Thakur, Singh, Thamaraiselvan, et al., 2019), respectively. Moreover, the microbial diversity in the biofilm can be changed in the colony, wherein a high concentration of EPS is released to electrically active bacteria by applying electric potential, implying that ECM shows selectivity in microorganism removal (L. Xu et al., 2020).

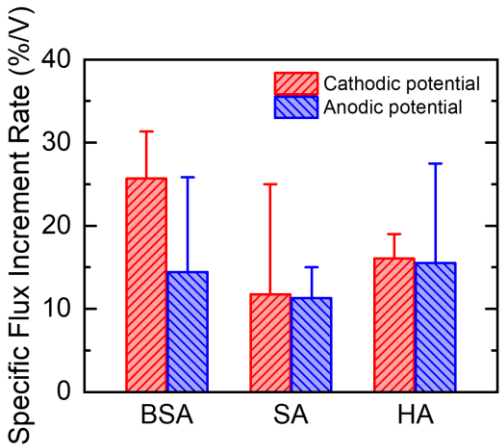

Figure 3-3 The specific flux increment rate of cathodic and anodic potential for each BSA, SA, and HA in electrically conductive MF/UF membranes.

As the applied potential to ECM is directly related to energy consumption, further elucidation of the specific cleaning efficiency against applied voltages for each organic foulant (i.e., BSA, SA, and HA) is presented in **Fig. 3-3**. The cathodic potential of ECM membrane alleviates the flux decline more than its anodic potential. Moreover, the large difference in specific flux increment rate (%/V) in BSA was attributed to the limitation of oxidizing BSA. Thus, the ECM membrane could effectively control the NOM fouling on both anodic/cathodic potential, but the types of anode coating material should be considered to produce more hydroxyl radicals for a high oxidation rate. Moreover, the water permeability can be increased by applying both anodic and cathodic potential to ECM. The electric field application between both sides of a membrane induced by applied voltage can cause the electrophoresis phenomenon, which decreases the rate of cake deposition and increases the rate of water permeation (Karkooti et al., 2020).

In conclusion, the severe organic fouling in MF/UF membrane could be controlled by applying both cathodic and anodic potential with ECM. For the cathodic potential, the electrolysis and electrostatic repulsion between negatively charged ECM surface and negatively-charged organics reduce the absorption of foulant to the membrane surface. On the other hand, although the electrolysis in anodic potential can mitigate

membrane fouling, the oxidation ability of ECM plays a significant role in fouling control. The lack of oxidation rate of organic foulant leads to the attraction of foulants to the membrane surface, resulting in low cleaning efficiency or deteriorating removal rates. Therefore, the ECM membrane with adequate coating materials is one of the attractive options to control membrane fouling in the MF/UF process.

3.3.1.1.2. Rejection enhancement

As the amounts of wastewater containing toxic chemicals have increased in the industry, the application of the membrane process has significantly increased due to its compactness, non-chemical dosage operation, and relatively low energy consumption than conventional treatment process (Cha et al., 2022). However, because of the low rejection of chemical species by the porous MF/UF process, a further non-porous membrane is needed, which requires more energy input to operate compared with MF/UF process. With this point of view, an electrically conductive MF/UF can potentially replace nanofiltration/reverse osmosis (NF/RO), wherein the electrochemical reaction via the applied voltage can increase the removal rate of toxic chemicals, which cannot be removed by a typical MF/UF membrane.

Chromium is one of the common toxic heavy metals that is widely used in various industrial fields, such as textile, dyeing, electroplating, and pigment manufacturing industries (Velazquez-Pena et al., 2012). Specifically, hexavalent chromium (Cr (VI)) has been found as a carcinogen that has a harmful effect on human health due to its high toxicity than trivalent chromium (Cr(III)) (L. Liu et al., 2019). Nowadays, membrane technology, such as NF and RO, has been an attractive option to remove chromium in wastewater, but high operation cost and energy demand are the barriers to its practical application (Barrera-Díaz et al., 2012). To overcome the limitation of NF and RO process, several studies reported that the UF membrane could remove chromium by applying electric potentials, while the conventional UF could not remove chromium due to relatively large pore size (Duan et al., 2017; L. Liu et al., 2019).

The removal mechanisms of chromium by ECM include: 1) electrostatic repulsion and 2) electrochemical reduction of Cr(VI) to Cr(III) and subsequently precipitation ($Cr(OH)_3$). As shown in **Fig. 3-4**, the rejection rate of Cr(VI) significantly increased with the increase in applied voltages, while the ECM membrane without applied voltage can not remove Cr(VI) due to the large pore size of the UF membrane. These results confirm that the ECM membrane with cathodic potential can

reject Cr(VI) ions (dominant species of Cr(VI) is CrO_4^{2-} in aqueous) by electrostatic repulsion. However, electrostatic repulsion only plays an important role in low ionic strength, but at high ionic strength, it has lesser effect as the high ion concentration reduces electrostatic force between membrane surface and Cr(VI) by compressing electrical double layers (Duan et al., 2017; L. Liu et al., 2019). For Cr(VI) to Cr(III) reduction, the electrochemical reactions can be expressed as (Duan et al., 2017):

$$CrO_4{}^{2-} + 3e^- + 5H^+ \rightarrow Cr(OH)_{3(S)} + H_2O \quad E° = -0.13V \qquad \textbf{(3-10)}$$

$$2H_2O - 4e^- \rightarrow O_2 + 4H^+ \quad E° = 1.23V \qquad \textbf{(3-11)}$$

Applying high cathodic potential on ECM membrane can significantly remove Cr(VI). As shown in **Fig. 3-4A**, there are two results at an applied of 5 V: high and low rejection rate. The main reason for the low rejection rate by applying 5 V is that there are not enough conditions to reduce Cr(VI) to Cr(III). Contrary to the results of the electrostatic repulsion, a higher electrolyte concentration enhanced electron transfer to promote the reduction of Cr(III) (Duan et al., 2017; L. Liu et al., 2019). Moreover, the optimum residence time is also important to increase Cr(VI) rejection

because increasing residence time causes a longer contact time between the ECM and chromium (L. Liu et al., 2019). Therefore, the sufficient electrolyte and residence time reduced the soluble Cr(IV) species to insoluble Cr(III), subsequently precipitating on the membrane surface as $Cr(OH)_3$.

Arsenic is also a hazardous metal to the human body, and the risk of arsenic exposure has recently increased (Jang et al., 2016). Specifically, As(III) is the most toxic species and more favor to exist in redox environments (Singh et al., 2015). As(III) in oxygen depleted conditions can be present in three dissociation forms, namely: H_3AsO_3, $H_2AsO_3^-$, and $HAsO_3^{2-}$ (Wu et al., 2017). The uncharged form of H_3AsO_3 is the dominant species in the neutral pH due to a high pKa of 9.23, leading to low rejection of conventional membrane processes (Boussouga et al., 2021). However, the ECM membrane can effectively remove As(III) by applying cathodic potential as shown in **Fig. 3-4A**. In the cathodic potential, the local pH (in the vicinity of membrane surface) can be increased due to the reduction reaction of water molecules and formation of OH^- (Tang et al., 2017). Thus, the As(III) are converted to charged form when the local pH raised more than pKa of 9.23. This charged arsenic form are then removed by the electrostatic repulsion between arsenic and ECM membrane in cathodic potential. One study reported

that a CNT-coated ECM achieved 72% of As(III) rejection in 7 V of cathodic potential condition, but nickel-CNT coated ECM membrane rejected 93% of As(III) (S. Ma et al., 2021). This is because the catalytic properties of nickel exhibit higher currents compared to only CNT coated ECM membrane (Hou et al., 2018).

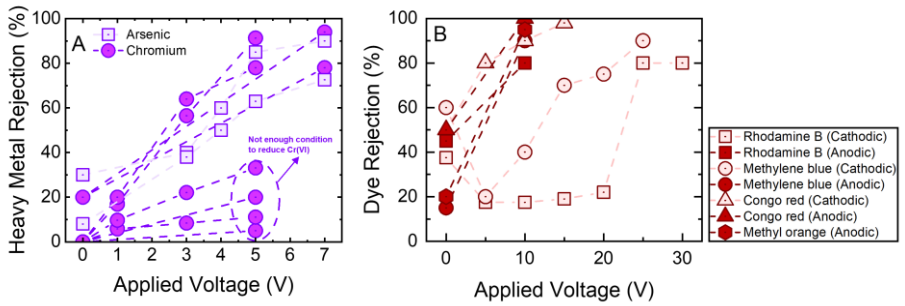

Figure 3-4 (A) Heavy metal rejection and (B) dye rejection of the cathodic potential in electrically conductive MF/UF membranes. The data of heavy metal rejection (A) are from (Duan et al., 2017; Hou et al., 2018; L. Liu et al., 2019; S. Ma et al., 2021) and dye rejection are from (Li et al., 2022; Yu et al., 2019).

Dye wastewater is one of the concerns in industrial wastewater treatment since dye is toxic and non-biodegradable (Melo et al., 2018). Due to the small molecular weight of dye molecules (~1,000 Da), the conventional UF membrane (>1kDa) is not a proper treatment for dye wastewater. However, the ECM UF membrane has shown to effectively remove dye molecules. Congo red (CR) was almost 100% rejected in cathodic potential (10 V) of ECM membrane by strong electrostatic

repulsion (**Fig. 3-4B)** (Yu et al., 2019). On the other hand, rhodamine B (RB) and methylene blue (MB) are positively charged, and electrostatic attraction occurs between the ECM membrane and dye molecules. At increasing applied cathodic voltage, the dye molecules could pass through the ECM membrane (leading to lower rejection). However, rejection was high (82% of RB and 100% of MB rejection) at 30 V applied voltage. Since the aeration on the ECM membrane surface has predominantly taken place, the dye molecules could have been extruded out of the membrane surface (Yu et al., 2019).

In anodic potential, RB, MB, CR, and methylene orange (MO) were completely removed as shown in **Fig. 3-4B**. Interestingly, the rejection of ECM membrane at 10V of anodic potential was increased from 44%, 20%, 56%, and 13% to 84%, 94%, 99%, and 93% for the various dyes, respectively. This result indicate that the oxidation reaction of dye molecules was effectively implemented by the ECM electrode (Li et al., 2022). Moreover, CR was completely oxidized at 10 V of anodic potential, even at negatively charged molecules. Therefore, the oxidation reaction is preferred over electrostatic repulsion in ECM to treat dye wastewater.

In summary, ECM could achieve high rejection of heavy metal and dye, which otherwise cannot be removed with the conventional MF/UF process. In heavy metal rejection, ECM was used as a cathodic electrode, and the heavy metal ion was rejected by electrostatic repulsion or electrochemical reduction to form solid precipitates with increasing local pH. Moreover, dye molecules were removed by not only electrostatic repulsion but also by electrochemical oxidation due to the production of micro-nano bubbles at the ECM surface.

3.3.1.2. Non-porous membrane process (NF, RO, and FO)

NF and RO membrane processes have become dominant desalination technologies, producing 65% of the global desalination capacity (Caldera et al., 2016; Shenvi et al., 2015). Typically, NF is widely used with high water flux and low energy consumption compared to RO (Boo et al., 2018). NF can remove multivalent ions, but low rejection of monovalent ions is its main challenge in satisfying desalination demands. To overcome the limitation of NF in desalination, electrically conductive NF coated with CNT and polyaniline (PANI) has shown to achieve high rejection of monovalent ions (from 53.9 to 82.4% of NaCl rejection) while retaining high water flux (14.5 LMH) (Zhang et al., 2018).

Applying a cathodic potential of 2.5 V makes the ECM surface more negatively charged, and the ion concentration difference between the ECM and bulk solution prevents ions from passing through the membrane (Zhang et al., 2018).

Although RO is favorable to remove monovalent ions that effectively meet desalination demand, the active layer of the RO membrane is vulnerable to chlorine attack (Al-Abri et al., 2019). Damaged RO membrane attacked by chlorine suffers low ion rejection and shortens the membrane lifespan (Tang et al., 2012). The reactive chlorine species (i.e., NaOCl) could be effectively reduced by employing ECM in RO (Khanzada et al., 2022). Previous report shows that chlorine was irreversibly reduced as described below:

$$HOCl + e^- \rightarrow Cl^- + OH\cdot \quad \textbf{(3-12)}$$

There are no significant changes in Fourier transform infrared (FTIR) and X-ray photoelectron spectroscopy (XPS) results, implying that the chemical structure of the RO membrane was not damaged by reactive chlorine species. After that, the ECM can remove Cl^- ion effectively more than 88% (Khanzada et al., 2022). Thus, ECM not only increases

the ion removal rate, but also increases the stability of the membrane via an electrochemical reaction.

Further, membrane fouling during desalination induces severe cost issues to NF/RO membrane, leading to a high cost of membrane replacement. Similar to ECM of MF/UF, the electrically conductive NF/RO membrane can control severe membrane fouling. In NF membrane coated with CNT, biofouling caused by bacteria deposition on the membrane surface was fully alleviated in 1.5 V of anodic potential, which was not recovered without electric potential (de Lannoy et al., 2013). Also, electrical cleaning by applying 5 V of cathodic potential was conducted for 20 min in an electrically conductive RO membrane, and the organic fouling layer on ECM was clearly removed by electrolysis (Ahmed et al., 2019a). The detailed information on electrically conductive NF/RO membrane, such as coating materials and counter electrodes, is summarized in **Table 3-1.**

Table 3-1 Overview of previous ECM application studies for NF/RO in current literature.

Process	Purpose	Modification material	Membrane usage for electrode	Counter electrode	Feed	Applied voltage	Reference
NF	Removal enhancement	CNT, PANI	Cathode	Titanium mesh	NaCl, Na_2SO_4, $CaCl_2$	0-3V	(Zhang et al., 2018)
	Biofouling control	CNT	Anode	Platinum	NaCl + LB	0-1.5V	(de Lannoy et al., 2013)
RO	Chlorine resistant	CNT	Cathode	Platinum	NaOCl	0-2V	(Khanzada et al., 2022)
	Fouling control	CNT	Cathode	Platinum	NaCl + HA	0-5V	(Ahmed et al., 2019a)

The forward osmosis (FO) process is a promising technology in seawater desalination and industrial wastewater treatment (Gwak et al., 2018; Lee et al., 2010b). Within the unique characteristics of non-pressurized FO compared to the RO process, there are several advantages, including lower energy consumption, a high rejection rate of a wide range of contaminants, and lower irreversible fouling tendency (Gwak et al., 2018). However, the polyamide active layer of the FO membrane has a high density of carboxyl groups that could increase the organic fouling under a high concentration of foulants (Mo et al., 2012). Several studies have been conducted to get anti-fouling features to the FO membrane by applying either anodic or cathodic potential (Cruz-Tato et al., 2019; Darbari et al., 2016; Liu et al., 2016; Rastgar et al., 2019; Shakeri et al., 2019; Wang et al., 2022b; M. Xu et al., 2022; X. Xu et al., 2021; X. Xu et al., 2020; X. Xu et al., 2019).

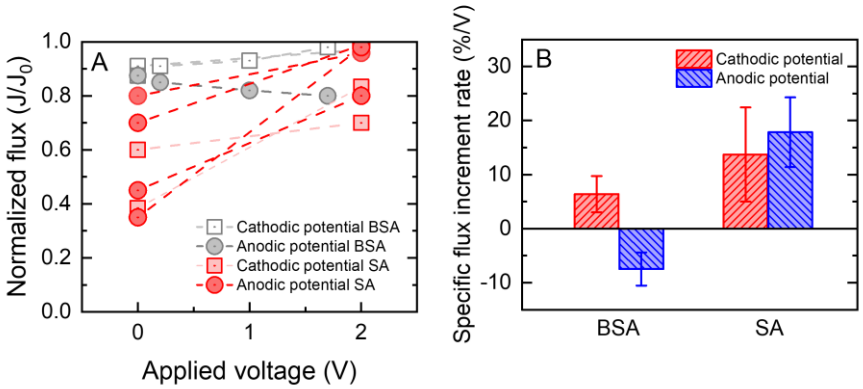

Figure 3-5 (A) Normalized flux as a function of applied voltage in continuous applied voltage operation for mitigating NOM fouling. (B) The specific flux increment rate of cathodic and anodic potential for each NOM in electrically conductive FO membranes. All data in the figure are from (Cruz-Tato et al., 2019; Liu et al., 2016; Rastgar et al., 2019; Shakeri et al., 2019; M. Xu et al., 2022; X. Xu et al., 2019).

As shown in **Fig. 3-5A**, the applied voltage is relatively lower than electrically conducted MF/UF membranes in **Fig. 3-2A**, because the non or low-pressurized FO process exhibits a lower irreversible fouling rate compared to MF/UF as well as to NF/RO membranes (Lee et al., 2010b). First, SA fouling was fully mitigated by applying continuously both anodic and cathodic potential (Cruz-Tato et al., 2019; Liu et al., 2016; Rastgar et al., 2019; Shakeri et al., 2019; M. Xu et al., 2022). The SA deposits on the conventional FO membrane (or non-applied voltage) surface with crosslinking to the polyamide active layer and subsequently forming cake layer formation (Mi & Elimelech, 2008). However, the ECM shows anti-fouling properties to SA with 2 V of anodic potential, and the water flux increased to 99% (Rastgar et al., 2019). Direct and indirect oxidation of the electrochemical oxidation reaction on the ECM surface degraded the SA fouling. Moreover, the water molecules could be dragged by electrostatic attraction to the ECM surface, leading to higher water flux. A similar result was observed in another study (Liu et al., 2016), when ECM with anodic potential increased the water flux

from 60% to 92% of its initial water flux. The cathodic potential of ECM effectively removes alginate fouling on the surface as well. Under no electric potential, the membrane surface was covered with SA fouling, but the foulant on the ECM surface was almost completely removed after an applied cathodic potential (Cruz-Tato et al., 2019). Furthermore, water flux decline was significantly reduced from 40% to 32.5% by continuously applying 2 V of cathodic potential (M. Xu et al., 2022).

The protein-like BSA fouling is affected by membrane properties to adhere to the membrane surface (Miao et al., 2017). When the potential was applied to ECM within the same charge of the BSA, the electrostatic repulsion between the ECM and BSA occurs and prevents the absorption of BSA on the membrane surface. Thereby, the water flux decline was alleviated by 5~10% more than the non-applied potential (M. Xu et al., 2022; X. Xu et al., 2019). However, BSA was attracted to the ECM membrane surface when the opposite potential of BSA was applied. Interestingly, the water flux was deteriorated on anodic potential, and the BSA adsorb to ECM surface and caused severe membrane fouling (X. Xu et al., 2019). Unlike MF/UF membrane, FO membrane is non-porous, which the BSA molecular cannot pass through the membrane pore. This result confirms well with **Fig. 3-5B**, that anodic potential of electrically

conducted FO membrane suffer severe organic fouling due to electrostatic attraction between ECM and BSA foulant.

Furthermore, fouling caused by calcium ions (gypsum scaling or organic-bridging fouling) can be minimized by electrostatic repulsive force between anode ECM and calcium cation (Rastgar et al., 2019; X. Xu et al., 2019). Especially, the formation of gypsum crystal on membrane surface changes at different applied potential. In the anodic potential, the calcium ions are repelled by positively charged ECM, while the gypsum crystal forms more favorably in homogenous nucleation (in the bulk solution), rather than heterogenous nucleation on the membrane surface. On the other hand, heterogenous nucleation of gypsum scaling was facilitated on cathodic potential via electrostatic attraction force (X. Xu et al., 2019).

The antimicrobial properties of electrically conductive FO membrane were observed by applying both cathodic and anodic potential. The PA/PES FO membrane was modified by coating carbon paper on PES support layer to utilize for the FO process in AL-DS (active layer is facing the draw solution) mode (Liu et al., 2016). AL-DS mode shows smaller internal concentration polarization (ICP) than AL-FS (active layer is facing the feed solution) but exhibits higher fouling potential

owing to its porous support layer (Gray et al., 2006; McCutcheon & Elimelech, 2006). The cathodic potential of 2 V on PES support layer has shown to repel bacteria and helped prevent the formation of biofilm on the ECM surface (Liu et al., 2016). Furthermore, generation of hydrogen peroxide near ECM surface could be fatal to biofilm formation and can decrease the viability of microorganisms (Ronen et al., 2015). Likewise, the CNT-interlayered FO membrane showed antimicrobial properties in anodic potential by generating reactive chlorine species (RCS) from Cl^- ion. The electro-generated RCS process (95% of flux recovery) has better cleaning performance than NaOCl dose (~70% of flux recovery) in terms of biofouling control. The fluorescence intensity results confirmed that live and dead cell were completely removed on ECM surface under anodic potential of 2.5 V (Wang et al., 2022a).

Membrane fouling in the FO process is an obstacle to practical development, but ECM can provide attractive opportunities to operate sustainably by mitigating fouling. Similar to electrically conductive MF/UF membrane, both the anodic and cathodic potential of electrically conductive FO can alleviate organic fouling with relatively low applied voltages. However, insufficient oxidation ability of ECM causes more severe fouling than non-applied potential, attracting counter-charged NOM to the membrane surface, subsequently forming a dense and thick

fouling layer. Further foulant with different surface charges, such as scaling precursor or microorganism, can be removed from membrane surface by applying potentials adequately to maintain water flux of FO. Therefore, customized with the proper coating material in FO is a feasible and promising technique to control various membrane fouling.

3.3.2. Hydrophobic membrane process

3.3.2.1. Water production process (Membrane distillation (MD))

Membrane distillation (MD) is a hybrid thermal-membrane separation process for desalination and water treatment using a hydrophobic membrane. In MD, water vapor passes through the MD membrane pores due to the vapor pressure difference between the feed and permeate solution channels (Kim, Kim, et al., 2022; Kim et al., 2018a; Kim et al., 2017a; Shin et al., 2020). Due to the unique characteristics of the MD process, it has a fouling tendency different from the typical membrane process using the hydrophilic membrane mentioned previously. In MD, in addition to fouling, which is basically caused by the accumulation of foulants on the membrane surface, wetting can cause performance degradation. The wetting phenomenon occurs when the hydrophobicity of the MD membrane is deteriorated by low surface tension and

hydrophobic substances such as surfactants including existing organic and inorganic foulant, so that the feed water passes through the membrane pore in the form of water molecule containing contaminants instead of vapor, resulting in performance degradation (Choudhury et al., 2019; Rezaei et al., 2018; Tijing et al., 2015). While organic fouling can be controlled by the typical pre-treatment method of the existing water treatment field, most of the wetting-inducing matters in MD have very small molecular weight and size, so it is difficult to remove them with the pre-treatment, which is based on the physical separation.

Therefore, the MD application of ECM is emerging. ECM has a comparative advantage in fouling and wetting control because it controls fouling by using electrochemical properties rather than the physical properties of the foulant. **Table 3-2** shows previous ECM application studies for MD in the current literature. There are two purposes: fouling and wetting control and detection.

3.3.2.1.1. Fouling and wetting control

Most of the ECM applications for MD fouling and wetting control were carried out through coating modification of electrically conductive materials on the existing hydrophobic polymer membrane. The most

commonly used MD base membranes are made of polypropylene (PP), polytetrafluoroethylene (PTFE), and polyvinylidene fluoride (PVDF). Most of the modification materials used were carbon-based materials such as CNT and graphene, are typical materials to increase both hydrophobicity and electrical conductivity of the membrane surface. A flat-sheet membrane in a direct contact membrane distillation (DCMD) configuration is the most widely studies for ECM application in MD.

Research on ECM for MD application is still in its infancy, and the level of technology is still far from maturing, so most of the studies are on simple feasibility evaluation. In many studies, performance evaluation was conducted by applying carbon-based material, which is the most basic material, to the most basic type and configuration of the process. In some cases, hydrophilic materials such as polyvinyl alcohol (PVA) and PANI were used with carbon-based materials. Hydrophilic layer (PVA or PANI/CNT) on hydrophobic MD membrane surface could lower the risk of fouling, especially for inorganic substances, due to its tightly-bound water layer at the water/layer interface (Rao et al., 2020). Due to this difference, in the case of ECM using only single carbon-based material, the direct contact angle (DCA), which is a hydrophobicity indicator, is increased before and after modification, and

in the case of PVA or PANI, the DCA value is decreased due to the hydrophilic layer of the ECM surface (**Fig. 3-6**).

In the case of foulant, various types were used, from basic organic substances (HA), surfactant (SDS), and inorganic foulant ($CaCO_3$, $CaSO_4$) to hexadecane, actual lake water, and geothermal brine. MD fouling and wetting control by ECM application could be achieved through electrostatic interactions, among them the repulsive force between the ECM surface and the foulant. When a cathodic potential is applied to the ECM, the ECM surface becomes negatively charged, and the negatively charged surface blocks or hinders access to the ECM surface while repulsing with organic foulant or surfactant in MD, which is mostly negatively charged. Applying a cathodic potential to the ECM, the ECM surface becomes negatively charged and prevents access of foulant to the ECM surface while repulsing organic foulant or surfactants. In the case of using a repulsion mechanism for ECM fouling control, the molecular weight and size of fouling and wetting inducing matter in MD were relatively small, so it was possible even at the low applied potential. On the other hand, when electrochemical oxidation was used together with repulsion mechanisms for fouling and wetting control, a higher potential range was used **(Table 3-2)**.

3.3.2.1.2. Fouling and wetting detection

In MD, fouling and wetting are one major limitation in its practical application and upscaling, and among them, wetting is even more fatal due to its special mechanism. However, if wetting occurs, performance degradation occurs such as immediate reduction in rejection. However, at the beginning of wetting, the removal rate reduced by the permeated water molecules is very limited in detection by measuring parameters such as electrical conductivity in bulk permeate solution because there are only partially pores with impaired hydrophobicity. By introducing ECM, performance degradation by wetting could be detected faster and earlier in-situ. If wetting occurs and the feed water flows into the permeate channel through the wetted pore, it could be detected immediately through electrochemical impedance monitoring of both channels. Through this, it is possible to immediately respond to the performance degradation during operation.

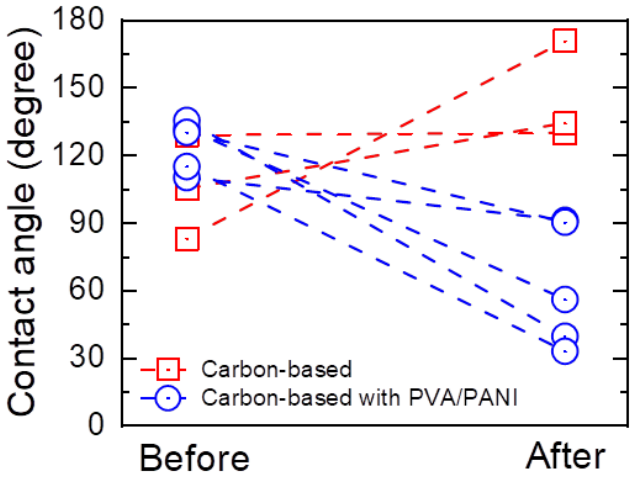

Figure 3-6 DCA change in ECM for MD before and after surface modification according to materials.

Table 3-2 Overview of previous ECM application studies for MD in current literature.

Purpose	Base material[1]	Modification[2]	Membrane type/ configuration[3]	Foulant and wetting inducing matter[4]	Electrical operating conditions	Contact angle[5] (°)	Mechanisms[6]	Reference
Fouling, wetting control	PP	· CNT/PVA thin film coating	Flat sheet / DCMD	· Geothermal brines	· Electrical potential (20 mA, membrane as cathode), 15 V / 3.6 V surface potential	83 / 170	EO	(Tang et al., 2017)
	PTFE	· MWCNT/graphene coating	Flat sheet / VMD	· 20 mg/L HA + 40 g/L NaOH + 3.5% NaCl	· 0.5, 1.0, 1.5 V/cm (electric field)	105 / 135	EI	(Huang et al., 2018)
	Fabrication	· Carbon nanostructures + Silica + PVA or NC with fluorination	Flat sheet / DCMD	· 200 mg/L colloidal silica + 2,000 mg/L NaCl	· Electrochemical impedance spectroscopy (EIS) < 100 Hz	- / 129	EI	(Ahmed et al., 2018)
	PTFE	· CNT + PVA coating	Flat sheet / DCMD	· Xuanwu Lake water	· 1.2 V (repulsion), 30 V (joule heating)	132 / 56	EI	(Jiang et al., 2019)
	PP	· CNT + PVA coating	Flat sheet / DCMD	· $CaSO_4$, silicate	· 0, 1, 2V / 1, 10 Hz	135.5 / 39.7	EI	(Rao et al., 2020)
	PVDF	· MWCNT + PVA coating	Flat sheet / DCMD	· 500, 1000, 2000 mg/L Hexadecane emulsion + 5g/L NaCl	1, 3 V	115/ 33	EI	(Han et al., 2021)
	PTFE	· Graphene coating	Flat sheet / DCMD	· 1000 mg/L Hexadecance + 200 mg/L SDS + 10 g/L NaCl	· 2, 10, 17, 23, 30 mA/cm^2 of Current density	130 / 90	EO, EI	(Jiang et al., 2021)
	PTFE	· CNT/PVA coating	Flat sheet / DCMD	· 2-chlorophenol	· 1, 2, 2.5, 3, 3.5 V	135 / 22	EO	(Lou et al., 2022)
Fouling, wetting detection	PVDF-HFP	· Heat pressing on Carbon cloth	Flat sheet / DCMD	· Tap water + table salt 20,000 mg/L	· 1 V	129 / 130	EI	(Ahmed et al., 2017)
	Fabrication	· PP support + PVDF + DMF + PANI + PVDF and PTFE layer	Flat sheet / DCMD	· 0.1 ~ 0.65 mM SDS	· 100 kHz	110 / 155	EI	(Deka et al., 2021)

[1] PP: Polypropylene; PTFE: Polytetrafluoroethylene; PVDF: Polyvinylidene fluoride; HFP: Hexafluoropropylene
[2] CNT: Carbon nanotube; PVA: Polyvinyl alcohol; MWCNT: Multi-wall carbon nanotube; PANI: Polyaniline; NC: Networked cellulose; DMF: Dimethylformamide
[3] DCMD: Direct contact membrane distillation; VMD: Vacuum membrane distillation
[4] HA: Humic acid; SDS: Sodium dodecyl sulfate
[5] These values are direct contact angle values of membrane before and after modification, respectively
[6] EO: Electrochemical oxidation and reduction; EI: Electrostatic interaction

3.3.2.2. Gas production process (MC)

The membrane contactor (MC) process is one of the membrane technologies for gas transfer between liquid and gas phases. MC processes aim to increase the contact area between the liquid-gas phases and improve the efficiency of gas diffusion. Especially, the MC process is commonly used in the environmental engineering process such as carbon capture and storage (CCS), ultra-pure water (UPW) and wastewater treatment processes (S. Lee et al., 2022). In the MC process, the gas phase carries target gas rapidly, so the pore of the membrane must be maintained in the dried condition. Thus, a challenge to developing an efficient process is controlling the pore wetting phenomenon (Mosadegh-Sedghi et al., 2014; Y. Xu et al., 2019). Because hydrophobicity of the membrane is a significant characteristic of improving the gas transfer performance, similar with MD, the materials of the membrane generally used are PVDF, PP, and PTFE (S. Kim et al., 2021). Further, fouling is also a critical phenomenon that decreases the robustness of the membrane (Velasco et al., 2021; Y. Xu et al., 2019). MC using a conventional polymer-based membrane is greatly affected by the feed water quality. Therefore, a study on the long-term MC operation attracts attention. To address this issue, ECM technology could provide the solution using its electrical characteristics. Additionally,

novel application processes for water decontamination are also developed via surface-modified membrane with applied electricity (Chen et al., 2017; Dagan-Jaldety et al., 2020; K. Li et al., 2019; K. Li et al., 2020; X. Li et al., 2020). Hence, ECM application in the MC process could allow performance improvement and utilization in fouling and wetting control and water decontamination.

3.3.2.2.1. Fouling and wetting control

In ECM, surface modification is the usual approach to improve the membrane resistance to pore wetting and fouling. Surface modification increases the contact angle and repulsive force to the organic matter, which are associated with the membrane zeta potential. This provides a significant advantage utilizing its own membrane surface potential in the MC process even without applied electricity.

To control the pore wetting phenomenon, the concept of breakthrough pressure (or termed as liquid entry pressure in MD) is employed, which could be calculated by using the membrane characteristics such as surface tension, contact angle, and the largest membrane pore size (Y. Xu et al., 2019). The value of breakthrough pressure is shown in **Eq. (3-13)** (Lu et al., 2008). The actual operation of the MC process affected by

the pore wetting is classified as non-wetting, partial-wetting, and overall wetting. If the operating pressure exceeds the breakthrough pressure, the pore is filled with water thoroughly, resulting in critical performance degradation (S. Lee et al., 2022). Therefore, maintaining the non-wetting condition is significantly necessary to obtain sustainable MC operation without performance degradation.

$$\Delta P_{breakthrough} = \frac{4\beta\gamma cos\theta}{d_p} \quad \textbf{(3-13)}$$

Where $\Delta P_{breakthrough}$ is the breakthrough pressure, β is the geometric factor, γ is the surface tension of the membrane, θ is the contact angle of the membrane, and d_p is the largest pore size of the membrane.

The electrical properties of the ECM such as zeta potential could affect the membrane hydrophobicity positively, by increasing the contact angle (Donaldson Jr et al., 2015; Kang, 2002; Tabassian et al., 2016). The zeta potential of water molecules is dependent on the pH value, but in most cases have a negative charge. Hence, controlling the surface potential of ECM could improve the hydrophobicity to repulse the water molecules, and obtain a high breakthrough pressure. It could maintain the condition

of ECM pores as a non-wetting condition and derives the increase of gas transfer performance.

In surface modification result of ECM, it shows that the increment rate of contact angle was high in the order: carbon-based > F-based/Si-based > surface modifying macromolecule (SMM) (**Fig. 3-7**). To determine the impact on wetting phenomenon only, all studies were reviewed on gas absorption and desorption processes from water without any foulants. A carbon-based surface-modified membrane obtained beneficial zeta potential and good structural advantage of the membrane surface. Carbon-based material has increased the membrane surface roughness, which in turn improved the membrane surface hydrophobicity, towards an omniphobic surface property (Wu et al., 2016). Further, the filler materials do not only carry electrical properties, but carbon-based surface modification materials such as CNT and graphene have innate hydrophobic characteristics as well. Si-based and F-based materials such as montmorillonite (MMT), zeolite, and hexafluoropropylene (HFP), when blended in a membrane, produces a typical asymmetric finger-like structure. These materials could increase the membrane surface roughness and electrical properties, but the increase was generally lower compared with carbon-based material (DashtArzhandi et al., 2015; Rezaei-DashtArzhandi et al., 2016; Rezaei et al., 2014; Zhang et al.,

2011). SMM on the other hand as been known as a material used for the most classical surface modification to obtain the asymmetric finger-like structure on the membrane. However, even though previous studies reported successful fabrication of finger-like structure, SMMs were not able to produce dramatical enhancement in hydrophobicity due to its typical characteristics compared to other filler materials (Bakeri, Ismail, et al., 2012; Bakeri, Matsuura, et al., 2012; Korminouri et al., 2014; Mansourizadeh et al., 2014; Rahbari-Sisakht et al., 2012a, 2012b; Rahbari-Sisakht et al., 2013).

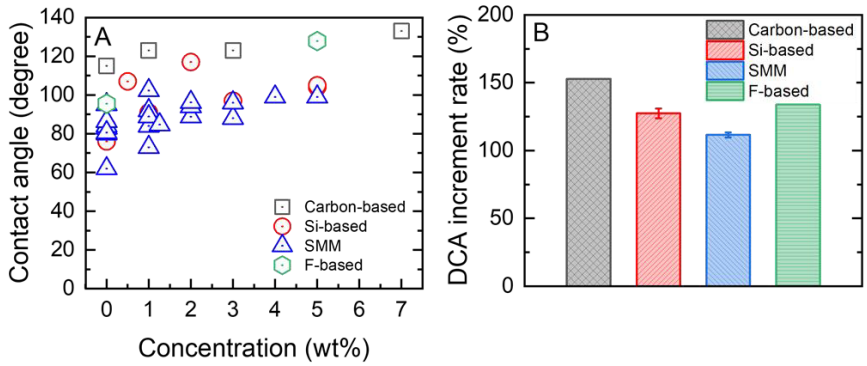

Figure 3-7 Results of surface modification in MC process according to the modifying materials: (A) Contact angle of surface modification before and after, (B) Contact angle increment rate ***(Bakeri, Ismail, et al., 2012; Bakeri, Matsuura, et al., 2012; DashtArzhandi et al., 2015; Korminouri et al., 2014; Mansourizadeh et al., 2014; Rahbari-Sisakht et al., 2012a, 2012b; Rahbari-Sisakht et al., 2013; Rezaei-DashtArzhandi et al., 2016; Rezaei et al., 2014; Wu et al., 2016; Zhang et al., 2011).***

Generally, surface modification method could potentially increase the roughness of the membrane surface and enhance hydrophobicity through its electrical property. Carbon-based modifying materials obtained the highest contact angle increment rate, significantly superior to the commonly used SMM. In conclusion, the introduction of ECM technology could solve the pore wetting phenomenon, which is a conventional challenge of the MC process.

Because the foulant interrupts the gas transfer through the membrane, the performance of the MC process is greatly affected by fouling. In particular, this is a significant problem in the CCS process, where the influent contains high organic concentration compared to other MC applications. In the CCS process, the liquid phase generally contains organic foulant such as amine-based material. The amine-based solution is a well-known absorbent of the carbon dioxide chemisorption process. Typically, monoethanolamine (MEA), diethanolamine (DEA), triethanolamine (TEA), and 2-amino-2-methyl-1-propanol (AMP) are commercialized in the CCS plant (El Hadri et al., 2017; Samanta et al., 2012). Further, those absorbents presented a high corrosion rate and low surface tension that can affect the membrane surface critically (Aguila-Hernández et al., 2001; Bernhardsen & Knuutila, 2017; El Hadri et al., 2017; Gunasekaran et al., 2013; Huang & Peng, 2017; Lampreia et al.,

2007; Vázquez et al., 1997; Vázquez et al., 1996; Veawab et al., 1999). Hence, those amines can lead to membrane degradation and absorbent fouling in the CCS process, so it is necessary to develop an anti-fouling strategy (Khaisri et al., 2011).

The ECM could prevent membrane degradation and absorbent fouling by electrical repulsion. In the membrane system, it is able to repulse the organic matter by the membrane's own zeta potential (Kim, Yun, et al., 2022; Tanudjaja & Chew, 2018). The DLVO theory presents the total interaction energy, which is combined with the LW and EL forces, and LW and EL forces represent the attraction and repulsion forces between the membrane and organic matter (Brant & Childress, 2002). The DLVO theory expresses the dominant force between organic matter and membrane. Those interaction forces are deeply associated with the zeta potentials of the membrane and organic matter. Hence, the performance of anti-fouling varies depending on the properties of the material for surface modification.

Fig. 3-8 presents some results from literature for the long-term operation of ECM membrane contactor with various modifying or filler materials. From the figure, it shows that better performance was observed for Si-based/Ti-based/carbon-based compared to Zr-based

surface-modified membrane. These ECMs maintained the flux, which dramatically increased the stable operating time. Si-based materials were classified as silica nanoparticles, fSiO_2, and silica aerogel (Amirabedi et al., 2019; Lin et al., 2013; Zhang & Wang, 2013). It showed that Si-based materials excluding silica aerogel maintained less than 10% decline in flux during 10 days of operation. Further, substrates such as PP, polyetherimide (PEI), and Al_2O_3 could affect the anti-fouling performance. The polymer-based substrate significantly increased the anti-fouling ability through the surface modification compared to the ceramic-based substrate. Ti-based and carbon-based surface-modified membranes also prevented fouling and maintained the flux at least 95% from its initial value (Lin et al., 2018; Talavari et al., 2020). Zr-based surface-modified membrane presented the flux retention during 3 days, but gradually decreased after that (Yu et al., 2015). Zr-based material could not significantly improve the electrical properties to provide electrical repulsion.

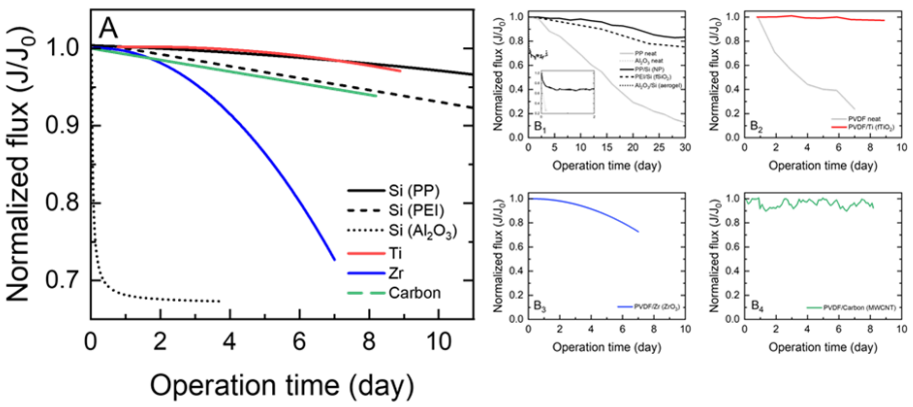

Figure 3-8 Long-term operation performance of ECM membrane contactor according to modifying materials: (A) Comparison of all modifying materials, (B_1) Si-based, (B_2) Ti-based, (B_3) Zr-based, and (B_4) carbon-based *(Amirabedi et al., 2019; Lin et al., 2018; Lin et al., 2013; Talavari et al., 2020; Yu et al., 2015; Zhang & Wang, 2013)*.

Therefore, the ECM can maintain performance during long-term operation by its electrical properties. Si-based, Ti-based, and carbon-based surface-modified membranes show the best performance to resist organic fouling in long-term operation. The surface modification allows the MC process to be applied in various fields without the classical maintainability issue of the membrane.

3.3.2.2.2 Water decontamination

Recently, electrochemical reactions have been applied in the MC process with ECM for various purposes. The electrochemical reaction in those novel MC processes is classified as electrochemical oxidation and

reduction. The electrochemical reaction on the membrane surface increases the performance of oxidation and reduction rather than the conventional processes of organic degradation and nitrate reduction. The MC for organic oxidation was applied to inject the ozone which is a well-known oxidant for organic degradation. The ECM in ozonation produces an electrocatalytic reduction of dissolved oxygen to H_2O_2, achieving the peroxone (O_3/H_2O_2) process that is a superior oxidation performance compared to a single ozonation without any chemical dosing. Further, ECM can alternate the existing nitrate reduction process which is dependent on anaerobic bacteria. The ECM can simplify the multi-step structure of the total nitrate reduction process, and it can reduce the energy consumption for bacterial culture and activation. Therefore, the ECM for MC is a promising technology to substitute for the conventional MC processes.

Electrochemical oxidation plays a significant role in the water treatment field to prevent membrane fouling. The application of ECM for MC could improve organic treatment performance rather than other oxidation processes such as conventional advanced oxidation processes (AOP). (Miklos et al., 2018). To decompose the organic matter, the MC process is applied to inject an ozone gas known as an oxidant (Atchariyawut et al., 2009; Bamperng et al., 2010; Jansen et al., 2005;

Miklos et al., 2018; Phattaranawik et al., 2005; Schmitt et al., 2020). Because the MC dramatically increases the contact area between gas and liquid, the ozonation process using MC has a higher organic degradation efficiency than conventional ozonation (Miklos et al., 2018). Because the ECM induces the electrocatalytic reduction to generate the H_2O_2 from dissolved oxygen, the ECM application for ozonation improves the organic degradation performance comparing to single ozonation. Further, electrical repulsion and nanobubble generation on the ECM surface could prevent membrane contamination, so it is more advantageous for sustained performance over a simple MC process.

Further, the electrochemical reaction can produce more oxidative species such as •OH. The MC process with electricity supply improves the organic degradation performance (K. Li et al., 2019; K. Li et al., 2020; X. Li et al., 2020). The surface-modified ECM could be used as the electrode in the MC module. Because the cathode membrane supplying the electricity converts the dissolved oxygen to ozone and activates the radical generation, oxidation performance can be significantly achieved higher than the single electrochemical oxidation (EO) process and ozonation using the MC process, as shown in **Eqs. (3-14) to (3-21).**

$$O_2 + 2H^+ + 2e^- \rightarrow H_2O_2 \quad \textbf{(3-14)}$$

$$H_2O_2 \rightarrow H^+ + HO_2^- \quad \textbf{(3-15)}$$

$$HO_2^- + O_3 \rightarrow HO_2 \cdot + O_3^- \cdot \quad \textbf{(3-16)}$$

$$HO_2 \cdot \leftrightarrow \cdot O_2^- + H^+ \quad \textbf{(3-17)}$$

$$\cdot O_2^- + O_3 \rightarrow O_2 + O_3^- \cdot \quad \textbf{(3-18)}$$

$$O_3^- \cdot + H^+ \leftrightarrow HO_3 \cdot \quad \textbf{(3-19)}$$

$$HO_3 \cdot \rightarrow \cdot OH + O_2 \quad \textbf{(3-20)}$$

$$O_3 + OH^- \rightarrow HO_2^- + O_2 \quad \textbf{(3-21)}$$

The MC process using ECM for ozonation presents the highest organic degradation performance, as shown in **Fig. 3-9**. It compared the performance of organic degradation processes such as EO, membrane contactor ozonation (MCO), and electrically conductive membrane contactor ozonation (ECMCO). Ibuprofen (IBU) and nitrobenzene (NB) are reported as the harmful pollutants detected in the surface water, groundwater, wastewater, and other environmental media (Guo et al., 2017; Xie et al., 2018; Q.-Q. Zhang et al., 2015). IBU and NB are typically organic matters that are hard to decompose by the conventional oxidation process due to their minute size and electron-withdrawing

group, respectively (Qiao et al., 2021; Q.-Q. Zhang et al., 2015). Because the •OH production rate of ECMCO is the highest among those oxidation processes, it can decompose more of those pollutants. The ECMCO process provides •OH from the dissolved ozone or oxygen to break the IBU structure, so it achieves the decomposition of almost IBU within 5 minutes. Thus, the ECMCO process improves IBU degradation performance at least twice as conventional processes such as EO and MCO. Likewise, the ECMCO process shows superior performance for NB degradation compared to others. NB is hard to decompose than IBU due to its nitro group. Accordingly, it needs to proceed much operating time to remove (Qiao et al., 2021). The EO and MCO achieved removal rates corresponding to 26.5% and 35.6%, while ECMCO removed 82.7% of NB in wastewater.

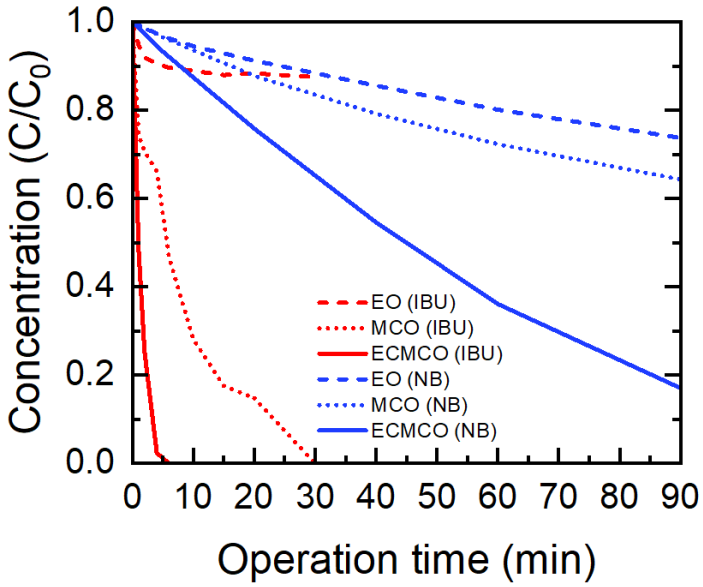

Figure 3-9 Performance of electrically conductive MC process for organic matters degradation (e.g., ibuprofen degradation by carbon fiber modified membrane and nitrobenzene degradation by TiO_2 nanoflower modified membrane) ***(K. Li et al., 2020; X. Li et al., 2020)***

Thus, the electrochemical MC could dramatically improve the organic foulant degradation performance. The ECM for foulant degradation can make the peroxone process without any chemical dosing and improves the degradation performance over the simple MC ozonation. Also, it can be predicted that the electrochemical MC process can maintain the organic degradation performance in long-term operation. Because the conductive cathode membrane surface repulses the organic matter, it

could be concluded that the electrochemical MC process could effectively mitigate membrane fouling.

In the wastewater treatment field, MC can remove or recover ammonia from denitrification. The nitrate concentration in the wastewater needs to be reduced for preventing eutrophication, and anammox process is commonly used despite the high energy consumption (Davey et al., 2022). Recently, ammonia, which can be obtained from wastewater, is noteworthy alternative energy source to the conventional energy source, so the ammonia stripping process by using MC not only reduces the energy consumption of the overall nitrate removal process but also generates renewable energy source (Kinidi et al., 2018; Morlanés et al., 2021; Zhang et al., 2012).

However, MC application for wastewater treatment is limited due to severe membrane fouling issues. The ECM for the MC process is potentially the most feasible strategy to remove nitrate and generate ammonia from wastewater without membrane fouling. The electrochemical reaction could lead to the nitrate reduction into ammonia so that it could remove the nitrate concentration (**Eq. (3-22)**) (Duca & Koper, 2012; M. Sun et al., 2021; Wu et al., 2021). Further, organic

repulsion and oxidation also occur, enabling stable use for wastewater treatment as described in the following equation:.

$$NO_3^- + 9H^+ + 8e^- \rightarrow NH_3 + 3H_2O \quad \textbf{(3-22)}$$

Table 3-3 shows the electrochemical MC processes in literature for nitrate reduction, and these studies achieved nitrate removal and ammonia synthesis. Electrochemical nitrate reduction rapidly produces nitrogen and ammonia to improve the nitrate removal time compared to the anammox process which is based on anaerobic bacteria. The low performance and high energy consumption due to slow bacterial growth time, bacterial activation, and multi-step structure of the anammox process can be improved through the ECM. The electrocatalytic reduction from the ECM surface has superior response and stability over the bacterial anaerobic digestion, and requires no energy to maintain the bacterial growth condition. In addition, the ammonia and nitrogen gases from nitrate reduction are immediately degassed from the water, so it is not necessary to apply an additional stripping process. In order to improve the electrochemical MC process in nitrate reduction, the membrane surface is usually modified with carbon-based materials. A membrane that has good hydrophobicity such as a carbon-based surface-

modified membrane is advantageous in the nitrate reduction process. Further, the carbon-based surface-modified membrane is a distinguished electrocatalytic reduction material due to its good electron conductivity incorporated with the chemical inertness, and it increases the nitrate removal efficiency. Finally, the converted ammonia is stripped from the liquid phase due to the ammonia partial pressure difference from the gas phase, and it could be used as a renewable energy source.

Table 3-3 Overview of previous ECM application studies of MC for nitrate reduction in current literature.

Base material	Modification material	Gas	Voltage (V)	Purpose	Reference
PP membrane	MWCNT	H_2, O_2	n/a	Nitrate removal, Ammonia synthesis	(Dagan-Jaldety et al., 2020)
Nafion membrane	Carbon paper	N_2	-2 ~ -1	Ammonia synthesis	(Chen et al., 2017)

In conclusion, the electrochemical MC process for nitrate reduction can obtain various benefits. While combining the anammox and ammonia stripping process, it redeems the challenges of the conventional nitrate removal process such as energy consumption. Also, it can generate ammonia which is well-known as a renewable energy source without membrane contamination.

3.4. ECM operation characteristics according application

ECM has been applied and studied in the hydrophilic membrane processes (MF, UF, NF, RO, and FO) and hydrophobic membrane processes (MD, MC). The basic purpose of ECM application is to control fouling. However, the electrical operating conditions and modification materials used vary slightly depending on the characteristics and purpose of each application process. Through an accurate understanding of each characteristic of the process and ECM, it is possible to improve performance and expand the field of application by customizing the ECM to the characteristics of feed water composition and process characteristics.

3.4.1. Electrical operating conditions

Fig. 3-10A shows the applied voltage range used for each process. MF/UF showed the highest applied voltage, followed by NF/RO, FO, MD, and MC. Since MF/UF mainly targets water with a high organic foulant content, a relatively high range of applied voltage is required for fouling control. Both cathodic and anodic potentials were in the high range, and the anodic potentials showed relatively higher values. This is attributed to the fact that it is more advantageous from the viewpoint of

the applied voltage to perform fouling control through electrostatic repulsion at cathodic potential rather than the fouling control effect obtained by oxidizing the entire organic matter at the anodic potential due to high concentration of organic matter.

In addition, the use of a high voltage range in MF/UF is also attributed to microbubble by electrolysis. Because MF/UF are a pressure-driven process within dead end filtration mode, the mechanical strength of the fouling layer is relatively high compared to other processes. The self-cleaning effect by microbubble is also relatively insignificant. To compensate this, the required applied voltage value is high for fouling control by microbubbles. However, this high applied voltage results in high energy consumption. Recently, in order to reduce energy consumption, research is also underway on intermittent operation, which does not apply electricity at all times during ECM operation, but finds and operates optimal operation points to the extent that fouling does not occur while applying electricity to the interval.

In the case of NF/RO, the applied voltage range was relatively low despite the similar pressure-driven process as MF/UF. This is because the NF/RO in ECM has a different utilization for a specific purpose. Both electrically conductive NF/RO membranes were used in desalination. NF was focused on removal enhancement for monovalent ions without any

decrease of water permeability or controlling biofouling within relatively low applied potentials. On the other hand, the active layer of RO membranes has a vulnerable characteristic to chlorine. The electrochemical reduction was implemented to deal with chlorine disinfectant. Further self-cleaning was conducted in the RO membrane. Unlike MF/UF, a relatively low concentration of organics was in the feed solution, and due to high concentration of electrolyte could remain stable current during the self-cleaning process, leading to effective fouling control operation even in a low applied voltage range.

Because of the unique features of FO as a non-pressurized process, the tendency of irreversible fouling is relatively lower than in other membrane processes. Even if the concentration of organics is quite high (200~2,000 ppm) with the presence of calcium ion, which causes the formation of calcium-organic bridging fouling, the fouling layer was effectively removed by applying relatively low voltages. However, if the organics were not completely oxidized in anodic potential, the foulant would be deposited on the non-porous FO membrane surface due to electrostatic attraction between organics and ECM and could subsequently cause water flux decline.

On the other hand, MD and MC using hydrophobic membrane showed a very low applied voltage range. The key to MD fouling control is

micro-organic pollutants and surfactants, which are substances that damage the hydrophobicity of the membrane due to the characteristics of the process, and electrostatic interaction was employed for this purpose. In the case of micro-organic pollutants and surfactants, since their molecular weight and size are small, fouling control is possible even with the interaction in the electric field generated with a relatively low applied voltage range.

In the case of MC, the applied voltage is similar to MD. Because the MC also uses a hydrophobic membrane and the foulant also has a small molecular weight and size similar to MD, it was possible to control fouling and wetting through effective ECM operation even at a small applied voltage. In the case of using the electrochemical oxidation mechanism for water decontamination, an effective oxidation reaction could be achieved even at a lower applied voltage condition by assisting oxidant generation through gas injection (O_2, O_3).

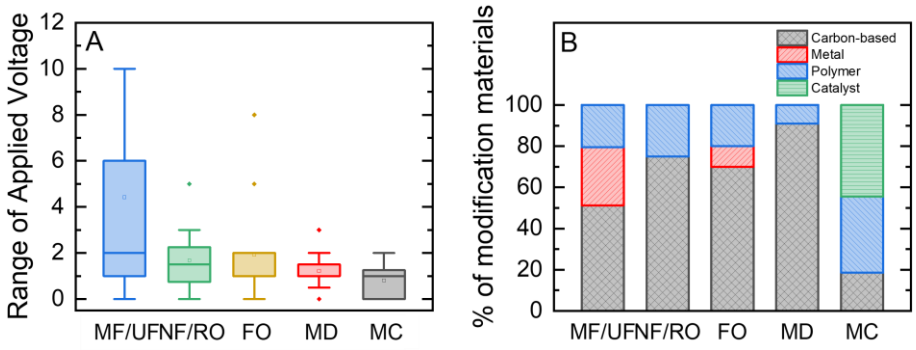

Figure 3-10 ECM operation parameters and characteristics according to the application processes; (A: range of applied voltage, B: the fraction of modification materials).

3.4.2. Modification materials

Since materials that can be used for ECM modification are basically used to increase the electrical conductivity of the membrane, carbon-based materials, metal, electrically conductive polymers, and electro-catalysts with high electrical conductivity are used for each process (**Fig. 3-10B**).

In MF/UF, the ECM uses a variety of the most basic forms of carbon-based materials, metal, and electrically conductive polymers, as it simply aims to increase electrical conductivity. Rather than customized modification for specific target foulant, most of the fouling control methods were based on electrochemical oxidation and electrostatic repulsion in bulk solution. NF/RO and FO also showed no significant

difference in trend with MF/UF, except for the use of metal. Unlike MF/UF, which focused on fouling control in bulk solution, the concentration of the foulant in the feed water and fouling potential are relatively low in ECM for FO, so the electrochemical reaction from the microscopic point of view of the foulant itself is more important. Therefore, carbon-based materials and conductive polymers, which could slightly increase the reactivity of oxidation rather than simple metal and are easy to control ECM surface charge, were mainly used. In addition, since it is difficult to control the pore size of metal, it is limited in its application to modification of the non-porous membrane process.

On the other hand, MD and MC using hydrophobic membrane showed a different trend from the previous cases. MD was found to be more than 90% of the modification of carbon-based materials to protect and increase the hydrophobicity of the membrane directly related to performance. Carbon-based materials not only can achieve the best increase in hydrophobicity, but also can prevent damage to the hydrophobicity of the membrane by acting as a protective layer instead of the base membrane materials even when there is direct contact with the foulant in harsh conditions.

In the MC process, conductive polymers and electro-catalysts accounted for most. Unlike MD, wetting by water molecules during

long-term operation is the most important obstacle for MC application in the actual process. Conductive polymers for wetting control were the most widely used, most of which were SMMs due to their ease of modification. In the case of MC for water decontamination by electrochemical oxidation and reduction, increasing the reactivity of the gas injection is a key factor in improving process efficiency. The application of electro-catalyst to increase reactivity has been studied a lot. As a result, the conductive polymer was used most frequently to increase hydrophobicity and electro-catalyst for water decontamination, respectively.

3.4.3. ECM fouling control efficiency

The previous section focused on the mechanism and qualitative analysis of ECM for fouling control. In this section, quantitative analysis was performed for a more accurate analysis of ECM fouling control efficiency. The factors that had the most significant influence on ECM fouling control efficiency were the applied voltage representing electrical phenomena and energy consumption and the foulant concentration representing the fouling potential of feed water, respectively. If the applied voltage is increased, the performance could be improved from the fouling control point of view, but it is accompanied

by the disadvantage of increasing additional energy consumption. In addition, since this fouling control performance is directly affected by the foulant concentration, both parameters should be considered in combination for an accurate analysis of the ECM fouling control efficiency.

3.4.3.1. ECM fouling control efficiency according to the application process

In order to quantitatively evaluate ECM fouling control efficiency, flux decline rate (FDR), a parameter for the degree of fouling, was employed. FDR is a value that quantifies the degree of flux reduction over time, and the effect of performance degradation due to fouling can be evaluated (J. Kim et al., 2019; Wang et al., 2007). FDR value is defined by **Eq. (3-23)**.

$$FDR = -\frac{1}{J_0^2} tan\,\theta \,|t = 0 = -\frac{1}{J_0^2}\frac{dJ}{dt}|t \qquad \textbf{(3-23)}$$

Where J_0 and J are the initial flux ($Lm^{-2}h^{-1}$) and the flux at time t, respectively, $\tan\theta\big|_{t=0}$ is the slope of the flux behavior at t = 0, and t is

the operation time (h). The decline rate of FDR is proportional to the efficiency of fouling control due to ECM. In addition, since the additional energy required for ECM operation is proportional to the applied voltage, a performance indicator parameter, the specific FDR decline rate, was introduced and calculated by dividing the FDR decline rate by the applied voltage value to evaluate the efficiency in terms of energy. As a result, the specific FDR decline rate is a parameter that can directly show how effectively the performance degradation of the membrane process due to fouling was mitigated from the ECM energy consumption point of view. The analysis of foulant concentration and specific FDR decline rate was performed for current ECM cases applied for fouling control **(Fig. 3-11)**.

Hydrophilic porous membrane processes (MF, UF) had the highest number of application cases compared to other processes. As the foulant concentration increased, the specific FDR decline rate decreased. This is because, as the foulant concentration increases, the fouling potential of the feed water increases, so a more considerable amount of energy is required to control it. Since the MF and UF processes target feedwater with a relatively high fouling potential compared to other membrane processes, foulant loading is extensive. However, it could be compensated by increasing the applied voltage. It showed stable

efficiency in all foulant concentration ranges at high applied voltage conditions.

For hydrophilic non-porous membrane processes (NF, RO, and FO), the number of NF and RO cases was minimal, and most were FO application cases. Employing ECM for NF and RO would be challenging performance (water flux and salt rejection), unlike the process using a porous membrane (M. Sun et al., 2021). Additionally, there is an issue of stability of modification materials under pressure conditions. Unlike the conventional pressure-driven membrane process, since the FO process uses only osmotic pressure as a driving force, the hydraulic flow direction inside the module is different, so performance reduction due to ECM is low, and the stability of modification materials could be easily secured. As a result, the hydrophilic non-porous membrane processes did not show a significant relationship between the foulant concentration and the specific FDR decline rate. It could be postulated that other parameter values are more critical than the foulant concentration.

On the other hand, in the case of the hydrophobic membrane processes (MD, MC), the tendency to decrease the specific FDR decline rate was intensified according to the increase in the foulant concentration. This is due to the specific rejection mechanism of hydrophobic membrane processes. In the MD and MC, an essential premise for effective process

operation is the maintenance of the hydrophobicity of the membrane. If the hydrophobicity of even some membrane pores is deteriorated by fouling and wetting, very immediate performance degradation occurs, unlike the hydrophilic membrane process. Therefore, the sensitivity to the foulant concentration is higher.

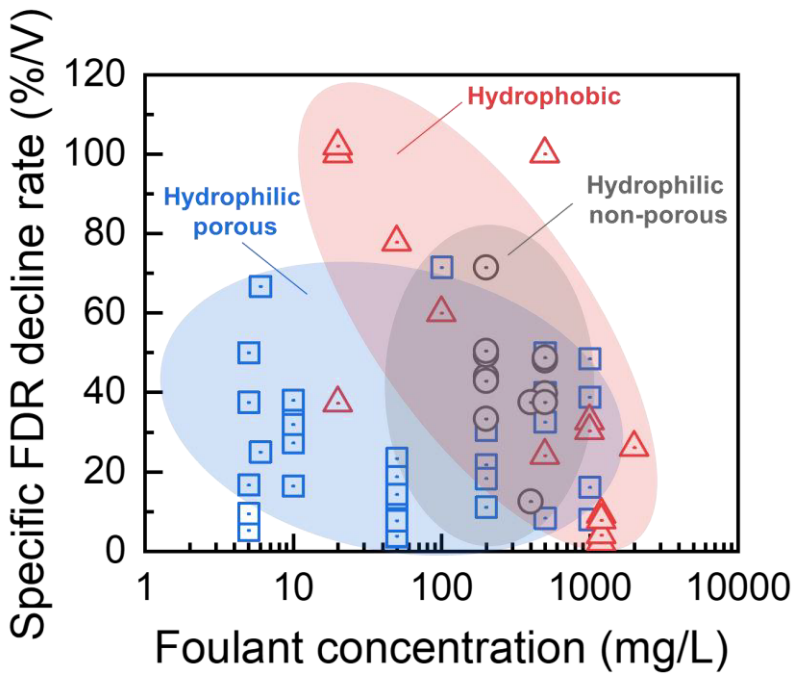

Figure 3-11 Specific FDR decline rate according to foulant concentration and application process.

3.4.3.2. Factors affecting ECM fouling control efficiency

For a more detailed and accurate quantitative analysis, the relationship between foulant concentration, applied voltage, and FDR decline rate,

which are the factors that have the most significant influence on ECM fouling control efficiency, were analyzed through multiple linear regression **(Fig. 3-12).**

In the hydrophilic porous membrane process, the FDR decline rate was inversely proportional to the foulant concentration and proportional to the applied voltage, respectively. This is consistent with the previous analysis of the specific FDR decline rate, and it is attributed that the ECM fouling control efficiency is lowered because the fouling potential of the feed water increases as the concentration of foulant increases. However, this could be overcome by increasing the applied voltage. In order to mitigate fouling in high foulant concentration conditions, it requires high energy consumption. In the applied voltage range of about 10 V or more, the FDR decline rate was about 75% or more, enabling sustainable operation of the process. Although it was possible to control a high concentration of foulant at a high applied voltage, the reduction of energy consumption through optimization of operating conditions still remains a task to be solved to increase the applicability of ECM.

On the other hand, in the case of the hydrophilic non-porous membrane process, the FDR decline rate was proportional to both the foulant concentration and the applied voltage. However, the degree of proportionality of the foulant concentration was not significant. This is

attributed to the fact that when the foulant concentration is low, the initial FDR value is very low because of the low fouling tendency of the FO process, which accounts for most of the hydrophilic non-porous membrane process cases. When the foulant concentration is high, the FDR value is increased due to the high fouling potential. However, a 100% FDR decline rate was possible through ECM in both conditions. As a result, fouling control was possible through ECM in all ranges regardless of foulant concentration. The fouling control could be achieved in a relatively very low applied voltage range (< 2V). In the applied voltage range of 2V or less, all showed an FDR decline rate of 75% or more, and effective fouling control was possible. This is because the FDR decline rate through the application of ECM was very high because the irreversibility and density of the fouling layer are low in these cases.

In the case of the hydrophobic membrane process, the FDR decline rate was inversely proportional to the foulant concentration and had no significant relationship with the applied voltage. This is also consistent with the specific FDR decline rate analysis. In the case of high foulant concentration, the hydrophobicity of the membrane is highly likely to be damaged, so it is fatal in the case of MD and MC processes, where even slight damage to the hydrophobicity could cause immediate performance degradation. On the other hand, the applied voltage had no significant

effect on the FDR decline rate. As a result, in the hydrophobic membrane process, effective fouling control could be achieved through ECM even at very low applied voltage conditions, and foulant concentration is a key factor.

As a result, in the hydrophilic porous membrane process and the hydrophilic non-porous membrane process, the applied voltage is a key factor, and it could become even more critical under relatively high and low voltage conditions, respectively. For effective energy consumption reduction, it is essential to study various methods that enable effective fouling control even at low applied voltage. In the case of the hydrophobic membrane process, the foulant concentration is a key factor. For the effective fouling control operation of ECM, a pretreatment process based on an accurate understanding of the feed water properties in view of ECM should be accompanied.

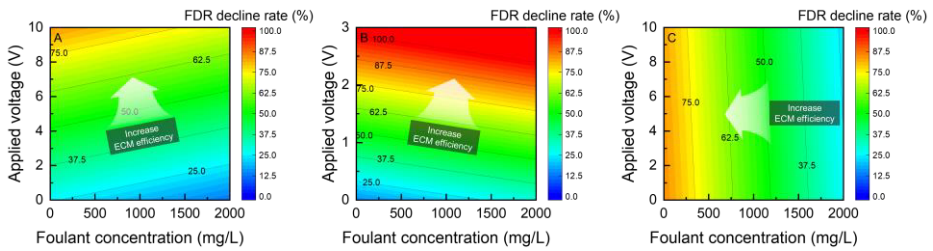

Figure 3-12 Factor analysis of ECM fouling control efficiency (A: hydrophilic porous membrane process, B: hydrophilic non-porous membrane process, and C: hydrophobic membrane process).

3.4.4. Summary

Although the membrane process is currently the most widely used in the water treatment field due to its excellent compactness, low energy consumption, and ease of operation and management, fouling still remains a priority challenge. ECM is emerging as a way to overcome this fouling. Unlike the existing physicochemical-based operation and fouling control in the conventional membrane process, ECM is an electrochemical-based technology, and thus has comparative advantages in control of micro-pollutants and self-cleaning without membrane damage. However, the maturity of the technology is still low, and there is a lack of fundamental understanding and research on critical mechanisms.

In order to increase the applicability of ECM, it is a prerequisite to study the fundamental mechanism used for fouling control. There are three main fouling control mechanisms: electrochemical oxidation and reduction, electrostatic interaction, and microbubble by electrolysis (**Fig. 3-13**). Electrochemical oxidation and reduction are methods of lowering the fouling potential of feed water itself by oxidizing the foulant to decompose or degrade it to a smaller size. Electrostatic interaction is a method to prevent the formation of a fouling layer by inducing electrostatic repulsion between the foulant and the ECM surface using

the surface charge of the foulant or attracting it toward the counter electrode to prevent the foulant from approaching the ECM surface. Finally, microbubble by electrolysis is an indirect fouling control method by hydrogen and oxygen gas bubbles generated by water evolution. By microbubble generation, fouling control could be achieved that the generated microbubble hinders the movement of foulant to the ECM surface. In addition to the fouling control effect, it is possible to self-cleaning the membrane by decomposing and removing the fouling layer already generated on the ECM surface.

In the cases where these mechanisms are applied to the processes (MF/UF, NF/RO, FO) using the hydrophilic membrane among the actual membrane processes. In addition to the basic fouling control, research is being conducted for self-cleaning and increasing the removal rate of metal, dye materials that have a low removal rate in the existing process (MF/UF) by using their surface charge. These fouling control mechanisms also play key roles in NF/RO, and ECM was used in FO to control fouling and increase cleaning efficiency. However, the oxidation ability of ECM should be guaranteed to oxidize foulants to ensure the cleaning efficiency by applying anodic potential, which partially oxidizes organics and causes severe membrane fouling than typical non-porous membrane without any applied potentials. Additionally, it is

being studied to increase ion rejection in NF membrane and chlorine resistance in RO membrane via electrostatic repulsion or electrochemical reduction reaction.

In the case of MD and MC, there is a difference in the application purpose and mechanism of ECM because the hydrophobic membrane is used, unlike the previous processes. In MD, ECM was mainly used for the purpose of fouling mitigation by increasing the hydrophobicity of the membrane. The electrostatic interaction mechanism was used to prevent direct contact with the membrane against substances such as surfactants that could cause wetting, which induces the most significant reduction in performance in MD and MC, which are processes using a hydrophobic membrane. In addition, wetting is challenging to be detected because there is a time gap until performance degradation occurs, but it could be detected more quickly through ECM technology. In the case of MC, ECM is used for two purposes: fouling & wetting control, and water decontamination. For fouling and wetting control, a method of increasing the surface charge value through ECM is mainly applied, and for water decontamination, a method of inducing effective oxidation of foulant by directly generating oxidant through gas injection is used, respectively.

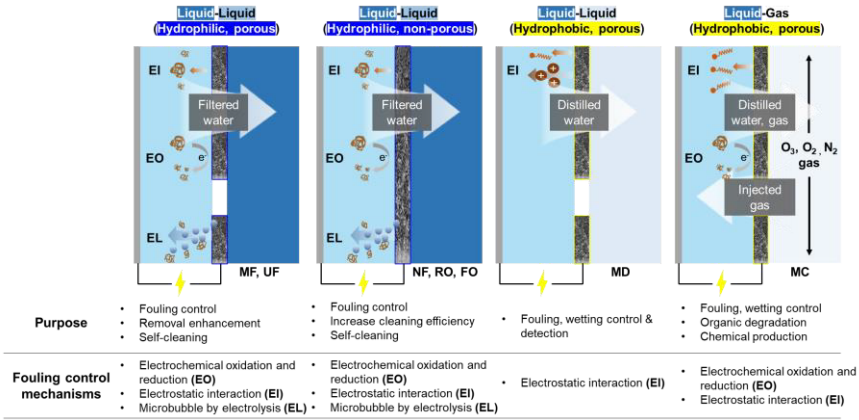

Figure 3-13 The overall summary of ECM application processes: purpose and fouling control mechanisms

3.5. Concluding remarks and future directions

In ECM, a complementary synergistic effect is expected because electrochemical phenomena work together in addition to the physical phenomena based on the conventional membrane process, but the mechanism is very complicated. Therefore, much systematic and fundamental research should be done beyond the simple applicability evaluation study, especially on the mechanism. Based on the review in this paper, future directions to increase the feasibility of ECM technology are suggested as follows: (1) Understanding feedwater composition from an ECM perspective, (2) Selection of appropriate modification materials, and (3) Effective and optimized low energy operation (**Fig. 3-14**).

- **Understanding feedwater composition from an ECM perspective:** In the case of the conventional membrane process, only the physico-chemical properties of the foulant were considered for fouling control. However, since the fouling control mechanism of ECM uses not only the physico-chemical phenomenon but also the electrochemical phenomenon, it is essential to understand the feed water composition from a complex perspective. For each foulant present in the feed water, it is possible to lower the fouling potential of the feed water by determining which mechanism among physical and electrochemical could control (size exclusion, electrochemical oxidation, electrostatic interaction). However, since the feed water composition is very different depending on the application field, the ECM process should be accompanied by the target feed water customized development for the actual application.
- **Selection of appropriate modification materials:** Modification materials have the most excellent effect on efficiency in ECM. The characteristics of the best modification materials are as follows: high electrical conductivity, surface characteristics suitable for the removal mechanism of the application process, and high electrochemical reactivity to target foulants. Energy

consumption could be reduced because the efficiency of the fouling control mechanism increases as the electrical conductivity increases. An increase in flux and rejection can also be expected depending on the removal mechanism of the application process. In addition, in the case of fouling control through electrochemical oxidation and reduction, since the reactivity is higher than that of the conventional polymer membrane, foulant degradation is energy efficient.

- **Effective and optimized low energy operation:** ECM has an advantage in fouling control, but has a disadvantage in that it requires additional energy. In order to overcome this, it is essential to study the optimization of the operation method. The additional energy consumption required for ECM operation is directly proportional to the applied voltage and operation time. Energy consumption could be reduced by optimizing the applied voltage based on an accurate understanding of the target foulant and the electrochemical fouling control mechanism. Additionally, the interval operation method could be a promising option. ECM is based on the constant electrical operation. Energy consumption reduction effect due to a significant reduction in operation time could be achieved by introducing the interval operation based on

flux and rejection behaviors instead of regular operation, which is a typical operation method of ECM.

Consequently, customized research is essential according to the application field in all three future directions to increase the applicability of ECM. Unlike the conventional membrane process, which is advantageous for general application, ECM has advantageous characteristics for specific target customization fields. Through these initiatives, with an accurate understanding and analysis of the fundamental fouling control mechanism, ECM technology could enable purposeful and beneficial applications and further enhance the economic sustainability of the industry.

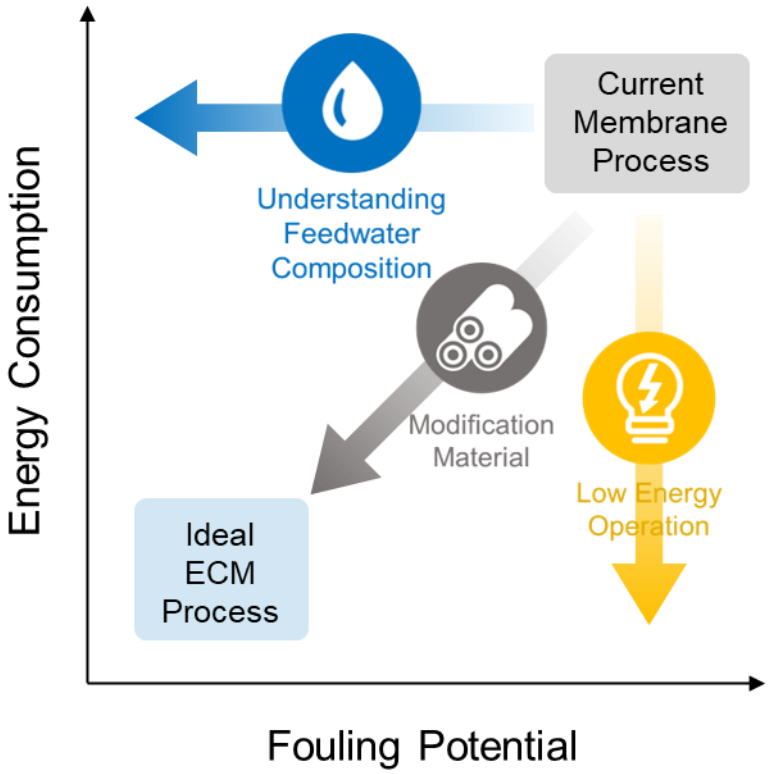

Figure 3-14 Future directions to increase the feasibility of ECM technology: (1) Understanding feedwater composition from an ECM perspective, (2) Selection of appropriate modification materials, and (3) Effective and optimized low energy operation

Chapter 4. Elucidation of physicochemical scaling mechanisms in membrane distillation: Implication to the control of inorganic fouling

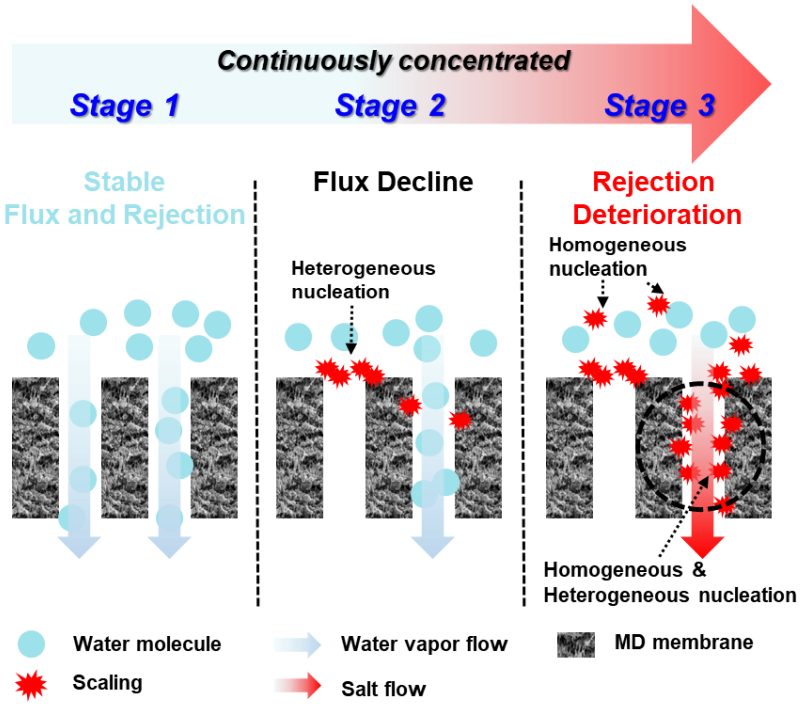

This chapter is based on:
Kim, J., Kim, H.-W., Tijing, L.D., Shon, H.K. and Hong, S. (2022a) Elucidation of physicochemical scaling mechanisms in membrane distillation (MD): Implication to the control of inorganic fouling. Desalination 527, 115573.

4.1. Introduction

MD processes can be operated by utilizing alternative renewable energy sources, such as solar energy (Fuzil et al., 2021; G. S. Kim et al., 2021; Q. Ma et al., 2021). Even though MD has been increasingly studied over the last few years (González et al., 2017), membrane scaling due to the formation of salt crystals and deposition on the membrane surface is still one of the major barriers to its more widespread use (Bush et al., 2016; El-Bourawi et al., 2006; Kim et al., 2018b; Kim et al., 2017b; Tijing et al., 2015). The existence of a scaling layer not only adds additional heat and mass transfer resistance (Gryta, 2008; Qtaishat et al., 2008), but also increases the risk of pore blockage and membrane wetting, and ultimately results in deterioration of MD performance (Dong et al., 2021; J. Liu et al., 2021; L. Liu et al., 2021). Therefore, it is necessary to find an effective means of controlling inorganic scaling (Anvari, Kekre, et al., 2020; Elcik et al., 2020; Naji et al., 2020; Qu et al., 2020).

Pretreatment of feed solution is one of the most commonly used methods for minimizing the scaling problem in MD (Gryta, 2009). Low pressure filtration techniques have been studied as pretreatment processes to reduce the scaling effects of the MD processes. Cartridge filter, microfilter, ultrafilter, and nanofilter were used to remove the hardness ions along with the other foulants (Cho et al., 2018;

Kamranvand et al., 2020). Since the scalant ions in the feed stream of the pretreatment system are mostly rejected, it lowers the scaling potential for the subsequent MD process, but it increases the scaling effects in the pretreatment processes. Magnetic field was also applied to minimize scaling. The magnetic field slows the nucleation and increases the size of the crystals. In addition, it makes the scalant more porous while reducing the effects of scaling on MD performance (Gryta, 2011). However, under the laminar flow condition, this process promotes the deposition of calcite. Controlling the pH of the feed solution is another solution to the scaling problem that has been studied rigorously. Reducing the pH by acidifying the feed solution increases the solubility of the alkaline salts that lowers the possibility of scale formation (He et al., 2009). But the additional chemical dosage to reduce the pH also leads to an increase in the expense of the process. Further, antiscalant materials are widely used to control the scaling effects. These materials reduce the scaling effects in various ways such as slowing the nucleation rate, changing the structure of the scale crystal and altering the concentration of the dissolved CO_2 (Hasson & Semiat, 2006). Usage of antiscalants is also limited by their low surface tension characteristic which leads to membrane pore wetting problem resulting in a significant reduction of the MD system performance (Franken et al., 1987).

Since these pretreatment techniques have their own limitations, few studies have found that the scaling layer on the membrane surface can be efficiently cleaned by regular membrane flushing as the MD processes do not apply very high hydraulic pressure. It is however, also observed that the effectiveness of cleaning declines after a certain period and it completely fails to recover the performance at a point if the operation is further continued (Nghiem & Cath, 2011). Therefore, to identify an optimal cleaning strategy, it is indispensable to study the physical and chemical mechanisms of the dynamics of scale formation and its effects on the mass transport through the membrane pores. Despite a significant attempt to understand the mechanism of scale formation, there is a huge research gap in optimizing the cleaning procedure relating to the transient growth of the scaling layer on the membrane surface. Especially, a more in-depth understanding of wetting and scaling is essential. Most of the existing MD wetting and scaling studies focused only on performance degradation such as flux decline. However, there is a large error in the step of generating scaling inside the pore and accurate prediction of the occurrence time of scaling.

This study aims at investigating the intricate physico-chemical mechanism of monovalent and multivalent inorganic scale formation on the MD membrane surface both theoretically and experimentally. In

addition to the scaling on the membrane surface, it was also aimed to confirm the generation of scaling inside the pores, and the prediction of the time of occurrence was also performed. Although there are many studies on the occurrence of wetting due to scaling and fouling and performance degradation, however, this paper focused on the generation and development stage of scaling, especially the expansion into the inside of the pore. In particular, it is the first time to directly confirm the occurrence of scaling on the surface and inside the pores and analyze it in relation to performance degradation and solubility. Transient flux decline resulting from the deposition of monovalent and multivalent scale was experimentally studied. Energy Dispersive X-Ray (EDX) spectroscopy was conducted to characterize the chemical composition of the scale formed on the membrane to confirm the existence of the scaling incident. Scanning Electron Microscopy (SEM) analysis was also carried out to investigate the morphological structure of the scaling layer and its effects on the mass transport through the membrane pores at different phases of distillation. For the more realistic investigation, the concepts of supersaturation (S) and saturation index (SI) employed for two multivalent ions, one monovalent ion, and their mixture were theoretically evaluated by employing the equilibrium principles of water chemistry. To determine an optimal cleaning strategy for efficient MD

operation, crystallization effects of these ions on the water flux through the membrane were experimentally measured. Then the accumulated scales were cleaned by generating high shear stress on the membrane surface at different stages of distillation using deionized (DI) water at high crossflow velocity.

Finally, through various analyses, the inorganic scaling formation stages of the MD process were confirmed. Also, the formation was predicted through S and SI value calculation. Additionally, an optimum cleaning strategy was developed based on the maximum flux recovery considering the transport resistance which resulted from the accumulation of inorganic scaling on the membrane surface. As a result, an inorganic scaling mechanism was suggested.

4.2 Materials and methods

This section outlines the theoretical and experimental methods employed to investigate the inorganic scaling in MD process. It also describes the chemicals and instruments used for the experimental analysis.

4.2.1. MD membrane and cell

A flat-sheet membrane (FGLP14250, Millipore), made of polytetrafluoroethylene (PTFE) polymer and supported by a polyethylene (PE) net was employed in this study. The principal characteristics of the flat-sheet membrane as provided by the manufacturer were 0.22 μm of average pore size, 150 μm of thickness, and 85% of porosity. In addition, the maximum operating temperature was 130℃. The acrylic membrane cell was employed with a total membrane area of 0.002 m^2.

4.2.2. MD scaling experiments

A series of MD scaling experiments were performed by using a lab-scale direct contact membrane distillation (DCMD) unit (**Fig. 4-1**). The feed solution was continuously circulated from a feed tank through the membrane cell with 25 cm/s of cross-flow velocity and maintained at 60 ± 0.5 ℃ by an electric heater. While the permeate solution was deionized (DI) water maintained at 20 ± 0.5 °C by an electric chiller. The volume of feed and permeate solutions were 2L, respectively. The analytical balance was employed to weigh permeated water through the membrane pores in the permeate reservoir. A conductivity meter (HACH® HQ40d) was employed to measure the electrical conductivity of the permeate water continuously. Each scaling experiment was

conducted until scaling occurred, and the operation time varied from 16 hour to 24 hours depending on the initial concentration.

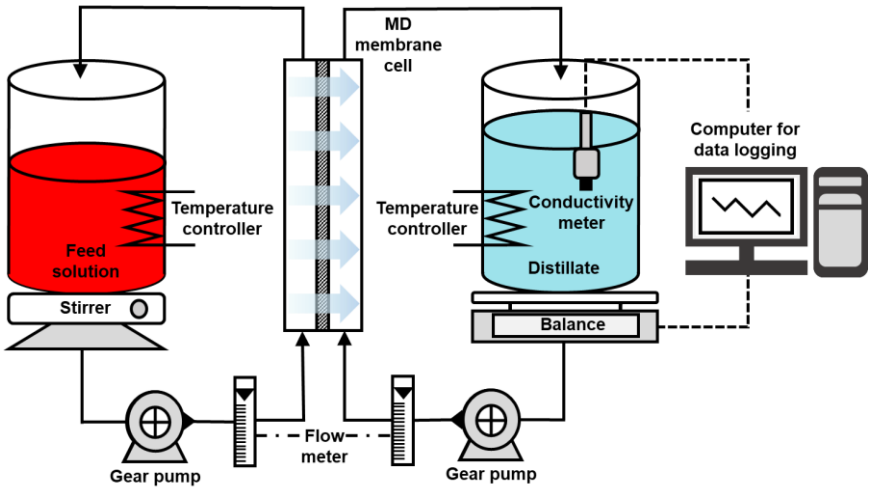

Figure 4-1 A scheme of lab-scale direct contact membrane distillation (DCMD) unit

In order to study the mechanism of inorganic scaling in the MD process, the most common scalant, NaCl, was used in the feed solution. The initial concentration of NaCl was chosen to investigate the formation of scaling by observing the transition of undersaturated feed solution to supersaturated solution. Therefore, 200,000 mg/L of NaCl solution was employed in this study, which is slightly lower than supersaturation. However, since the effects of monovalent ion (NaCl) scaling is less than the multivalent ion scaling, this study also conducted MD experiments

with multivalent scalants, namely, $CaCO_3$ and $CaSO_4$. For more realistic analysis, feed solution with a mixture of NaCl, $CaCO_3$, and $CaSO_4$ was also used to study the MD scaling. Due to the limited membrane area at the lab-scale, there were constraints on conducting concentration experiments to increase the CF. Therefore, we set the feed solution at a very high concentration, below saturation levels, to ensure practical experimentation. In this study, the monovalent solution was NaCl (200,000 mg L^{-1}) and the multivalent solution was composed of NaCl (197,000 mg L^{-1}), CaCO3 (2,000 mg L^{-1}), and CaSO4 (1,000 mg L^{-1}). These ion concentration ratios were assumed to represent reverse osmosis (RO) brine, a common high salinity solution, and their corresponding saturation indices (SI) were -0.54, 1.55, and -1.17, respectively.

4.2.3. Theoretical prediction of inorganic scaling formation

Inorganic scaling in MD process occurs mainly in two ways such as bulk crystallization (homogeneous nucleation) and surface crystallization (heterogeneous nucleation). Bulk crystallization results from the supersaturation of feed solution containing dissolved ions which leads to the deposition of scalants on the MD membrane surface, whereas the surface crystallization occurs due to the heterogeneous nucleation of scaling crystals on the membrane surface. Bulk crystallization in the MD process is highly dependent on the solubility

constant (S), and the saturation index (SI). The ion dissolution/association model to predict the $CaCO_3$ scaling, which is one of the most common scalants in desalination systems scaling is as follows,

$$Ca^{2+} + {CO_3}^{2-} \leftrightarrow CaCO_3 \downarrow \quad \textbf{(4-1)}$$

According to this model the solubility product K_{sp} of $CaCO_3$ is given by,

$$K_{sp} = \frac{\{Ca^{2+}\}_e \left\{{CO_3}^{2-}\right\}_e}{\{CaCO_3\}_e} \quad \textbf{(4-2)}$$

Where, $\{Ca^{2+}\}_e$ and $\left\{{CO_3}^{2-}\right\}_e$ are the activity coefficients of Ca^{2+} and ${CO_3}^{2-}$, respectively at equilibrium. $\{CaCO_3\}$ is considered as 1 since the solute is in the solid phase. However, a real solution may not be in a state of equilibrium. This non-equilibrium state is described by the ion activity product (IAP) which is expressed by,

$$IAP = \{Ca^{2+}\}\{CO_3{}^{2-}\} \quad \textbf{(4-3)}$$

Where, $\{Ca^{2+}\}$ and $\{CO_3{}^{2-}\}$ are the activity coefficients of the respective electrolyte compounds, Ca^{2+} and $CO_3{}^{2-}$. SI is another useful parameter to define whether the substances will be dissolved or precipitated in a solution, which is given by (Q. Liu et al., 2019),

$$SI = log_{10}\left(\frac{IAP}{K_{sp}}\right) \quad \textbf{(4-4)}$$

Here, IAP is the ion activity product of a solution, and Ksp is the solubility product in terms of activity. The conditions for determining the saturation of a solution are,

if SI = 0 (IAP = K_{sp}): the solution is in equilibrium,

if SI < 0 (IAP < K_{sp}): the solution is undersaturated which means more solute will be dissociated,

if SI > 0 (IAP > K_{sp}): the solution is supersaturated, i.e. ions will precipitate as the solute.

Supersaturation is another important term to quantify the scaling in the system. It is defined by,

$$S = IAP - K_{sp} \quad \textbf{(4-5)}$$

The S and SI of $CaSO_4$ and NaCl were also calculated similarly in this study as representatives of the most common monovalent and multivalent scalants. A computer software, PHREEQC version 3.6.2 was employed to calculate the solubility constant (K_{sp}), IAP and the SI of the potential scales. Moreover, to observe the transition effects of solution from undersaturation to supersaturation state, the MD performance and the SI of the solution were determined at various concentration factors which is expressed by,

$$CF = C_i \left[\frac{ln\left(\frac{1}{1-R}\right)}{R} \right] \quad \textbf{(4-6)}$$

where CF represents the concentration factor, C_i (mg/L) is the

initial concentration of the solution and R is the system recovery rate.

4.2.4. Real-time scaling visualization system

The real-time scaling visualization system consisted of a charged-coupled device (CCD) camera and a light source. The CCD monochrome camera with 1.4 megapixel 16mm lens was employed to detect the light intentsity on the membrane surface. The membrane surface image was captured every 5 minutes. Illumination of lights to the membrane suface was conducted by visible LED light (H.-W. Kim et al., 2019).

4.2.5. Cleaning experiments

The scaled membrane surface was cleaned by high fluid shear force (i.e., by flowing a solution at a high crossflow velocity of 50 cm/s) in the feed channel of the MD experimental setup for 30 min. In this study, only DI water was used in the hydraulic flushing to focus only on the effect of scaling formation stage on membrane cleaning. To determine the optimal cleaning strategy, the scaling layer was cleaned at various stages of distillation and the flux recovery rates for these stages were compared. Finally, according to the maximum flux recovery rate, the optimal cleaning strategy was determined.

4.3. Results and discussions

4.3.1. Identification of monovalent inorganic scaling formation

4.3.1.1. MD performance: flux and rejection behavior

To analyze the most basic scaling condition, MD experiments were carried out using sodium chloride (NaCl), a representative monovalent-ion. The initial concentration of NaCl was chosen to investigate the formation of scaling by observing the transition of undersaturated feed solution to supersaturated solution. Therefore, 200,000 mg/L of NaCl solution was employed in this study.

Fig. 4-2 shows the MD performance with NaCl solution as feed in terms of transient water flux and distillate conductivity. The experiment was repeated three times to improve reproducibility and accuracy. Almost similar flux and conductivity behavior were found for all three experiments. Both water flux and distillate conductivity remained almost stable up to 900 min. Although there were slight reductions in water flux, this is because the vapor pressure decreases due to the concentration of the feed solution, and is independent of scaling. However, a sharp flux decline occurred after 900 min, but the distillate conductivity still remained unchanged for some time afterward. Then the distillate

conductivity increased rapidly at 1,200 min, when the water flux continued to decrease, reaching nearly zero.

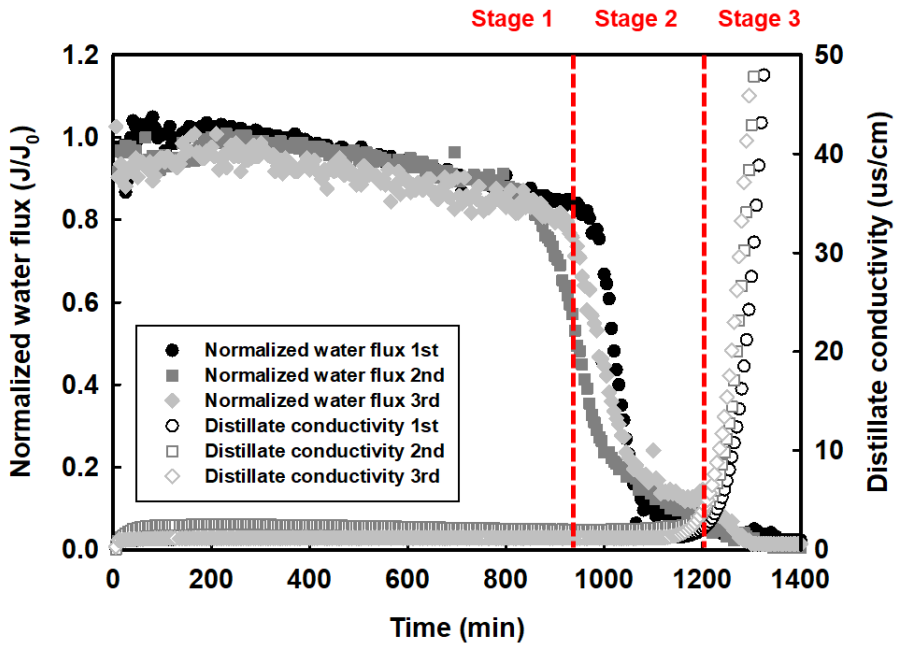

Figure 4-2 Normalized water flux and distillate conductivity as a function of time in the MD scaling experiment of NaCl solution (200,000 mg/L). Feed and permeate solution temperature was set at 60 ± 0.5 °C, 20 ± 0.5 °C, respectively. Cross-flow velocity of 25 cm/s was employed for feed and permeate streams.

Based from the results, it can be observed that there were three stages in the scaling formation during the MD process that can affect its process performance as shown in **Fig. 4-2.** The first stage is the interval from the beginning of the experiment before the flux decreases sharply (0 ~ 900 min). In the second stage, the water flux starts to decrease rapidly, but the distillate conductivity is maintained (900 ~ 1,200min). The third

stage is where the distillate conductivity begins to increase and the water flux reaches almost zero (1,200 min ~). Later sections will analyze this dynamic stages of inorganic scaling formation during the MD operation.

4.3.1.2. Composition and morphology of the scales

In order to further analyze the reason for the flux and rejection decline during the scaling experiment, SEM-EDX analysis was performed by sampling the membrane coupon after each experiment (**Fig. 4-3**).

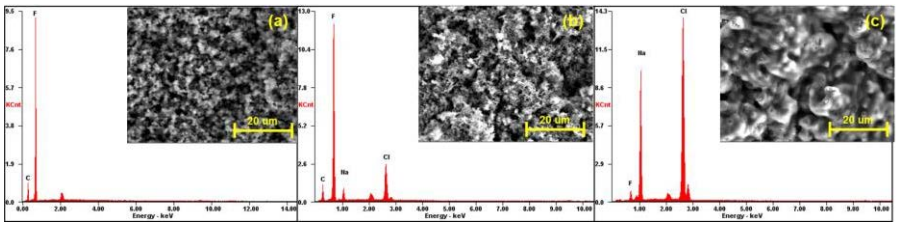

Figure 4-3 SEM image of membrane surface and SEM-EDX analysis of formed scale at (a) stage 1, (b) stage 2, and (c) stage 3.

Fig. 4-3a, b, and **c** show the SEM images of the membrane surfaces of stages 1, 2, and 3, respectively. From **Fig. 4-3a**, almost no scale was found during stage 1, whereas some scales started to deposit and partially covered the membrane surface in stage 2, and then became more severe in stage 3 (**Fig. 4-3c**) where the membrane surface is completely covered with scales, making it difficult to distinguish between the membrane and

the scales. This trend was identified through SEM-EDX analysis. In the case of the SEM-EDX analysis on stage 1, only C, F peak, which means membrane was identified. In the case of Stage 2, some Na and Cl peaks were identified, but the value was not large. However, very high Na and Cl peaks were identified in the SEM-EDX analysis on stage 3. It revealed that a large amount of generated scale is composed of NaCl (**Fig. 4-3c**). This trend is consistent with earlier transient flux decline behavior. In MD processes, water vapor passes through the membrane pores due to the vapor pressure difference between the feed and the distillate side. Consequently, the water flux decreases when the effective pores of the membrane are reduced by the deposited NaCl crystals or scale. As a result, the flux was decreased due to the scaling and the trend of flux behavior was in agreement with the transition of stages of flux and rejection behaviors (**Fig. 4-2**).

4.3.1.3. Development of scale formation stage

In order to understand the physical mechanism of scale formation in MD processes, SEM-EDX mapping analysis was performed by sampling the membrane after each scaling stage. **Fig. 4-4** shows the cross-sectional SEM and the EDX mapping images for each stage, which indicate the distribution of C, Cl and Na elements using different colors. The C

element represents the PTFE membrane. Cl and Na elements represent NaCl scale.

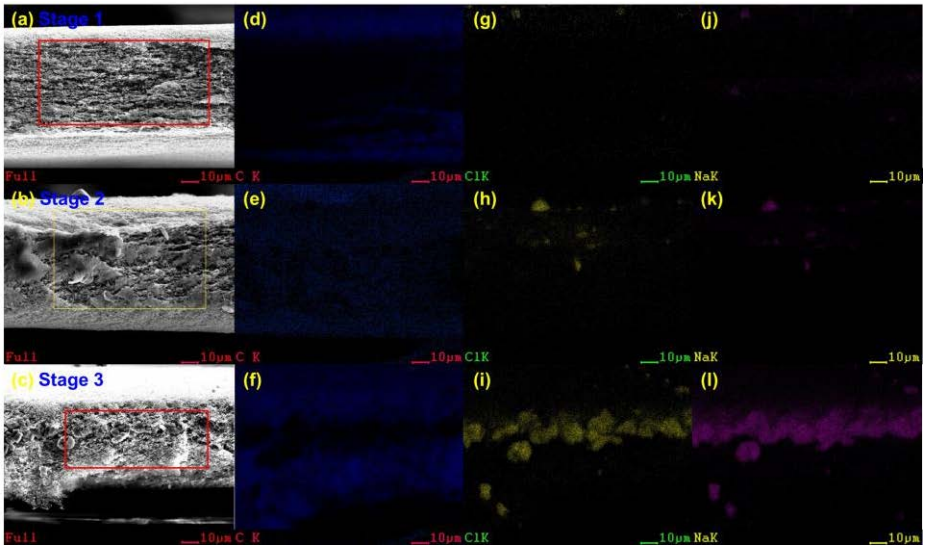

Figure 4-4 SEM cross-sectional images and corresponding EDX mapping images for elements C, Cl, and Na in each scaling formation stage. Stage 1: a, d, g, j; Stage 2: b, e, h, k; Stage 3: c, f, i, l.

In the case of stage 1, the cross-section image revealed almost no scale formation on the membrane surface and inside the membrane pores (**Fig. 4-4a**), which is also corroborated by the EDX mapping images (**Fig. 4-4d, g, j**) where only very small amount of yellow and purple images representing Cl and Na were found on the membrane surface. The amount of Cl and Na elements was found to slightly increase in stage 2 as indicated in the EDX mapping, but the scale deposits cannot be clearly viewed in the depth of the membrane based from the SEM cross-section

image, though small amounts of deposits can be seen on the surface. The surface scaling and pore blocking resulted to a flux decline in stage 2. However, the distillate conductivity during stage 2 did not increase significantly due to the fact that the scale was not fully developed into the inside of the pores. In stage 3, NaCl scale formation was clearly evident in the depth of the membrane as revealed in the cross-sectional SEM image (**Fig. 4-4c**) and supported by the corresponding EDX mapping showing presence of Cl and Na elements in both the surface and in the pores of the membrane. Consequently, pore wetting occurs and the distillate conductivity rapidly increased as the feed water penetrated the pores and mixed with the distillate solution. Then, after some time, scaling expanded further into the inside of the pores as well as on the membrane surface, leading to complete pore blockage that consequently declined the flux until no more water vapor permeation through the membrane.

As a result, the mapping analysis revealed that scaling starts from the membrane surface and gradually expands into the pores along the scaling formation stage. In addition, the MD performance (water flux and distillate conductivity) is significantly dependent on the location of scaling during different stages of operation. This result is in good

agreement with flux and rejection behavior and SEM-EDX analysis explained in the previous section.

4.3.2 Identification and prediction of multivalent inorganic scaling formation

4.3.2.1. Identification of multivalent inorganic scaling formation with in-situ scale visualization

4.3.2.1.1. MD performance: flux and rejection behavior

In the previous section, the monovalent scaling phenomenon was investigated. However, monovalent scaling is the most fundamental condition, while the multivalent ions are considered to be the major scalants in real water treatment field due to their higher scaling potential. Therefore, for a more realistic scaling analysis, the scaling of multivalent ions and mixtures (both monovalent and multivalents) was examined in this section. $CaCO_3$ and $CaSO_4$ were employed as multivalent scalants, since these are the most critical scalants in the field. The initial concentrations of $CaCO_3$ and $CaSO_4$ were 1,000 and 2,000 mg/L, respectively, as these are the appropriate concentrations to properly observe the transition of solution from under-saturated to a super-saturated state similar to the monovalent ion (NaCl) case.

In the case of normalized water flux (**Fig. 4-5**), it was observed that there was only a slight decline until volume concentration factor (VCF) 1.3 which was mainly attributed to the effect of vapor pressure reduction due to feed concentration change (stage 1). After VCF 1.3, the water flux begins to rapidly decrease. The distillate conductivity, representing rejection, was found to not change in this section (stage 2). From above VCF 1.4, the distillate conductivity starts to increase, and the water flux continues to decrease until zero (stage 3). This flux and rejection trend is the same as with the result in the previous monovalent scaling (NaCl) test. However, the observed main difference is on the rate of flux decrease in stage 2, where it is less rapid than that of monovalent ion test result. This is because NaCl is the only ion present in the solution in the case of monovalent scaling, so all ions are precipitated at once and a large amount of scaling occurs at supersaturation state. On the other hand, in the case of the multivalent scaling, other multivalent ions also exist in the solution. The degree of supersaturation of NaCl is lower than that of the monovalent scaling case, so that the degree of flux reduction is less in multivalent scaling case. As a result, in a multivalent scaling experiment, MD performance was found to be affected by the scaling formation stage, and this trend was similar to that of the monovalent scaling case.

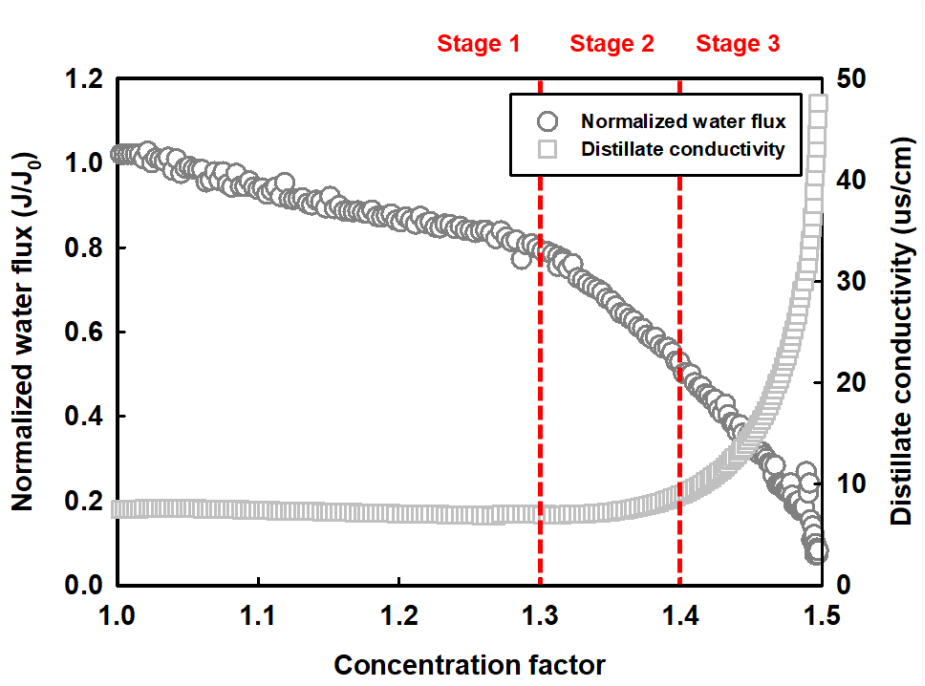

Figure 4-5 Normalized water flux and distillate conductivity as a function of concentration factor in the multivalent scaling experiment of the mixture solution (NaCl: 200,000 mg/L, $CaCO_3$: 1,000 mg/L, and $CaSO_4$: 2,000 mg/L). Feed and permeate solution temperature were set at 60 ± 0.5 °C, 20 ± 0.5 °C, respectively. Cross-flow velocity of 25 cm/s was employed for feed and permeate streams.

4.3.2.1.2 Composition and morphology of the scales

In multivalent scaling experiment, SEM-EDX analysis was performed to identify when and which scaling occurred for each stage. **Fig. 4-6** shows the SEM images of the scales generated on the membrane surface for each stage and the result of the component analysis. In the case of VCF 1.05, which refers to stage 1, it is identified that no scaling has occurred as no scaling element have been detected except for the fluorine

which refers to the membrane material (**Fig. 4-6a, d**). In the case of VCF 1.3, which represents stage 2, it was confirmed that a small amount of scale was generated on the membrane surface (**Fig. 4-6b**). It was verified that the shape of the scale was also mixed with NaCl and calcium-based scale by component analysis. However, considering that the peak of calcium element is higher than that of NaCl, the calcium-based scale is considered dominant in this section (**Fig. 4-6e**). As a result of the component analysis, the calcium-based scale is estimated to be $CaCO_3$, considering that there are a large amount of C and O elements and the shape of the scale also has a rounded grain shape (Rodriguez-Blanco et al., 2011). In the case of VCF 1.4, which represents stage 3, it was observed that the scale extensively covered the membrane surface (**Fig. 4-6c**). In small-scale SEM images, a number of NaCl scales having a cube shape were observed on the membrane surface (**Fig. 4-6f**). As a result of SEM-EDX analysis, there was a difference in the formed scale component according to the VCF. In stage 2, the calcium-based scale was dominant, and in stage 3, a large amount of cube-shaped NaCl scale was generated. This is related to the flux rejection behavior in the previous section. The decrease in flux from the VCF 1.3 can be attributed to the membrane surface pore blocking by calcium-based crystal, and the reduction from the VCF 1.4 is due to pore wetting due to a large amount

of NaCl crystal. As the VCF increases further, NaCl scaling covers the membrane surface, completely blocking all pores, and the flux eventually reaches zero.

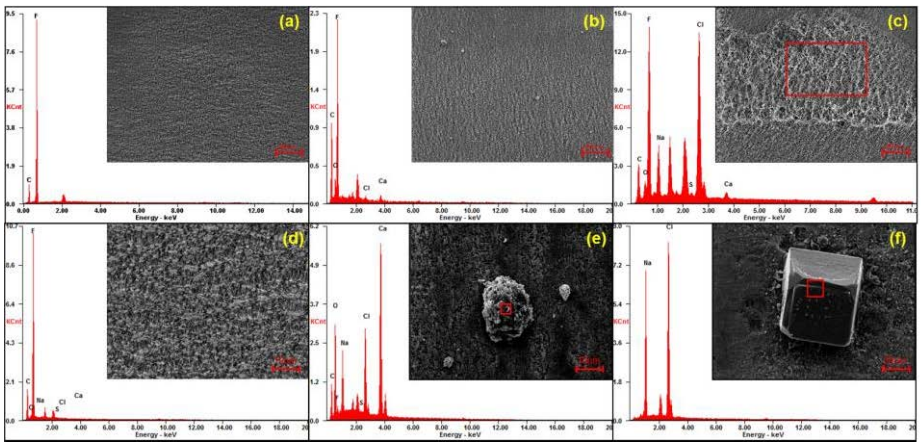

Figure 4-6 Large scale SEM image of membrane surface and SEM-EDX analysis of formed scale at (a), (b) VCF 1.05, (b), (d) VCF 1.3, and (c), (f) VCF 1.4, respectively.

4.3.2.1.3. Development of scale formation stage

In order to more accurately confirm the scale formation inside the membrane pore as well as membrane surface, SEM-EDX mapping analysis was performed on the membrane cross-section. In the case of VCF 1.05 (stage 1), no specific scale was observed in the mapping results. In **Fig. 4-7d**, only the F peak representing the membrane material was observed, and the Na, Cl, and Ca peaks representing the scaling material were not observed at all. For VCF 1.3 (stage 2), some Na, Cl, and Ca peaks were observed on the membrane surface. In particular, Na and Cl

peaks were clearly observed on the membrane surface (**Fig. 4-7h, k**). On the other hand, the Ca peak seemed to be slightly increased compared to stage 1, but it was still not significant. In the last VCF 1.4 case (stage 3), a large amount of Na and Cl peaks were observed not only on the membrane surface but also inside the membrane (**Fig. 4-7i, l**). The Ca peak also increased more than in stages 1 and 2, which was more pronounced at the membrane surface than inside the pore (**Fig. 4-7o**). In other words, in stage 2, the scale starts to develop on the membrane surface, which intensifies in stage 3 and extends to the inside of the membrane pore. This trend is exactly the same as the previous monovalent scaling formation.

As a result, through all the data of flux and rejection behavior, SEM-EDX component analysis and mapping analysis, it was found that multivalent scaling formation started to generate small scales on the membrane surface from VCF 1.3 (stage 2), causing flux reduction. As scaling expands into the membrane pores in the VCF 1.4 or higher, wetted pores are generated and salt rejection is reduced. Eventually, all pores are blocked and the flux reaches zero. This trend is consistent with monovalent scaling, with only slight differences in the components of the scale.

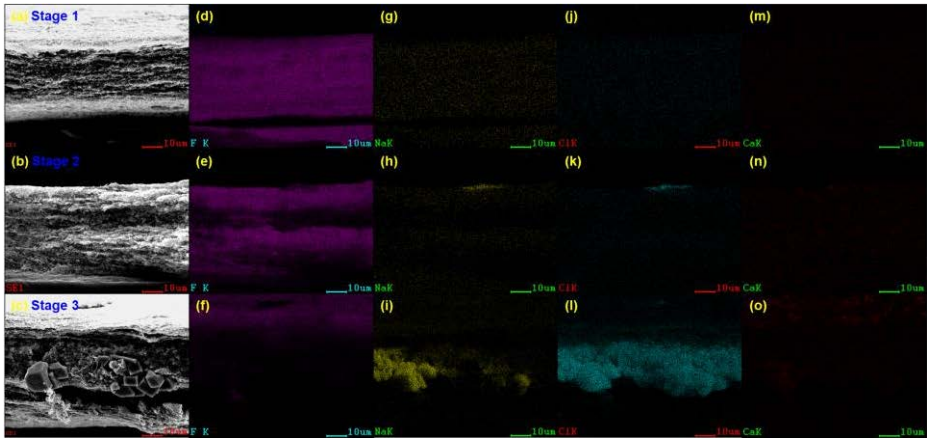

Figure 4-7 SEM cross-section images and their corresponding EDX mapping images for elements F, Na, Cl and Ca in each scaling formation stage. Stage 1 at VCF 1.05: a, d, g, j m; Stage 2 at VCF 1.3: b, e, h, k, n; Stage 3 at VCF 1.4: c, f, i, l, o.

4.3.2.1.4. Identification of inorganic scaling on membrane surface by real-time visualization

In the previous section, it was confirmed that scaling occurs on the membrane surface and gradually expand to the pores. A real-time visualization technique was introduced in order to more accurately compare the membrane surface scaling occurrence point with the scaling formation stage analyzed through flux and rejection behavior (H.-W. Kim et al., 2019). **Fig. 4-8a** shows the intensity value according to VCF. The higher the intensity value, the higher the light transmittance of the membrane surface, which means that scaling and wetting occurred more on the membrane surface. **Fig. 4-8b, c, d**, and **e** are captured images of

the actual membrane surface light transmission in each VCF. For the first time in VCF 1.2, a white spot was found, indicating scaling and wetting. This white spot gradually expands and increases rapidly at VCF 1.3. This trend is in exact agreement with the previous flux and rejection behavior and SEM-EDX analysis results in which MD performance decreases due to rapid increase in scaling from VCF 1.3. Especially, from VCF 1.2, white spots start to occur gradually, and it seems to be the calcium-based scale confirmed in SEM-EDX analysis as it does not affect the flux and rejection behavior if in a small amount. From VCF 1.3 and above, the white spot begins to increase rapidly. This coincides exactly with the starting point of stage 2, where the flux begins to decrease rapidly. As a result, it was confirmed that from VCF 1.2 (stage 2), scaling begins to occur on the membrane surface, which increases from VCF 1.3 and begins to cover the entire membrane surface by real-time visualization. Therefore, the flux decline in stage 2 of the MD performance experiment was attributed to this surface scaling. However, real-time visualization has limitations, such as that it cannot visualize through the depth of the membrane especially inside the membrane pores. Therefore, this visualization technique should be performed with SEM-EDX and mapping analysis, to fully consider not only the membrane surface but also the inside of the pores.

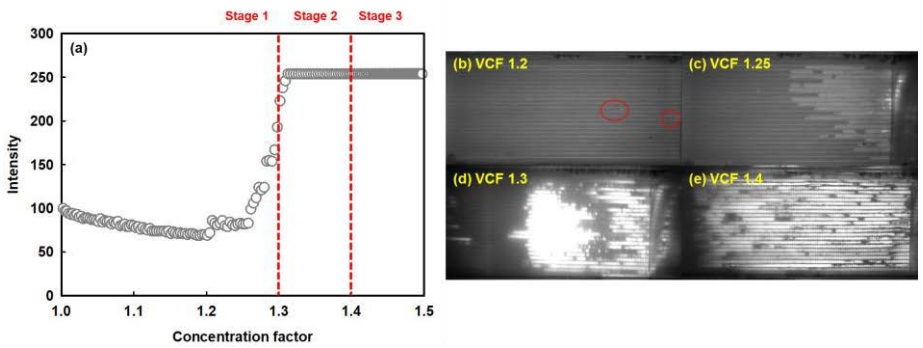

Figure 4-8 The real-time scaling visualization analysis: (a) light intensity value and the captured images from the real-time visualization system as a function of VCF at (b) 1.2, (c) 1.25, (d) 1.3, and (e) 1.4.

4.3.2.2. Prediction of multivalent inorganic scaling formation by calculating saturation index and supersaturation

In the previous section, through lab-scale experiments and analysis, the scaling formation stage was confirmed, and the relationship between the substances and timing of scaling occurrence and MD performance reduction was analyzed. However, for optimal operation of the process, even if the ionic composition of the feed water changes, it is important to have the ability to predict the occurrence of scaling. Therefore, in this section, the substance and the time of occurrence of scaling are predicted through the ionic composition of feed water, and the effect is verified by comparing it with the experimental results. Saturation index and supersaturation of the solutions were theoretically calculated to anticipate the feed solution concentration at which the nucleation

initiates. To justify the theoretical predictions, experimentally measured normalized flux (actual flux/initial flux) declines for the solutions due to the scaling were also compared.

Fig. 4-9 compares the supersaturation (S), and saturation index (SI) of each scalant solution as a function of concentration factor. The performance degradation behavior according to scaling of this mixture solution can be interpreted through the analysis of the SI and S values (**Fig. 4-9**). According to **Fig. 4-9a**, $CaSO_4$ is under-saturated with SI value of less than 0 throughout the concentration factor range (1 ~ 1.9) and does not affect the nucleation behavior of the mixture solution. On the other hand, only $CaCO_3$ solution is super-saturated with SI value greater than 0, at the concentration factor equal or less than 1.3. At the concentration factor equal to or greater than 1.3, the SI value of NaCl is greater than zero. As a result, only $CaCO_3$ is supersaturated in the range of 1 to 1.3 of the VCF, and NaCl also transforms from undersaturated to supersaturated state from the VCF value of 1.3 or higher.

However, the flux and rejection behavior does not change significantly below VCF 1.3, but changes rapidly from 1.3 or above. Therefore, it can be interpreted that MD performance is more affected by NaCl scaling than $CaCO_3$. This can be explained by the supersaturation, S value. **Fig.4- 9b** shows the S value of each potential

scale of the mixture solution. As in the result of the SI value above, $CaSO_4$ is supersaturated only at VCF 1.9 or higher, so the S value can also be calculated only at VCF 1.9 or higher. Since the scaling experiment is stopped at VCF 1.5, $CaSO_4$ is unsaturated in all VCF conditions of the experiment and does not affect the scaling phenomenon. The S value of $CaCO_3$ is supersaturated under all VCF conditions, and the S value is in the range of $7.38 \times 10^{-8} \sim 2.35 \times 10^{-6}$. On the other hand, in the case of NaCl, it gradually begins to be supersaturated after VCF 1.3, and the S value ranges from 0.9 to 4,500. As a result of S-value modeling, $CaCO_3$ is supersaturated under all VCF conditions, however the S value is very small and the amount of scaling is very limited. On the other hand, although NaCl is supersaturated only at VCF 1.3 or higher, the S value is very large and increases rapidly. Therefore, the amount of generated NaCl scaling is relatively large, so the effect on MD performance is significant.

As a result, it was confirmed that the scaling phenomenon of the mixture solution also has a scaling formation stage like the NaCl solution in the previous section. The ion composition affected scaling formation and the change in MD performance, which can be interpreted and predicted through analysis of solubility constant or saturation parameters such as S and SI.

In particular, it was identified that the time, material and amount of scaling occurrence can be predicted by analyzing SI and S value of each potential scale of mixture solution, respectively. This is significant in enabling simple prediction in the treatment of actual concentrated water and high-concentration wastewater, which has limitations in prediction and modeling due to the presence of various potential scale when actual inorganic scaling occurs. However, since each ion's interaction and quantitative analysis of the relationship between S value and MD performance were not considered in this stage, it is essential for further research.

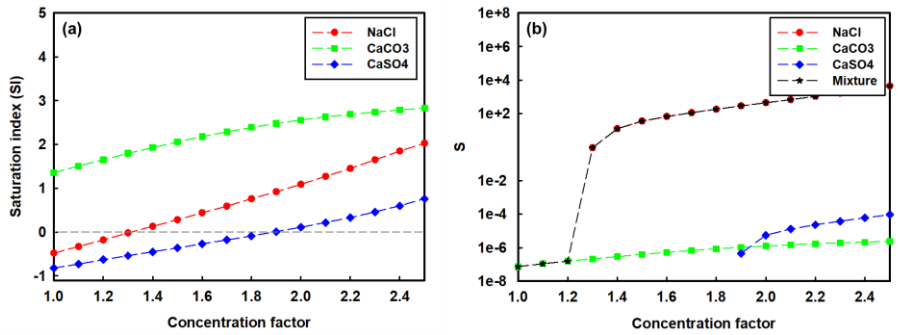

Figure 4-9 (a) saturation index (SI) of each potential scale and (b) supersaturation of each potential scale at various concentration factor for mixture solution, respectively.

4.3.3 Implications

4.3.3.1. Mechanisms of scaling formation stage

The anticipation and prediction of inorganic scaling primarily depends on two key factors, namely scalant material and dynamics of scaling. To minimize the scaling effect, it is essential to know which scaling materials are presented in the feed solution. In addition, it is equally important to predict the onset of scaling incident. According to the scaling formation stage analysis, the end of stage 1 and the beginning of stage 2 represent the point at which flux decline occurs. Determining the operating condition when the scaling occurs allows for proper consideration of an optimal cleaning strategy for efficient MD operation.

In detail, possible scaling matter can be predicted by ion association modeling using PHREEQC program. Material whose SI is higher than or close to zero is considered to be expected scaling matters. If the SI value of the matter is less than 0, scaling does not occur in theory. However, in the case of heterogeneous nucleation (surface crystallization) that can occur on the membrane surface, scaling is possible even at SI ranges less than 0 because the required Gibbs free energy is smaller than that of the homogeneous nucleation (bulk crystallization) that occurs in bulk solutions. The prediction of when scaling occurs is more

complicated. According to the classical nucleation theory (CNT), scaling does not occur just because concentration exceeds solubility. The nucleation, which is the basic stage of scaling, does not begin until it reaches a minimum concentration that can cause heterogeneous or homogeneous nucleation higher than the critical value. After that, crystal growth occurs at higher concentrations than solubility. Therefore, supersaturation calculation and modeling according to the concentration factor was employed to predict the scaling behavior of the solution. By calculating S and SI values, possible scaling matter and time of nucleation can be predicted. Especially, it is possible to predict the type and time of scale formation that can occur through the SI value, and the amount of scaling through the S value. However, there is a limit to finding the exact starting point by considering only homogeneous nucleation or bulk crystallization, because the heterogeneous nucleation or surface crystallization which occurs on the membrane surface depends on various conditions such as hydrodynamic conditions, membrane materials and the interaction between scalant particles in high concentration. Therefore, an analysis that considers the result of supersaturation analysis and the actual experimental value is necessary. Through supersaturation analysis, the point where scaling starts is theoretically known, and its accuracy can be further improved by

comparative analysis with the point of flux decline from actual experimental value.

The scaling formation mechanism according to these stages is shown in **Fig 4-10. Fig. 4-10** shows scaling stage 1 which is operating stably, and there is no performance degradation with flux and rejection behavior. In scaling stage 2, scaling occurs due to heterogeneous nucleation on a part of the membrane surface. This occurs only in some pores on the membrane surface as well and blocks the pores to reduce flux (**Fig. 4-10**). Some heterogeneous nucleation occurs in the pores near the membrane surface towards the pore wall, but the amount is very insignificant. In stage 3, as the concentration of the solution increases, homogeneous nucleation in the bulk solution also occurs. In addition, heterogeneous nucleation, which occurred on the surface of the membrane, also expands into the inside of pores, causing pore wetting. This causes not only flux decline, but also salt flux, which reduces rejection. After that, as scaling has deteriorated, all pores are covered by scaling, and the flux value continues to decrease and becomes zero.

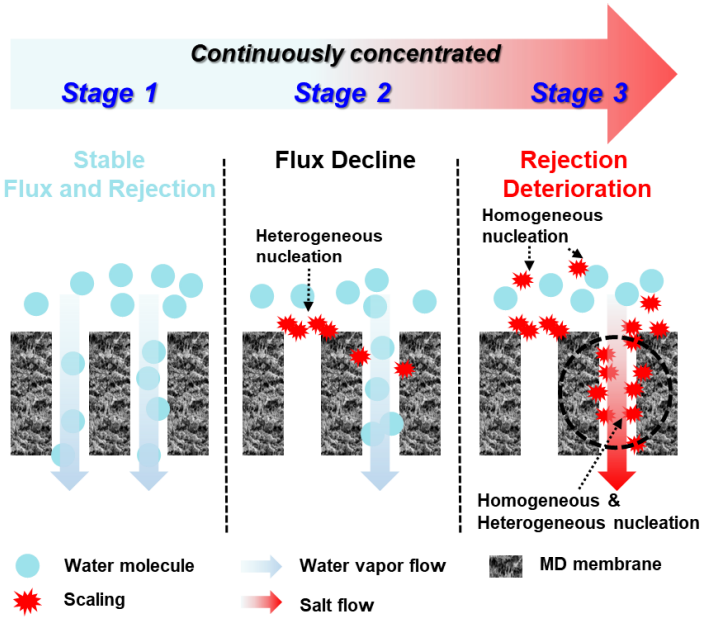

Figure 4-10 Mechanisms of scaling formation stage: Stage 1, Stage 2 (scaling on membrane surface by heterogeneous nucleation), and Stage 3 (scaling on membrane inside pore by homogeneous and heterogeneous nucleation)

As a result, scaling formation can be predicted by flux and rejection behavior experiments and calculation and modeling of supersaturation and saturation index. However, since the scaling phenomenon is greatly affected by the membrane surface material and hydrodynamic conditions, such complex considerations are required. Further analysis of these relationships will enable the development of new scaling index and operation guidelines that can be used in actual operations.

4.4. Conclusion

This study thoroughly investigated the physicochemical mechanism of inorganic scaling in MD processes. Transient flux decline and change in distillate conductivity due to inorganic scaling were experimentally measured. Moreover, SEM-EDX analysis was carried out to characterize the composition of scales formed and to observe the growth of the scale layers over the membrane surface and within the pores. Further, supersaturation and saturation index calculation and modeling were employed to predict the scaling formation. An optimal cleaning strategy was then decided based on the maximum flux recovery after cleaning at various stages. The major findings of this study are listed below:

- Changes in water flux and distillate conductivity during the MD operation resulted from the formation of inorganic scaling showed three distinct stages of the MD process. During stage 1, almost stable water flux and distillate conductivity were found. At the following stage, although the distillate conductivity remains steady, water flux decreases rapidly. At the final stage, water flux almost reduces to zero and the conductivity increases sharply.
- The physical characteristics of scaling formation were confirmed by SEM-EDX and in-situ scale visualization analysis. The scale

was not formed over the membrane surface at stage 1, whereas the scaling layer started depositing on the membrane surface at stage 2. At stage 3, scaling extends to the inside pore and the membrane pores were completely blocked by the scaling.

- The substance and time of occurrence of the scaling formation can be predicted through saturation index and supersaturation calculation and modeling, respectively. Especially, the behavior of the supersaturation value exactly coincides with the substance and time point of the scaling formation.
- In terms of membrane cleaning, more than 94% flux recovery was confirmed in every cleaning cycle of stage 1. This is attributed to the fact that the scaling is limited to only the membrane surface and the amount is very insignificant in stage 1. Based on this, the mechanism of inorganic scaling formation according to stages was proposed.

Chapter 5. Electrically conductive membrane distillation (ECMD) via an alternating current operation for zero liquid discharge (ZLD)

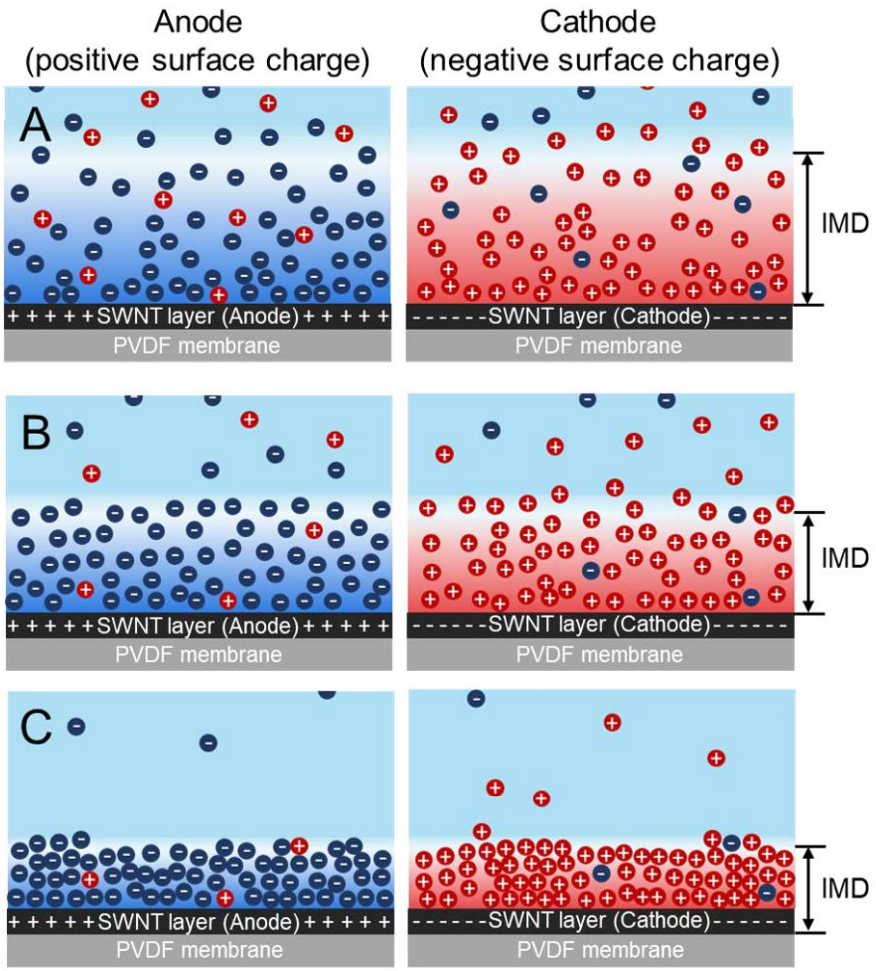

This chapter is based on:
Kim, J., Tijing, L.D., Shon, H.K. and Hong (2023), S. Electrically conductive membrane distillation via an alternating current operation for zero liquid discharge. Water Research 244, 120510.

5.1. Introductions

Stress on traditional freshwater resources such as rivers and groundwater is increasing due to population growth and climate change, and the need for non-traditional water resources is emerging (M. Liu et al., 2022; Stenzel et al., 2021; Zhu et al., 2022). However, considering the overall water cycle, the potential for new water resources is locally and temporally limited (Chagas et al., 2022; Pistocchi et al., 2020). Consequently, enhanced water recycling and additional extraction from traditional freshwater resources are becoming increasingly essential. As a strategy to increase the water recovery rate from the water resource, it is necessary to develop water treatment technology that is multifunctional, scalable, resilient, chemical resistant, and energy efficient. Ultimately, it also poses as a challenge for zero liquid discharge (ZLD). In order to achieve ZLD, it must be preempted with the development of a process capable of sufficiently coping with a concentration of contaminants and salinity at a high recovery rate (Boo & Elimelech, 2017; W. Xie et al., 2022; C. Zhang et al., 2021; Zuo et al., 2020).

In recent decades, fouling and scaling issues, which cause a reduction in water productivity and shortened membrane lifespan due to the concentration of contaminants and salts under high recovery

conditions for ZLD, remain obstacles to be solved before practical application (Choudhury et al., 2019; Costa et al., 2021; C. Liu et al., 2018; Naidu et al., 2015; Yan et al., 2021). Research has been conducted to solve various fouling and scaling problems, but it is still impossible to cope perfectly with high-recovery conditions (Kim, Yun, et al., 2022; Zhao et al., 2021).

Recently, research on the electrically conductive membrane (ECM) has been increasing because of the potential for fouling and scaling control using electrical-based phenomena by introducing electrical activity as a membrane function beyond existing physical and chemical characteristics (Ahmed et al., 2016; Barbhuiya et al., 2021; Mo et al., 2022; M. Sun et al., 2021; Z. Zhang et al., 2022; Zhu & Jassby, 2019). ECM has electrical conductivity by fabricating a membrane with an electrically conductive material (carbon-based, conductive polymer, and metal) or modifying a new layer using the conventional polymer membrane as a base. By applying an electric potential to the ECM to generate an electric charge on the surface, there is a promising possibility for controlling fouling and scaling through mechanisms such as electrostatic interaction, electrochemical oxidation & reduction, and electrolysis. Direct current (DC) is applied in most cases. Since most of the organic contaminants (bacteria, polysaccharides, NOM, and oil)

present in the water system are negatively charged, it is easy to induce electrostatic repulsion with each other using ECM as a cathode, enough to control organic fouling effectively (Han et al., 2021; Jiang et al., 2021; Kim, Kim, et al., 2022; Lou et al., 2022). The application for organic scaling mitigation is also being attempted, but since both cations and anions must be controlled simultaneously, there is a limit to DC operation using only changes in local pH (Zhu & Jassby, 2019).

As a new alternative to these disadvantages of DC operation, AC operation has been newly proposed, and studies aimed at fouling and scaling mitigation are in progress (Fan et al., 2016; Jung et al., 2023; Rao et al., 2020; Thamaraiselvan et al., 2018; Zhang et al., 2017; Zhou et al., 2018). Most of them were applied for biofouling alleviation of microfiltration (MF) and ultrafiltration (UF) membrane processes. In AC operation, negatively charged bacteria induce repulsion to the cathodic ECM and promote electron transfer to the anodic ECM due to the potential difference between the ECM and the bacteria. Bacteria that lose electrons cause reactive oxygen species (ROS) bursts to be killed or inactivated (Wang et al., 2018). In the case of organic fouling, it has been proven that sufficient control is possible even in DC operation, so there have been few studies on AC operation (Kim, Yun, et al., 2022). Despite the unique advantage of AC operation of its potential to simultaneously

control both anions and cations, there are almost no application cases for inorganic scaling mitigation, and those few reported application cases are even just simply performance evaluations using a single solution. As the applied voltage was still maintained at a high value, adverse effects such as water electrolysis have not been solved.

In this study, the objective was to maximize the water recovery rate by controlling and mitigating inorganic scaling by applying AC operation to the MD process, which is advantageous for high-salinity water sources. Systematic experimental performance evaluation for all predictable operating conditions (frequency, waveform, ionic composition, and applied voltage), verification of the theoretical mechanism based on the data, and ECMD AC operation optimization in energy consumption were performed. Through this research, the fouling and scaling control performance of the ECM will be maximized, ultimately achieving high water recovery, including ZLD. Furthermore, it is expected to increase the value of ECM, which has tremendous potential for use in fuel cells, catalysts, and sensors in addition to water treatment (Alvarez et al., 2018; Boo & Elimelech, 2017; Chen et al., 2018; Dudchenko et al., 2017; Qi et al., 2017; Seo et al., 2018; Surwade et al., 2015; B. Zhang et al., 2022; Zuo et al., 2020).

5.2. Materials and methods

5.2.1. Reagents

The following reagents were used without purification or treatment: sodium chloride (Sigma-Aldrich), sodium carbonate (Sigma-Aldrich), calcium chloride (Sigma-Aldrich), sodium sulfate (Sigma-Aldrich), 2-Propanol (Sigma-Aldrich), nafion perfluorinated resin solution (Sigma-Aldrich), and SWNT powder (d1.5L1-5-S, Nanolab). All the chemicals used were of reagent grade, and ultrapure deionized water (>18.2 MΩ·cm) produced from a Milli-Q water purification system was used to make the reagent solutions.

5.2.2. Modification methods of SWNT ECM

For stable and homogeneous SWNT ECM modification, uniform SWNT-IPA-Nafion solution was prepared by appropriate ultrasonication for more than 3 hours with SWNT powder 0.8g, IPA 250 mL, and Nafion 750 μg and then centrifuged at 8,000 rpm for 30 min, after which the supernatant was collected. Finally, the uniform solution was stabilized in the laboratory for more than 24 hours. SWNT ECM modification was achieved by vacuum filtering the uniform solution 10 mL at once through a flat-sheet PVDF membrane (GVHP14250, Millipore) and drying at 60 °C for more than 30 minutes to remove excess IPA. In the case of

multilayered ECM, the above process was repeated up to 4 times. The optimal membrane was selected as SWNT-4 membrane in consideration of both the physicochemical and electrochemical characteristics of the modified membrane.

5.2.3. Characterization and analytic methods of SWNT ECM

The physicochemical morphologies of the SWNT ECM were characterized by field emission scanning electron microscopy (FE-SEM, Inspect F50, FEI), and atomic force microscope (AFM, HR-AFM, AFM Workshop). The chemical functions and characteristics of SWNT ECM were confirmed by x-ray photoelectron spectroscopy (XPS, ThermoFisher Scientific) and contact angle goniometer (DCA, Phoenix-300, SEO Corporation). Additionally, electrochemical properties were measured by cyclic voltammetry (CV) and electrochemical impedance spectroscopy (EIS) using a potentiostat (PGSTAT204, Metrohm Autolab) in a conventional three-electrode setup: SWNT ECM, a silver/silver chloride (Ag/AgCl) electrode, and a platinum plate electrode were used as the working, reference, and counter electrodes, respectively.

5.2.4. ECMD inorganic scaling mitigation experiments

The inorganic scaling mitigation effect of AC operation was evaluated using a laboratory-scale ECMD unit. In each experiment, pristine PVDF, SWNT-1, and SWNT-4 membranes with an effective area of 20.02 cm^2 were used with an acrylic cell of a channel height of 3 mm. For the scaling experiment, two solutions (monovalent ion, multivalent ion solution) in 2L volume were continuously supplied to the ECMD cell by a pump, and the compositions of the feed solutions were NaCl 200,000 mg l^{-1}, and NaCl 193,802.4 mg l^{-1}, $CaCl_2$ 3033.45 mg l^{-1}, Na_2CO_3 2,120 mg l^{-1}, Na_2SO_4 1044.12 mg l^{-1} with same TDS value, respectively. These extreme conditions were applied in order to shorten the experimental time as much as possible due to the small membrane-effective area of the laboratory-scale experiments. Ultrapure deionized water was used for the distillate solution and was supplied and circulated to the ECMD cell by the same gear pump, and the temperature of each solution was maintained at 60 ± 1, 20 ± 1 °C by thermostatic baths (AD-RC08, AND), respectively. The weight and conductivity of the distillate solution were continuously monitored by an electronic balance (GF8202M, AND) and conductivity meter (HQ40d, HACH). The power supply was performed through a potentiostat (PGSTAT204, Metrohm Autolab) and effectively controlled through customized software. A function/arbitrary waveform

generator (DG1000Z, Rigol) was used to generate and change AC waveforms.

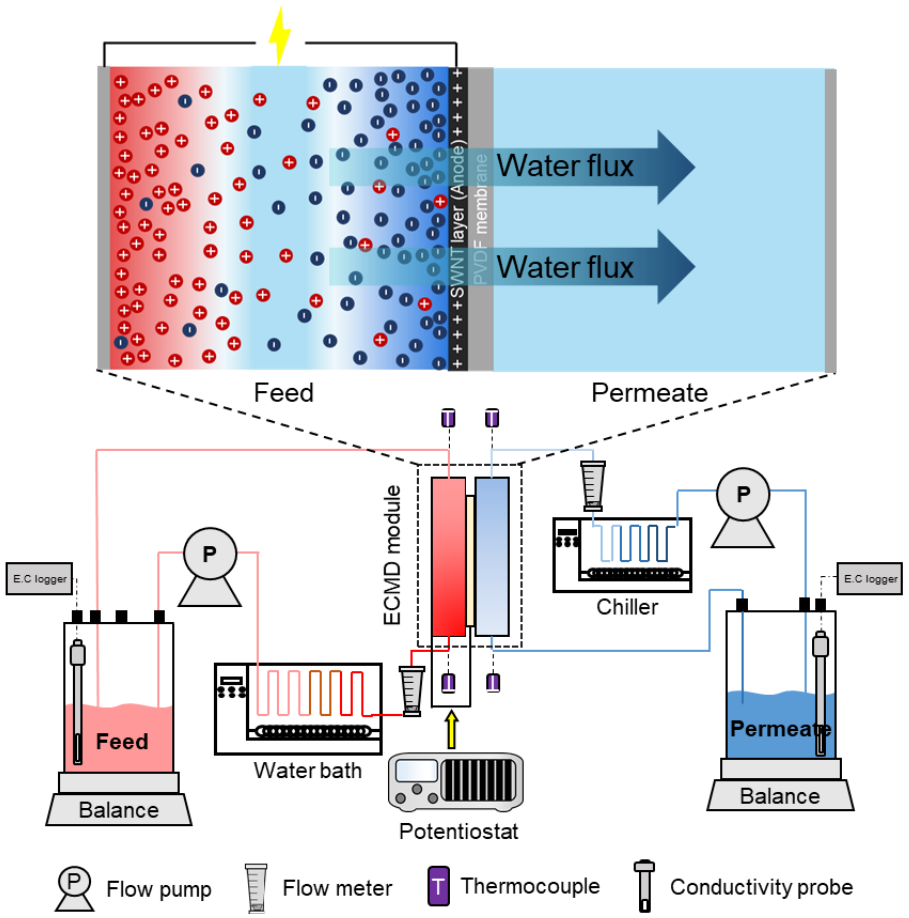

Figure 5-1 Schematic of the lab-scale electrically conductive membrane distillation (ECMD) system.

5.2.5. ECMD performance and energy consumption assessment

To evaluate the performance and energy consumption of ECMD, the following parameters were considered, along with their respective

equations: (1) FDR, (2) Ion velocity, (3) IMD, and (4) SEEC (J. Kim et al., 2019; Kim, Yun, et al., 2022; Varcoe et al., 2014).

$$FDR = -\frac{1}{J_0^2} tan\,\theta \,|t = 0 = -\frac{1}{J_0^2}\frac{dJ}{dt}|t \quad \textbf{(5-1)}$$

where J_0 and J are the initial fluxes ($Lm^{-2}h$), respectively, the fluxes at time t are the slopes of the flux behavior at t = 0, respectively, and t is the operation time (h).

$$Ion\ velocity = Ion\ mobility \times Electrical\ field \quad \textbf{(5-2)}$$

Ion velocity (ms^{-1}) is calculated as the product of each ion mobility ($m^2s^{-1}V^{-1}$) and electrical field ($m^{-1}V$). Ion mobility is proportional to ion charge and inversely proportional to solution viscosity and ion hydrodynamic radius. The ion mobility value of each ion was calculated based on the feed solution temperature of 60 °C. Like the multivalent ion solution, the ion velocity of the mixed solution was considered as an average value based on each ion concentration ratio with the total energy difference according to the waveform.

$$IMD = \frac{Ion\ velocity}{Frequency} \quad \textbf{(5-3)}$$

Considering that the ion moving time changes according to the frequency, the IMD (m) was calculated by dividing the ion velocity by the frequency.

$$SEEC = \frac{Applied\ electrical\ energy}{Volume\ of\ additional\ water\ production\ by\ ECMD} = \frac{V_{ECMD} \times I \times t}{V_{water}} \quad \textbf{(5-4)}$$

The SEEC value ($kWhm^{-3}$) was calculated by dividing the additional electrical energy used for ECMD AC operation by the amount of additional water produced through fouling mitigation. Where V_{ECMD} is the applied voltage (V), I is the applied current (A), t is the operation time (h), and V_{water} (m^3) is the increased yield compared to the pristine PVDF experiment.

5.3. Results and discussions

5.3.1. Modification and characterization of SWNT ECM

Polyvinylidene fluoride (PVDF) membranes are most commonly used in MD processing because of their inherent hydrophobicity, low thermal conductivity, and mechanical robustness (Im et al., 2021; X. Wang et al., 2016; Ye et al., 2022). However, the hydrophobic PVDF membrane is easily wetted and vulnerable to inorganic scaling caused by heterogeneous nucleation on the membrane surface under high recovery conditions. In response, the hydrophobicity and electrical conductivity of the PVDF membrane were supplemented through single-wall carbon nanotube (SWNT) surface modification, thereby enabling scaling mitigation ECMD operation. Accurate characterizations of the SWNT ECM were performed in terms of physical, chemical, and electrical aspects on pristine PVDF, SWNT-1 (single-layered), and SWNT-4 (4-layered) membranes.

To analyze the physical properties and surface morphology of the SWNT ECM, scanning electron microscope (SEM) imaging and atomic force microscope (AFM) analysis of the membrane surface and cross-section were performed (**Fig. 5-2**). In the SEM image of the pristine PVDF membrane, the sponge-like porous surface of PVDF was clearly visualized (**Fig. 5-2A$_1$**). On the other hand, on the surface of the SWNT-

1 membrane, it was confirmed that the PVDF membrane surface was covered with SWNTs. This tendency was further maximized in the SWNT-4 membrane with more SWNT layers. However, in cross-sectional SEM images, there was no significant difference between each membrane. This is because the thickness of the SWNT layer (about 2 μm) is minimal compared to the entire film (115 μm). A similar trend was confirmed in the AFM analysis (**Fig. 5-2B**). In the case of the pristine PVDF membrane, it was identified that the membrane surface height was widely distributed from 0.1 to 3.6 μm due to the porous surface in the form of a sponge. Whereas, in the case of SWNT-1 and SWNT-4 membranes, the surface height distribution was reduced to 0 ~ 1.4 and 1.8 μm, respectively by the SWNT layer on the surface, and the morphology of the membrane surface was changed to a more uniform and flatter shape overall. Due to these changes, the roughness values of the SWNT-1, and SWNT-4 membranes also decreased to 225.4 and 145.8 nm compared to the pristine PVDF membrane of 614.33 nm, respectively. This reduction in roughness can provide more inactive nucleation sites with an increased activation energy barrier to heterogeneous nucleation. So, the resistance of SWNT ECM to inorganic scaling can be increased (M. Sun et al., 2021). As a result, through membrane surface and cross-sectional analysis, it was confirmed that the

SWNT layer was stably coated on the PVDF surface, and the physical properties of the SWNT ECM were changed to be more advantageous to inorganic scaling.

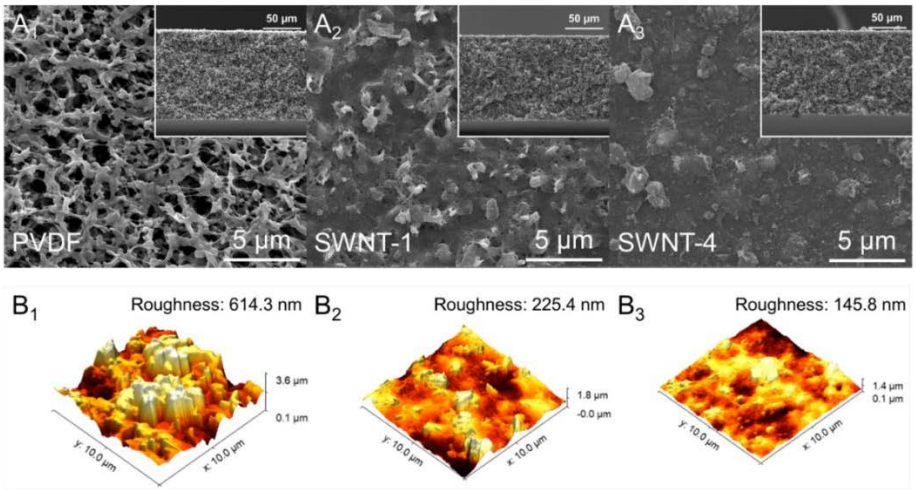

Figure 5-2 Characterization of physical properties and surface morphology of membranes. A_1, A_2, and A_3 are membrane surface and cross-sectional SEM images, and B_1, B_2, and B_3 are AFM images of the pristine PVDF, SWNT-1, and SWNT-4 membranes, respectively.

The chemical properties of the SWNT ECM were characterized by X-ray photoelectron spectroscopy (XPS) and direct contact angle (DCA) analysis. XPS analysis was introduced to detect the chemical structure and functional groups of SWNT ECM. **Fig. 5-3A** shows the XPS spectra of pristine PVDF, SWNT-1, and SWNT-4 membranes. As a result, as the SWNT layer increases, the peak of C1s at 285 eV increases, and the peak of F1s at 686 eV decreases. The peak of C1s and F1s corresponds

to sp2 bonds mainly composed of SWNTs and pristine PVDF, respectively(Kaspar et al., 2021; Kaspar et al., 2020). This indicates that as the SWNT layer increases, a more considerable amount of SWNT is stably coated on the surface of the pristine PVDF membrane, and thus the chemical properties of the SWNT ECM surface are modified to the characteristics of SWNT rather than the existing PVDF. DCA is a representative indicator of membrane hydrophobicity and is commonly used in the MD process. DCA measurements were performed in deionized (DI) water and NaCl 200,000 mg l^{-1} solution to consider both the basic properties of the membrane and the properties under high recovery conditions (**Fig. 5-3B**). In DI water case, the DCA of the pristine PVDF membrane was 124.95 ± 5.71°, which is consistent with the intrinsic properties of the PVDF material. It was confirmed that the DCAs of the SWNT layer slightly increased to 129.74 ± 7.25 and 133.29 ± 7.02° in the SWNT-1 and SWNT-4 membranes, respectively. This is because the chemical properties of the SWNT ECM are affected by the pure aromatic carbon layer of the SWNT effectively coated on the membrane surface. This trend was also consistent with NaCl 200,000 mg l^{-1} case. The DCAs of pristine PVDF, SWNT-1, and SWNT-4 were 123.41 ± 6.25, 128.54 ± 6.54, and 131.74 ± 5.86°, respectively. The overall DCA decreased slightly than in the DI water cases, but the

increasing trend with the number of SWNT layers was maintained. In conclusion, as the SWNT layer was coated on the surface of the pristine PVDF membrane, the chemical properties of the SWNT ECM became closer to those of the SWNT, and an apparent increase was confirmed in the DCA value representing the hydrophobicity of the membrane.

Finally, the electrochemical impedance spectroscopy (EIS) and cyclic voltammetry (CV) analyses were performed to evaluate the electrical characteristics of the SWNT ECM (**Fig. 5-3C, D**). The EIS results are shown in **Fig. 5-3C** in Nyquist plots where the fictitious component of impedance ($-Z''$) is plotted against the real component (Z'). The impedance of the pristine PVDF membrane is much higher than that of SWNT-1 and SWNT-4, suggesting that SWNT plays an important role in membrane conductivity. Compared to SWNT-4, the impedance of SWNT-1 was higher, implying that the addition of the SWNT layer increased the membrane electrical conductivity. The charge transfer resistance (Rct) also showed a similar trend. Compared to the pristine PVDF membrane, as the SWNT layer increased, the Rct value significantly decreased. The Rct values of pristine PVDF, SWNT-1, and SWNT-4 were 1903.9, 59.6, and 3.6 Ω, respectively. This can be interpreted that the dense layer of SWCNTs exhibits high ionic mobility with excellent electrical conductivity. The CV curve analysis in **Fig. 5-**

3D was performed to examine the electrochemical performance of the pristine PVDF, SWNT-1, and SWNT-4 membranes and to investigate the inorganic scaling mitigation potential of the membranes. The CV curve of the pristine PVDF membrane shows little change over the entire scan range, indicating that the electrochemical properties are very inferior. In the case of SWNT-1, the CV curve slightly increased from -0.2 to 0.2 mA/cm^2 over the entire scan range. In particular, the CV curve was narrow and thin in the scanning range of -0.5 to 0.0 V, but relatively wide in the range of 0.0 to 0.5 V, which means that the oxidation tendency was limited after SWNT modification, indicating better stability as an anode. On the other hand, in the case of SWNT-4, the current density in the entire applied voltage range showed a dramatic increase from -0.7 to 0.7 mA/cm^2, and stable performance was shown as both anode and cathode. This indicates that the SWNT layer positively affects the electrochemical properties of the membrane, consistent with previous EIS results.

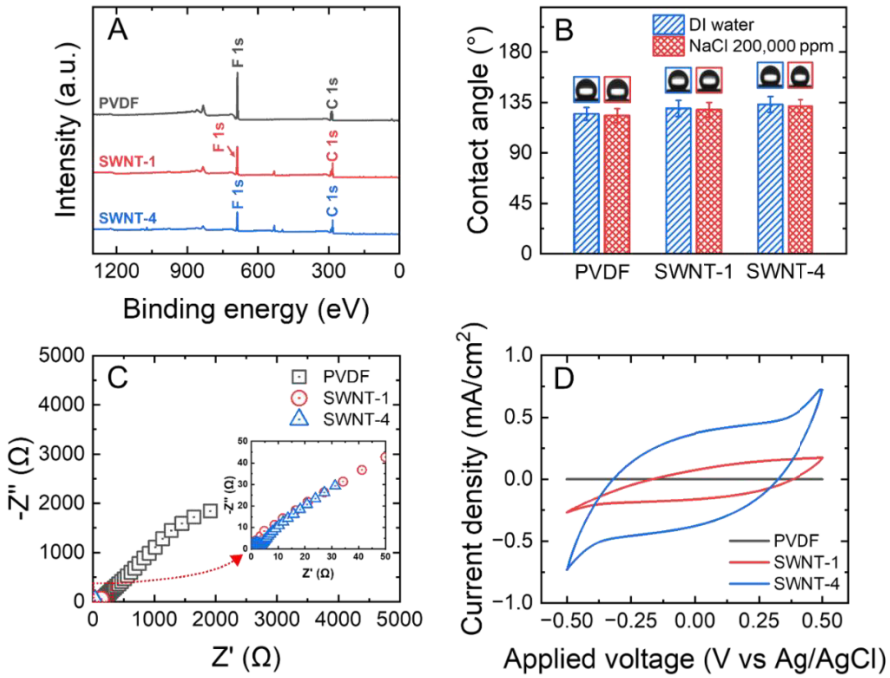

Figure 5-3 Characterization of chemical and electrical properties of membranes. A: XPS spectra using a monochromatic Al-Kα X-ray source (1486.6 eV), B: DCA values and sessile drop images in DI water and NaCl 200,000 mg l^{-1} solution, C: Nyquist plots of real and imaginary impedance by EIS measurement, and D: CV curves of the pristine PVDF, SWNT-1, and SWNT-4 membranes, respectively.

SWNT modification improved the physicochemical and electrochemical properties of SWNT ECM for inorganic scaling mitigation. The SWNT-4 membrane was selected as the optimal membrane considering all properties, and a basic experimental evaluation of inorganic scaling mitigation was performed. **Fig. 5-4** shows the normalized flux behavior in each operating condition

according to the concentration factor (CF). In the case of pristine PVDF membrane, rapid flux decline due to inorganic scaling occurred from CF 1.4, and the final CF 1.6 showed the lowest water productivity. In the case of SWNT-4 without applied voltage, although the flux decline was slightly delayed than that of the pristine PVDF due to the hydrophobicity increase by the SWNT layer, the final CF was limited at 1.7. In the case of SWNT-4 (DC), unlike the excellent performance in organic fouling control, a flux trend similar to that of SWNT-4 without applied voltage case was confirmed (Kim, Yun, et al., 2022). Finally, in the case of SWNT-4 (AC), stable flux was maintained from the beginning of the experiment, and sustainable operation was possible without any flux decline until the final CF 1.8. AC operation had a very dramatic increase in inorganic scaling mitigation compared to DC. This is presumed to be because AC operation can control both cations and anions as the surface charge of SWNT ECM is continuously changed, unlike DC operation. As a result, AC operation is essential for inorganic scaling mitigation in the ECMD process, and the sensitivity assessment and analysis of operating conditions and optimization from an energy perspective are required for practical application.

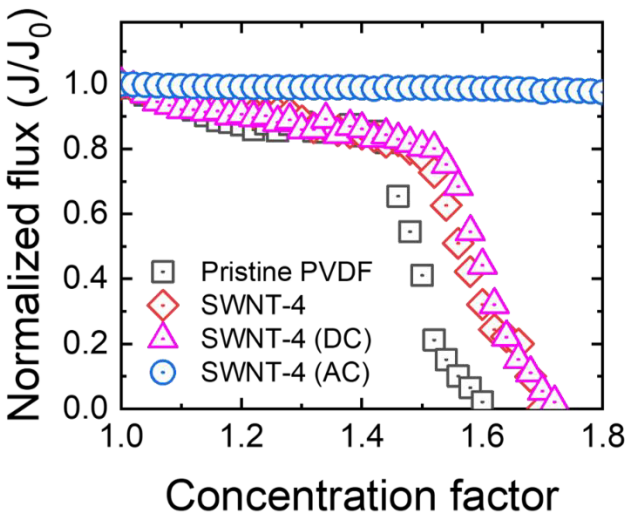

Figure 5-4 ECMD performance behaviors under various membrane and electrical operation conditions. The pristine PVDF and SWNT-4 membranes were used with a feed solution NaCl concentration of 200,000 mg l^{-1}. Especially, the SWNT-4 membrane was used under non-ECM, DC, and AC operation conditions.

5.3.2. Evaluation of scaling mitigation effect in ECMD according to operating parameters

Direct contact membrane distillation (DCMD) experiments were systematically conducted using a high salinity feed solution to evaluate the inorganic scaling mitigation performance of AC operation using SWNT ECM. Frequency, waveform, feed solution ionic composition, and applied voltage were selected as the key operating conditions of AC operation, and MD performance behavior (water flux, distillation conductivity) according to concentration factor (CF) for each operating condition was monitored.

Fig. 5-5 shows MD performance behavior according to frequency (1, 5, and 10 Hz). In order to investigate the effect of frequency on inorganic scaling mitigation, other operating conditions were fixed at monovalent ion solution (NaCl 200,000 mg l^{-1}), sine wave, and 0.5 V. In the case of 1 Hz, a gradual and gentle flux decline was observed from the beginning of the experiment, and a more rapid flux decline appeared after CF 1.5. Eventually, the normalized flux decreased to less than 0.6 at the final CF 1.8 point, failing to maintain performance under high recovery conditions. While in the 5 Hz condition, the vapor pressure decreased according to the feed water concentration, so there was a slight flux decrease, but a rapid decrease in flux due to scaling was not

observed. The stable operation was possible while maintaining a normalized flux of 0.8 or more up to CF 1.8. In the 10 Hz condition, a gradual flux decline was identified, similar to the 1 Hz condition until CF 1.4. However, a dramatic flux decrease occurred, and the normalized flux decreased to zero around CF 1.7. In the distillate conductivity, which represents the rejection of the MD process, no significant change was observed in the case of 1 and 5 Hz, but a rapid increase was confirmed from CF 1.6 or higher in the case of 10 Hz.

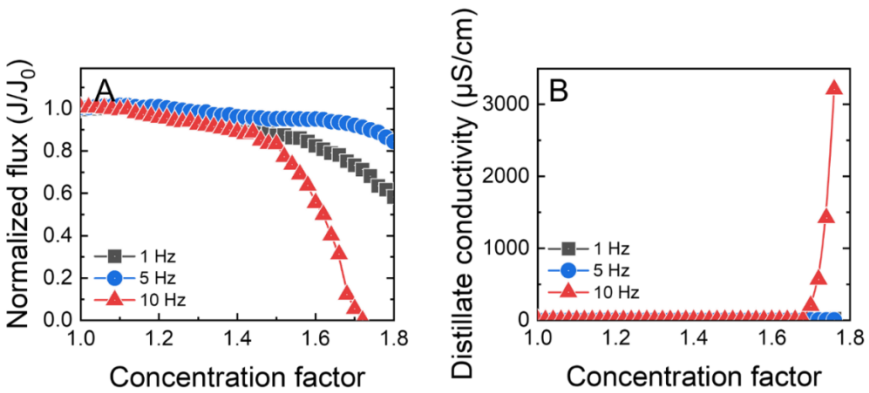

Figure 5-5 ECMD performance behaviors under various frequency conditions. A: normalized water flux, B: distillate conductivity. The SWNT-4 membrane was used with a feed solution concentration of 200,000 mg l^{-1} (NaCl single solution).

These results can be elucidated by the inorganic scaling formation stage and the electrophoresis of ions by AC operation. In the MD process, scaling formation is divided into three stages. Stage 1 is the gradual flux

decline due to a small amount of heterogeneous nucleation, stage 2 is the rapid flux decline due to homogeneous nucleation, and stage 3 is wherein flux approaches to zero and distillate conductivity increases (Karanikola et al., 2018; Kim, Kim, et al., 2022). In the 1 Hz condition, only a gradual decrease in flux occurred, and no distillate conductivity increased. Therefore, it corresponds to scaling stage 1, and changes in MD performance behavior in this stage are usually caused by the deposition of scaling caused by heterogeneous nucleation under high recovery conditions (Kim, Kim, et al., 2022). The 1 Hz AC operation induced electrophoresis of ions by switching the charge on the SWNT ECM surface, and the formation of scaling on the ECM surface was suppressed by repeating the process of attraction and repulsion of cations and anions according to the change of ECM surface charge. However, the effect was postulated to be insignificant. In the case of the 5 Hz condition, only a gradual flux decrease occurred as in the 1 Hz condition, so it corresponds to scaling stage 1. In particular, even the gradual flux reduction was not severe compared to the 1 Hz condition, so it is assumed that cations and anions control through AC operation was more effective. In the case of the last 10 Hz, a gradual flux decrease was confirmed up to CF 1.5, after which a rapid flux decline occurred and the desalination function was completely lost. The result showed that the normalized flux approached

zero at CF 1.7. In addition, the distillate conductivity also rapidly increased, showing a decrease in salt removal efficiency around CF 1.7. This corresponds to scaling stage 3, and changes in MD performance behavior in this stage are usually affected by wetting caused by scaling on the surface of the membrane and inside the pores by homogeneous nucleation under high recovery conditions. As a result, AC operation under the condition of 10 Hz rather rapidly converts the attraction and repulsion of cations and anions, causing a peripheral mixing effect, which is presumed to promote inorganic scaling. This caused performance degradation by entering scaling stage 3. On the other hand, AC operation under the conditions of 1 and 5 Hz had the effect of mitigating inorganic scaling and sustaining at scaling stage 1 and had a more dramatic effect under the 5 Hz condition than at 1 Hz. It is considered that the inorganic scaling formation could be controlled by affecting the difference in attraction and repulsion of cations and anions with SWNT ECM, but additional detailed analysis is essential.

Systematic additional ECMD experiments were performed to analyze the scaling mitigation effect of AC operation according to the remaining operating conditions (waveform, feed solution ionic composition, and applied voltage) (**Fig. 5-6**). **Fig. 5-6A** shows the MD performance behavior according to the waveform. In the 1 Hz condition,

a more gentle curve was observed for the flux decline when the square wave was applied, compared to the basic condition of the sine wave. However, although the slope of flux decline was reduced, it was not completely overcome. Under the 5 Hz condition, the stable MD operation was sustainable by maintaining almost complete initial flux compared to the gentle flux decline of the sine wave condition under the square wave condition, except for the negligible flux decline due to the concentration of the feed solution. Whereas, in the 10 Hz condition, the rather rapid flux decline point was advanced to around CF 1.3 under the square wave condition, and performance degradation was observed earlier. Distillate conductivity was also similar to the previous trend. This is due to the total amount of energy according to the AC waveform. The total energy of the square wave is about 1.414 times higher than that of the sine wave due to its high RMS value (Sun et al., 2022). So, the trend of the scaling mitigation effect in the sine wave condition does not change and the degree of the effect is strengthened by the relatively high total energy of the square wave. As a result, since the trend was maintained unchanged, frequency is still a critical operating condition that is more important and sensitive than waveform.

In **Fig. 5-6B**, in order to evaluate the performance change of AC operation according to the ionic composition of the feed solution and its

applicability in harsh conditions, a mixture solution with the addition of multivalent ions (NaCl 197,000 mg l^{-1}, $CaCO_3$ 2,000 mg l^{-1}, and $CaSO_4$ 1,000 mg l^{-1}) but under the same TDS condition was employed in the ECMD experiments. Compared to the results of the monovalent ion solution (**Fig. 5-6A**), a dramatic flux decline was confirmed earlier in all conditions (**Fig. 5-6B**). In the 1 Hz condition, the flux reduction was also severe, and the final CF value significantly decreased from about 1.8 to 1.5. In the 5 Hz condition, although less than in the 1 Hz condition, an increase in flux decline was confirmed with a final CF of 1.5. The most severe flux drop in the 10 Hz condition was observed as the final CF decreased to 1.4. Distillate conductivity was also similar to the previous trend. This is due to the high scaling potential of the solution, and the kind of production scale. As multivalent ions are added, homogeneous nucleation by high scaling potential of multivalent ions becomes possible even at a lower CF, and membrane wetting may be induced by the deposition of generated nuclei, which affects the flux (Kim et al., 2018a). In addition, in the case of a monovalent ion solution, only the NaCl scale could occur, so only gradual flux decline occurs until scaling stage 3. In the case of a mixture solution including multivalent ions, the Ca-based scale could be generated by high scaling potential even in stages 1 to 2, The gradual flux decline was accelerated and maximized, and the final

CF was also reduced. This is also affected by the change in local pH according to the ECM surface charge (Zhu & Jassby, 2019). As a result, the increase in scaling potential and the change in the type of generated scale caused by the change in ionic composition with the addition of multivalent ions deteriorated the scaling mitigation effect by AC operation and caused additional MD performance degradation. Nevertheless, under the optimal condition of 5 Hz, the normalized flux was maintained above 0.9 in all experimental time ranges, confirming the practical applicability.

ECMD experiments were performed by increasing the voltage from 0.5 to 1.0 V to supplement and improve the reduction of the inorganic scaling mitigation effect of AC operation by multivalent ions (**Fig. 5-6C**). In the 1 Hz condition, the final CF did not increase. However, flux decline was reduced in both sine and square wave conditions, enough to maintain a normalized flux of 0.8 or more at final CF 1.5. In the 5 Hz condition, not only the flux increased, but also the final CF increased to 1.6. On the other hand, at 10 Hz, the final CF was significantly reduced by about 0.1 compared to the 0.5 V condition. Still, similar distillate conductivity trends were observed. When the voltage was increased to 1.0 V, except for the 10 Hz condition, the inorganic scaling mitigation effect was improved along with the increase in flux and final CF. This is

due to increased electrical force between the SWNT ECM surface and both cations and anions. As the voltage increases, the SWNT ECM surface charge increases, and the control effect by electrostatic interaction (attraction, repulsion) and electrophoresis between ECM and both ions increase, so the probability of nucleation could be lowered. While, at 10 Hz conditions, nucleation by mixing was already present due to excessive ions movement, so it is further promoted, and more scales are generated, adversely affecting MD performance.

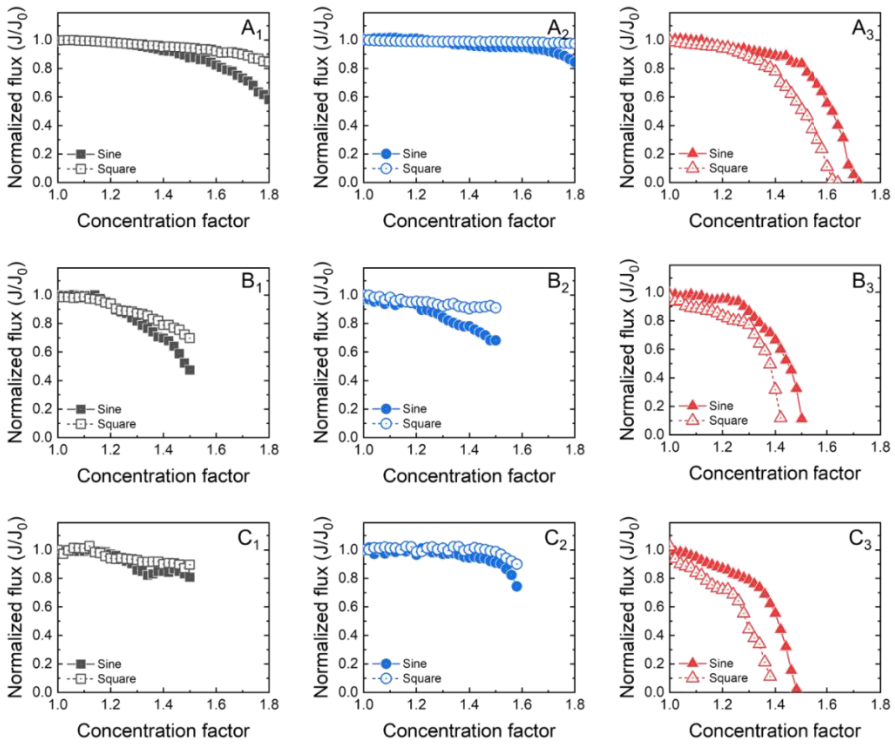

Figure 5-6 ECMD normalized flux under various operating conditions. A_1, A_2, and A_3 are results of square wave, B_1, B_2, and B_3 are results of multivalent ion solution, and C_1, C_2, and C_3 are results

of 1.0 V of the 1, 5, and 10 Hz conditions, respectively. The SWNT-4 membrane was used with a feed solution concentration of 200,000 mg l^{-1} (NaCl single, mixture solution).

As a result, AC operation using SWNT ECM showed a promising opportunity to achieve sustainable operation through inorganic scaling alleviation of the MD process. Frequency, waveform, ionic composition, and applied voltage were evaluated systematically and experimentally from the viewpoint of inorganic scaling mitigation effects. The frequency, which showed the most significant effect on performance was the most important operating condition. Further, the scaling mitigation effect was different according to the energy difference of the waveform, and the AC operation performance decreased as the scaling potential increased according to the ionic composition of the feed solution. The reduced scaling mitigation effect could be improved by increasing the electrostatic interaction between the ions and the ECM surface by increasing the applied voltage. However, since this analysis is only qualitative, additional quantitative analysis of the effect of SWNT ECM AC operation on MD performance should be preempted to understand the mechanism more accurately and evaluate the process applicability.

5.3.3. Optimization of operating parameters and identification of scaling mitigation mechanisms for practical application

Practical application of AC operation using ECM can begin with accurately identifying the scaling mitigation mechanism and a detailed understanding of the effects of each operating condition. For a thorough valorization of AC operation, a quantitative comparative evaluation was performed for each operating condition for flux decline rate (FDR) and final CF, which are the most intuitive and representative MD performance parameters. In addition, it is essential to consider the behavior of ions for an accurate understanding of the scaling mitigation mechanism. The ion velocity and ion moving distance (IMD), the most direct parameters related to the movement of ions in the solution, were calculated and evaluated for each operating condition.

Fig. 5-7A shows the flux change, or FDR, from the water production point of view of the MD process. Under the 1 Hz condition, FDR decreased to 0.1829 under the square wave condition compared to 0.4457 under the most basic condition of 0.5 V / Sine / Monovalent, and increased to 1.0218 and 0.5876 under the multivalent condition under the sine and square wave conditions, respectively. In the 1.0 V condition, it decreased again to 0.3885 and 0.2092, respectively. This tendency was similarly confirmed in the 5 Hz condition, but the overall FDR value was

about 50% lower than that in the 1 Hz condition. On the other hand, a sharp increase in the FDR value was observed in the 10 Hz condition. The trend was reversed as opposed to the 1 and 5 Hz conditions. A square wave showed a higher FDR value than a sine wave and 1.0 V higher than 0.5 V. Under the condition of 1.0 V / Square / 10 Hz, the FDR value was the highest at 3.1686. The average FDR values for all conditions for 1, 5, and 10 Hz were 0.4726, 0.1946, and 1.7148, respectively. Compared to the average FDR value of 1.5815 in the non-ECM experiment (pristine PVDF case), there was a clear decrease in FDR in the 1 and 5 Hz conditions, and a slight increase in FDR in the 10 Hz condition. As a result, the most significant change in FDR was confirmed according to the frequency in accordance with the results of the experiment, the 5 Hz condition was confirmed to be optimal for the purpose of scaling mitigation, and the 10 Hz condition aggravated water production enough to increase the FDR by about 9 times or more.

Another water production performance indicator, final CF, was also evaluated for each operating condition (**Fig. 5-7B**). In the 1, 5 Hz condition, the final CF was the highest in the monovalent condition and was further increased in the square wave condition. In the multivalent condition, the overall final CF was reduced and slightly increased when the 1.0 V condition was applied. While, under the 10 Hz condition, the

final CF decreased under the square wave condition and tended to decrease under both the multivalent condition and the 1.0 V condition. The average final CF values for all conditions at 1, 5, and 10 Hz were 1.3767, 1.5867, and 1.1950, respectively. Compared to the average final CF value of 1.2467 in the non-ECM experiment (pristine PVDF case), an apparent increase in the final CF was confirmed in the 1 and 5 Hz conditions, and a slight decrease in the final CF was confirmed in the 10 Hz condition. This trend coincides with the FDR value, and 1 and 5 Hz conditions are suitable for maintaining the performance of AC operation, and among them, the 5 Hz condition is found to be optimal with a CF increase of about 27%. In the 10 Hz condition, it was confirmed that scaling worsened and caused performance degradation.

For an accurate theoretical analysis of the mechanism based on quantitative analysis of performance parameters, ion velocity and IMD, which are key factors related to the behavior of ions according to AC operation, were newly considered (**Fig. 5-7C, D**). Ion velocity was 3.28 $\times 10^{-8}$ m/s under the most basic condition of 0.5 V / Sine / Monovalent, and increased to 4.63 $\times 10^{-8}$ m/s when a square wave was applied. In contrast, there was almost no change in the multivalent condition because the ratio of multivalent ions was low. As the voltage increased from 0.5 to 1.0 V, the ion velocity was found to have a proportional

relationship with the applied voltage due to the increased electrostatic force on the ions and ECM surfaces. By contrast, the frequency did not affect the ion velocity at all. In the case of IMD, the 1 Hz condition equals the value of ion velocity because it oscillates once per second. In the conditions of 5 and 10 Hz, as the frequency increases, the movement time is inversely proportional, so the IMD values are exactly inversely proportional. The average IMD values for 1, 5, and 10 Hz were 3.96×10^{-8}, 1.58×10^{-8}, and 3.96×10^{-9} m, respectively. The previous FDR and final CF analysis concluded that the most important operating condition was the frequency and the optimal point was 5 Hz. Since the ion velocity is not affected by the frequency, it was found that it is not an important factor influencing the mechanism, and the IMD value of about 1.58×10^{-8} m under the condition of the optimal frequency of 5 Hz is considered to be near the optimal operating condition.

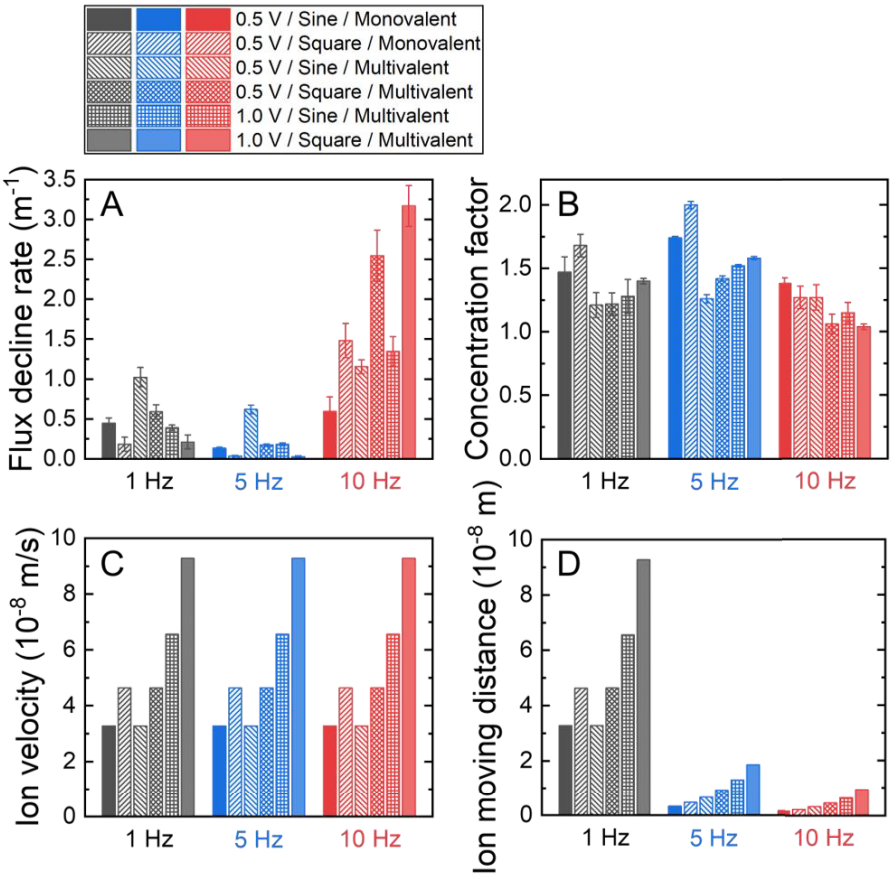

Figure 5-7 Quantitative analyses for ECMD performance parameters under various operating conditions. A: FDR, B: Final CF, C: ion velocity, and D: IMD. Each value was measured and calculated for each ECMD operating condition (frequency, waveform, ionic composition, and voltage).

Among the operating conditions revealed, frequency and applied voltage are the ones that have the most influence on scaling mitigation and can be easily controlled from an operation point of view. Therefore, FDR decline rate, CF increase, and Specific electrical energy

consumption (SEEC) in terms of energy consumption were introduced to quantitatively compare the actual scaling mitigation effect, rather than simple MD performance behavior, such as flux, rejection, according to frequency and applied voltage. **Fig. 5-8A** shows the change in FDR decline rate with frequency and applied voltage. In the range of 1 ~ 5 Hz, the FDR decline rate increased as the frequency increased, but it showed a tendency to decrease in the range of 5 ~ 10 Hz. In the case of applied voltage, there was a proportional relationship with the FDR decline rate within all ranges. These results can be interpreted as ion velocity, IMD. The higher the FDR decline rate, the more the flux decline by scaling is alleviated and the water production is increased, which was confirmed at the frequency optimal point around 5 Hz. The IMD at this time was about 1.0×10^{-8} m, which is consistent with the previous FDR and final CF analysis results. In the similar IMD range, the ion velocity, which increases with voltage, and the FDR decline rate also increased to about 100%. As a result, IMD 1.0×10^{-8} m is the optimum condition for AC operation to mitigate scaling, and within such range, higher ion velocity according to the applied voltage results in better performance. In the case of CF increase, the overall trend was similar to that of the FDR decline rate. The frequency condition of 5 Hz was the optimal point, and the IMD value at that time was 1.0×10^{-8} m (**Fig. 5-8B**). The higher the ion

velocity according to the applied voltage, the higher the CF increase, reaching 0.5 in the optimal condition compared to the lowest – 0.3 (10 Hz condition), showing an increase of about 0.8.

However, SEEC showed a different pattern. SEEC was decreased as the frequency and voltage were lowered, and the energy efficiency increased (**Fig. 5-8C**). At 5 Hz / 1.0 V, which was optimal in terms of water production, the SEEC was rather close to 75 kWh/m^3, and the energy efficiency was relatively low compared to 34 kWh/m^3 of optimal condition (1 Hz / 0.5 V). This can be the basis that ECM AC operation needs to be optimized comprehensively considering energy consumption, not just water production. Under the 5 Hz / 1.0 V condition, the water recovery rate was increased due to the effective control of scaling, but the water production efficiency was not high considering the continuous electrical energy input, increasing the SEEC value. However, in the 1 Hz / 0.5 V condition, although the increase in the water recovery rate was not high compared to the 5 Hz / 1.0 V condition, the additional electrical energy consumption time was short, so the SEEC value of excellent efficiency was achieved through an appropriate amount of additional water recovery in a short time. As such, it is expected that integrated process modeling from the energy perspective of ECMD AC operation will be required as a prerequisite for practical application in the future.

However, the optimum value of SEEC is 34 kWh/m^3, which may be slightly higher than the conventional enrichment process (Jamil & Zubair, 2017; Lin & Malmali, 2023). However, the modules and operating conditions of the ECMD AC operation have not been optimized yet, and the ECMD process is very advantageous in connecting with new and renewable energy, such as waste heat and electrical energy, compared to the conventional process, so there is much potential for further improvement. Therefore, it has excellent potential in the future industrial market where zero liquid discharge and carbon neutrality are required.

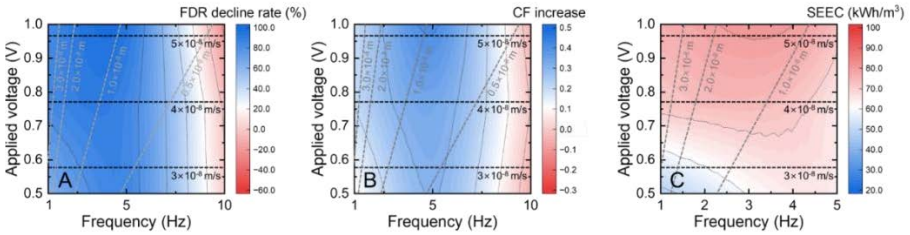

Figure 5-8 Evaluation of the scaling mitigation effect for each critical operating condition in terms of water production and energy consumption. A: FDR decline rate, B: CF increase, and C: SEEC.

A scaling mitigation mechanism for ECMD AC operation was proposed based on a quantitative and comparative analysis of parameters related to MD performance for each operating condition (**Fig. 5-9**). AC is applied to convert the charge on the SWNT ECM surface continuously,

and it is possible to control both cations and anions with high concentration by concentration polarization (CP) on the surface. In detail, SWNT ECM is used as an anode to attract anions and repulse cations when the surface is positively charged, and conversely to attract cations and repulse anions when the surface is negatively charged when used as a cathode. It lowers the scaling potential by fundamentally preventing collisions or nucleation between each other by separating anions and cations into ECM and counter electrode, respectively. This tends to vary depending on IMD, and if IMD is more significant than 1.0×10^{-8} m, the ion separation effect is insignificant, and if it is small, the ion is rather too concentrated, increasing the possibility of collision, which promotes scaling. 1.0×10^{-8} m is the optimal point of IMD, and the inorganic scaling mitigation effect is the greatest due to proper ion separation without the possibility of additional ion collisions. IMD is proportional to the applied voltage and inversely proportional to frequency, but the effect of frequency is greater in the range of normal AC operation operating conditions. As a result, in the experimental range of this study, the scaling mitigation effect at the optimal frequency of 5 Hz was much better than that of other frequency ranges, and this increased as the applied voltage increased within the same frequency level. As a result, controlling the IMD in an appropriate range through optimization of

operating conditions for each ion composition and concentration, that is, properly maintaining the formation and disturbance of the electrical double layer (EDL) on the surface of the membrane, is the optimal operating strategy of ECMD AC operation. This makes it possible to take a step closer to ZLD by enabling sustainable low-energy MD operations in high recovery conditions.

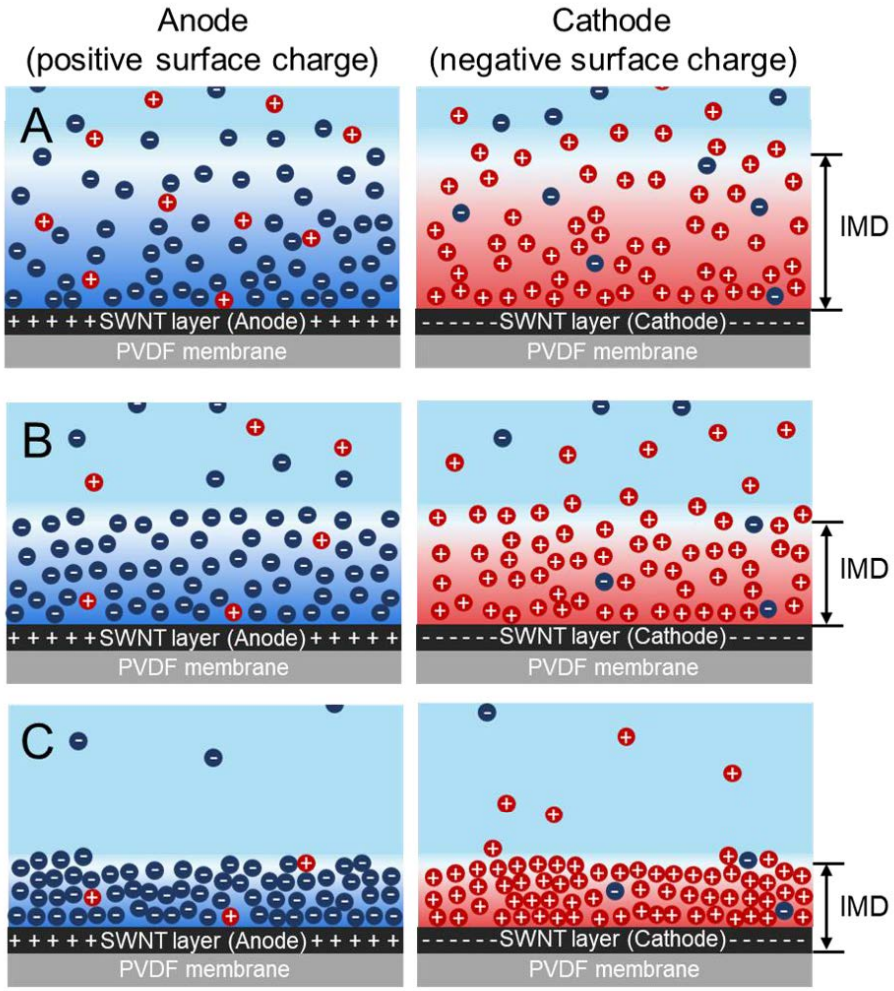

Figure 5-9 Scaling mitigation mechanisms for ECMD AC operation based on quantitative comparative analyses of parameters related to MD performance for each operating condition. A: IMD > 1.0×10^{-8} m case, B: IMD ≈ 1.0×10^{-8} m case, and C: IMD < 1.0×10^{-8} m case.

5.4. Conclusions

In this study, SWNT ECMD AC operation with excellent salt rejection and strong anti-scaling performance was developed and evaluated for ZLD through sustainable MD operation. The efficient modification of SWNT not only secured the ECM's anti-scaling physicochemical characteristics (low roughness, high DCA), but also enabled electrostatic interaction between ECM and ions to alleviate heterogeneous nucleation caused by solution concentration following continuous moisture-vapor conversion on the membrane surface, and electrophoresis of ions induced by the sufficient electrical conductivity of SWNT.

The applicability evaluation of AC operation was conducted through a systematic ECMD performance experimental set according to operating conditions (frequency, waveform, ionic composition, and applied voltage). Based on an accurate understanding of the mechanism, a quantitative comparative evaluation was performed for each operating condition for the performance parameters (FDR, final CF) to achieve the ultimate practical application. Frequency was the most important factor in ECMD AC operation and was optimized with excellent anti-scaling (88% of FDR decrease) and water production performance (27% of CF increase) compared to the existing MD process. The optimum value of SEEC was 34 kWh/m^3, which confirmed its competitiveness compared

to the conventional process, but the need for additional research in terms of energy consumption was also confirmed. Theoretical scaling mitigation mechanisms of ECMD AC operation based on experimental data were proposed, and it was reconfirmed that frequency is one of the main factors because it is possible to control both the EDL on the membrane surface and cations and anions in the solution together by adjusting the IMD.

In conclusion of this study, the development of SWNT ECM and AC operation for efficient and sustainable MD operation were proposed. An anti-scaling, electrically conductive surface was constructed on the pristine PVDF membrane through SWNT modification, and inorganic scaling mitigation was achieved by controlling IMD and EDL on the membrane surface through critical operating conditions (frequency, applied voltage) control. It is expected that this microscopic understanding of ionic interactions not only presents an effective route for water treatment to realize ZLD, but also has promising potential to help the electrocatalyst field that can be combined with future energy production.

Chapter 6. Electrochemical cleaning (EC) in electrically conductive membrane distillation (ECMD): Its mechanisms and operation strategies

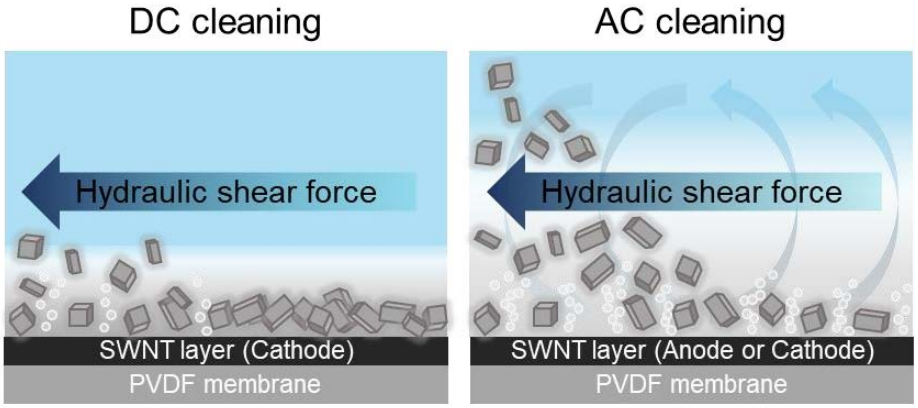

This chapter is based on:
Kim, J., Tijing, L.D., Shon, H.K. and Hong, S. Electrochemical cleaning (EC) in electrically conductive membrane distillation (ECMD): Its mechanisms and operation strategies.

6.1. Introduction

MD can achieve high water recovery and high-quality permeate, but its performance can be limited by fouling and scaling on the membrane surface. In particular, scaling control in the MD process has different efficiency depending on the scaling stage, and permanent membrane damage may not be perfectly controlled even with cleaning under optimal conditions (Karanikola et al., 2018; Kim et al., 2017a; Wang et al., 2021; Xie et al., 2023).

To address this issue, researchers have explored the application of electrically conductive membranes (ECM) in MD to enhance performance and control scaling (Han et al., 2021; Jiang et al., 2019; Kim, Yun, et al., 2022; Shin et al., 2020). ECM can generate an electric field across the membrane surface and modify the transport properties of ions and water molecules, which can enhance the separation efficiency and reduce fouling and scaling (Chen et al., 2022; Huang et al., 2023; L. L. Xu et al., 2021). Moreover, electrochemical cleaning (EC) can be performed on the membrane surface using direct current (DC) or alternating current (AC) to remove scaling and restore the membrane performance (Barbhuiya et al., 2021; Jung et al., 2023; J. H. Lee et al., 2022; Y. Zhang et al., 2021).

There are two types of EC methods: DC and AC. DC EC operates by inducing an electric field across the membrane surface, which attracts ions in the feed solution to the oppositely charged ions on the membrane surface. This flow of ions can help to prevent fouling and scaling on the membrane surface. However, if scaling and fouling deposits have already formed on the membrane surface, DC alone may not be sufficient to remove them (Rao et al., 2020).

On the other hand, AC EC operates by inducing an oscillating electric field across the membrane surface. This oscillating field causes the water molecules to vibrate, generating heat through a process known as joule heating (Ahmed et al., 2022; Dudchenko et al., 2017; Zuo et al., 2020). This heat can help to soften and loosen the inorganic scaling and fouling deposits, making them easier to remove from the membrane surface (Anvari, Kekre, et al., 2020; Duong et al., 2016; Han et al., 2022; Lohaus et al., 2020). In addition, AC can induce mechanical forces to remove scaling and fouling deposits, which makes it more effective than DC for inorganic scaling cleaning.

This study aims to evaluate the feasibility of EC cleaning for inorganic scaling using DC, and AC operation in the ECMD process. Specifically, we will discuss the advantages of the membrane process in water treatment compared to the conventional process, the benefits of

membrane distillation in terms of high water recovery and high-quality permeate, the application of electrically conductive membrane to MD for intensifying performance, and the advantages and mechanisms of EC with DC, AC operation. The proposed method could contribute to increasing the potential of ECMD technology for inorganic scaling control in water treatment and identify the research gaps and future directions.

6.2. Materials and methods

6.2.1. Modification methods of SWNT ECM

A commercial polyvinylidene fluoride (PVDF) membrane (GVHP14250, Millipore) was used as the base for ECM production. A homogeneous SWNT solution was prepared by stirring 0.08 g of single-wall carbon nanotube powder (SWNTs) (D1.5L1-5-S, Nanolab), 250 mL of 2-propanol (Sigma-Aldrich), and 75 μL of 5 wt% Nafion (Sigma-Aldrich) solution. This solution was filtered onto the PVDF membrane and dried to be stably coated on the surface. This process was repeated up to four times to enhance the electrical conductivity of the ECM.

6.2.2. MD inorganic scaling EC experiments

MD inorganic scaling EC experiments were conducted using a lab-scale MD unit. NaCl solution with a relatively high concentration of 200,000 ppm was employed as the feed solution for the scaling experiments to overcome the limitations of the small effective membrane area of 20.02 cm^2, and DI water was used as the distillate solution, with 2L. MD operation was performed in a DCMD configuration using SWNT ECM prepared as described above. The feed and distillate solutions were circulated stably at a flow rate of 0.6 LPM using a gear pump, and were maintained at 60 and 20 °C, respectively, using a

constant temperature bath. To measure water production and quality, the weight and electrical conductivity of the distillate were monitored throughout the entire experiment using an electrical balance and a conductivity meter (HACH® HQ40d). After the scaling experiments were completed, EC experiments were performed according to the scaling stage. Power was provided stably by a potentiostat (Autolab, PGSTAT204) for EC, and DI water was used for hydraulic flushing, which was circulated in the feed channel for 15 minutes at a flow rate of 1.2 LPM. The applied voltage in the EC experiment was 0.5, 1.0 V, and the frequency was 20 kHz.

6.3. Results and discussions

6.3.1. Optimal scaling cleaning strategy for sustainable MD operation

Scaling can not only affect the performance of the MD process, but also cause permanent damage to the membrane, limiting the recovery of flux through cleaning. In addition, the cleaning efficiency is determined by the flux recovery and maintenance through cycle repetition. Hydraulic flushing experiments were performed for each scaling stage to evaluate the efficiency of cleaning methods.

Fig. 6-1 shows the average flux recovery rates based on flux behavior and hydraulic flushing for each scaling stage. During three cycles of MD operation over 24 hours, similar flux decline trends were observed for all three conditions from 0 to 24 hours during the first cycle. From 14 hours onwards, a gradual decline in flux occurred, which intensified after 17 hours. The MD operation was maintained until the normalized flux values reached 0.8, 0.3, and 0.0 for scaling stages 1, 2, and 3, respectively. In the second and third cycles (24-48 and 48-72 hours, respectively) following the first hydraulic flushing, only initial flux differences were observed based on cleaning efficiency, while the flux decline trends were similar to those in the first cycle.

Flux recovery rates were calculated for a quantitative comparison of cleaning efficiency by hydraulic flushing at each scaling stage. In **Fig. 6-1B**, after 24 hours of operation and hydraulic flushing (cleaning cycle 1), the flux recovery rates for each scaling stage were 95.22, 77.54, and 42.12% for stages 1, 2, and 3, respectively. After 48 hours of operation (cleaning cycle 2), the flux recovery rates were 92.84, 62.11, and 18.42% for stages 1, 2, and 3, respectively. Ultimately, the flux recovery rate by the hydraulic flushing was highest under scaling stage 1 conditions, and decreased with increasing cleaning cycles. Scaling stage 2 conditions showed a slight decrease in flux recovery rate, and this trend was further exacerbated under scaling stage 3 conditions.

This is due to the difference in the location of scaling formation between scaling stages. Scaling was easily removed by hydraulic flushing in Stage 1 because scale deposits only accumulated on the membrane surface and had not yet extended into the membrane pores. In contrast, in Stages 2 and 3, cleaning led to a significant decrease in flux recovery due to increased cleaning cycles. Particularly in Stage 3 cleaning, the flux recovery rate decreased to less than 40% in all cycles compared to the previous stages. In Stages 2 and 3, scales are deposited on the membrane surface and partially block the membrane pore surface, and some scale deposits even penetrate the pore. Although some scale

layers on the membrane surface are removed during cleaning, the scale deposits formed inside the pores cannot be removed. As a result, partially blocked pores lead to higher transport resistance of the membrane, contributing to lower flux recovery in the cleaning process of Stages 2 and 3.

Considering the scaling formation stages, membrane cleaning in Stage 1 showed excellent flux recovery of over 92% for all scalants. In Stages 2 and 3, irreversible scaling effects were found inside the membrane pores, indicating a significant decrease in cleaning efficiency. In this regard, to achieve sustainable MD operation, membrane cleaning before reaching Stage 2 after Stage 1 can be optimally considered. However, hydraulic cleaning after Stage 1 may increase the number of cleaning, resulting in additional cost increases. Therefore, it is essential to develop a new cleaning method that can achieve flux recovery of over 90% through cleaning after Stages 2 and 3.

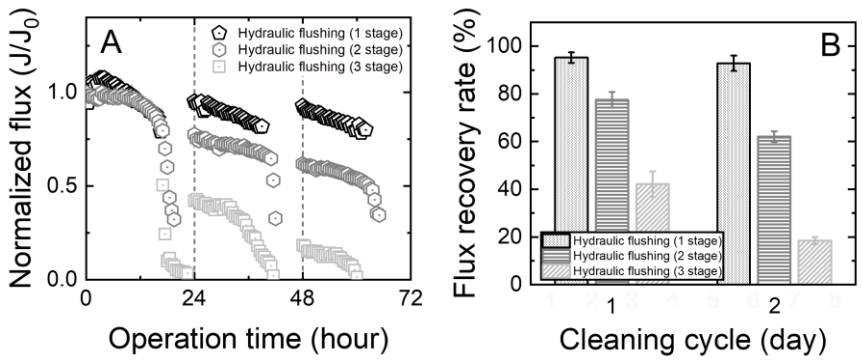

Figure 6-1 Effect of hydraulic flushing on MD performance parameters by scaling stage: (A) Normalized flux behavior, (B) flux recovery rate.

6.3.2. Evaluation of cleaning efficiency according to operation conditions (DC, AC)

To remove scaling in stages 2 and 3 that was not eliminated by conventional hydraulic flushing, a new cleaning method (EC) was introduced. The EC aims to improve overall flux recovery by not only removing scaling on the membrane surface but also targeting the cleaning of scaling inside the inlet of the pore. This is achieved not only by simple fluid dynamic flow-based removal but also by inducing detachment of scaling from the membrane itself.

Fig. 6-2 shows the performance behavior of EC using DC. To compare the performance of EC with conventional cleaning methods, hydraulic flushing (stage 3) is also presented. It was observed that EC (DC) maintained a high normalized flux value despite the stage 3 cleaning. This trend was maintained even after repeated cleaning cycles. However, this varied depending on the voltage conditions. At 0.5 V conditions, EC (DC) maintained a generally higher normalized flux than hydraulic flushing, but a gradual decrease in flux was observed as the cleaning cycle increased. On the other hand, at 1.0 V conditions, even with an increased cleaning cycle, a stable normalized flux of around 0.8 or higher was maintained.

The flux recovery rate was calculated for each condition to analyze these results quantitatively. For a cleaning cycle of 1 day, the flux recovery rates for hydraulic flushing, EC (DC 0.5 V), and EC (DC 1.0 V) were 42.12, 85.48, and 91.46%, respectively. For a cleaning cycle of 2 days, the flux recovery rates were 18.42, 72.85, and 87.88%, respectively. Hydraulic flushing showed meager flux recovery rates in all conditions and was limited to applying inorganic scaling cleaning. Although the EC (DC 0.5 V) condition exhibited a dramatic increase in flux recovery rate, it revealed a weakness in maintaining stable performance as it decreased with increasing cleaning cycles. On the other hand, the EC (DC 1.0 V) condition showed a somewhat reduced trend in the decrease of flux recovery rate with cleaning cycles, but it was still below the stable cleaning efficiency criterion of 90% even after two cycles, indicating a limitation in achieving complete cleaning of the scaling stages 2 and 3.

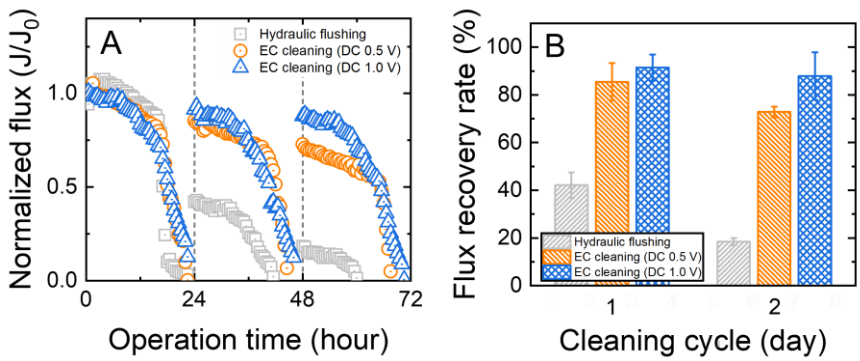

Figure 6-2 Effect of EC (DC) on MD performance parameters by operation conditions: (A) Normalized flux behavior, (B) flux recovery rate.

To overcome the drawbacks of DC operation, AC operation has been introduced. It is expected that the cleaning efficiency will be enhanced by the periodic change in membrane surface charge using AC. **Fig 6-3** shows the performance of EC using AC. After 0-24 hours of operation, the normalized flux was maintained at a high level similar to EC (DC) when EC (AC) was used. In particular, a higher cleaning efficiency was indirectly confirmed by the delayed flux decline point compared to EC (DC) during 24-48 hours of operation. This trend was more clearly observed after the second EC (AC) operation. Unlike the decrease in initial flux observed after the second EC (DC), there was no significant decrease in initial flux after the second EC (AC), and it was maintained similarly to the value at the start of the experiment. This is believed to be due to the additional removal of scaling on the membrane surface that was not cleaned by EC (DC).

For quantitative comparison, the flux recovery rate was calculated. For the cleaning cycle of 1 day, the flux recovery rates for hydraulic flushing, EC (AC 0.5 V), and EC (AC 1.0 V) conditions were 42.12, 94.88, and 97.88%, respectively. For the cleaning cycle of 2 days, the flux recovery

rates were 18.42, 90.16, and 95.78%, respectively. As a result, EC (AC) showed a cleaning efficiency of over 90% in all cycles and applied voltage conditions, and was found to be a highly suitable method for inorganic scaling cleaning. In particular, the disadvantage of EC (DC), which was the gradual decrease in cleaning efficiency with repeated cycles, was improved and a cleaning efficiency of over 95% was achieved after two cycles.

Overall, it was confirmed that inorganic scaling cleaning in the MD process was limited by hydraulic flushing and EC was introduced to solve this issue. While the cleaning efficiency of EC (DC) was improved, there was a gradual decrease in cleaning efficiency with repeated cycles, making it impractical for the actual application. On the other hand, EC (AC) maintained a high flux recovery rate of over 95% even with repeated cycles, and effective cleaning performance was secured after scaling stages 2 and 3. However, this is only a simple performance evaluation, and for practical application, a detailed quantitative evaluation of each method and a thorough understanding of the cleaning mechanism are required.

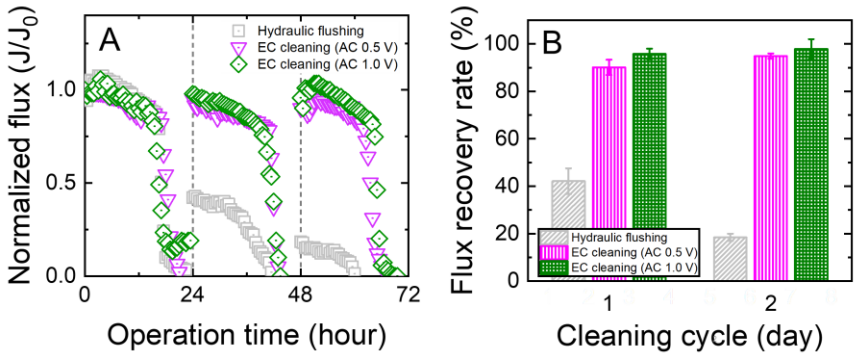

Figure 6-3 Effect of EC (AC) on MD performance parameters by operation conditions: (A) Normalized flux behavior, (B) flux recovery rate.

6.3.3. Identification of mechanisms and optimization of AC cleaning

In the previous section, experiments were conducted to evaluate the performance of EC (DC, AC). To quantitatively compare the cleaning efficiency according to each EC method and operating condition, the flux decline rate (FDR) was introduced. FDR is an indicator of the flux decrease over time, which can consider not only simple flux recovery due to membrane cleaning, but also the effect on the membrane performance change.

Fig 6-4 shows the change in FDR according to EC cleaning methods and operating conditions. In the case of hydraulic flushing, the initial FDR values were similar, but a sharp increase occurred from the second day, indicating a significant deterioration in cleaning performance. In particular, on the third day, the FDR value was confirmed to be over 10, making it impossible for practical use. EC was revealed to have good cleaning efficiency, maintaining low FDR values compared to hydraulic flushing for all conditions. A comparison of the performance of EC under different operating conditions was performed at a low FDR range (**Fig. 6-4B**). Under the EC (DC 0.5 V) condition, the initial FDR value was high at 4.49 %/h on the first day, increasing to 5.19 %/h on the second and third days, limiting the sustainability of MD performance due to the decrease in cleaning efficiency. As the FDR value continued to increase,

it was postulated that complete control of inorganic scaling was impossible under the EC (DC 0.5 V) condition, and that irreversible membrane damage would remain, making sustainable MD operation impossible. For the EC (DC 1.0 V) condition, an outstanding cleaning efficiency was confirmed with an initial FDR value of 3.44 %/h. However, as MD operation continued, a sharp increase in FDR occurred, ultimately reaching 5.23 %/h on the third day, indicating a deterioration in cleaning efficiency similar to that of the EC (DC 0.5 V) condition. As a result, although the initial decrease in FDR value, indicating an increase in cleaning efficiency, was observed as the applied voltage increased under the EC (DC) condition, complete scaling control was impossible with continued MD operation, resulting in irreversible membrane damage and an unavoidable increase in FDR.

The EC (AC 0.5 V) condition showed a tendency similar to the previous conditions. The FDR value on the first day was slightly lower than that of the EC (DC 0.5 V) condition at 4.09 %/h, but the difference was insignificant. However, the FDR value increased to 4.87 %/h on the second and third days. It showed a trend similar to the EC (DC 0.5 V) condition. On the other hand, the EC (AC 1.0 V) condition had a low FDR value of 3.88 %/h on the first day, and there was no significant increase in FDR even with continuous MD operation. Furthermore, the

FDR remained low at 4.15 %/h on the third day, indicating a very efficient cleaning performance compared to other conditions. Unlike other conditions where an increase in FDR due to irreversible membrane damage occurs with prolonged MD operation, the FDR increase rate over time was very low for the EC (AC 0.5 V) condition, making it the most efficient cleaning condition for long-term operation. In comparing the cleaning efficiency for different EC conditions, higher applied voltage resulted in lower FDR values and superior cleaning performance, with better performance observed in AC compared to DC. Especially, the EC (AC 1.0 V) condition was identified as the optimal cleaning condition for long-term operation, as the low initial FDR value was maintained stably throughout the experimental period.

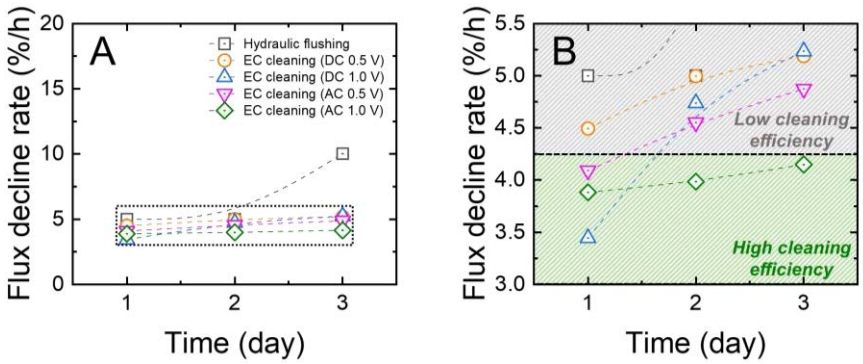

Figure 6-4 FDR changes according to EC method and operating conditions

Fig 6-5 shows the inorganic scaling cleaning mechanism (DC, AC) by EC. In ECMD, inorganic scaling and fouling deposits can occur on the membrane surface over time, reducing the efficiency of the distillation process. Various cleaning methods, including EC with DC and AC, have been studied to mitigate this issue. While both DC and AC can remove inorganic scaling, AC has been found to be more effective in some cases.

When DC is applied to the membrane surface, the charged ions in the feed solution are attracted to the oppositely charged ions on the membrane surface, creating a water flow in a single direction. This flow can help to prevent fouling and scaling on the membrane surface by sweeping away any particles or impurities that may adhere to the membrane. However, if scaling and fouling deposits have already formed on the membrane surface, DC alone may not be sufficient to remove them.

On the other hand, when an AC is applied to the membrane surface, the water molecules start to vibrate, generating heat through the joule heating (Ahmed et al., 2022; Lohaus et al., 2020; W. Ma et al., 2021). This heat can help to soften and loosen the inorganic scaling and fouling deposits, making them easier to remove from the membrane surface. In addition to joule heating, AC can also induce mechanical forces to remove scaling and fouling deposits. AC can cause the water molecules

to oscillate rapidly, creating a mechanical force that can help to dislodge the scaling and fouling from the membrane surface. This process is known as acoustic cavitation (Lee et al., 2017; J. Wang et al., 2016).

The combination of joule heating and acoustic cavitation makes AC more effective than DC for inorganic scaling cleaning. The heat generated by AC can help to dissolve or detach scaling and fouling deposits, while the mechanical forces can break them up and remove them from the membrane surface.

The behavior of water and the generation of air bubbles on the membrane surface can also differ between AC and DC cleaning methods. With DC, water flow is unidirectional, meaning that any air bubbles generated on the membrane surface during cleaning will be swept away in the same direction. However, with AC, the oscillating electric field can cause the water molecules to vibrate, creating a more turbulent water flow. This turbulence can cause air bubbles on the membrane surface, which can help dislodge and remove scaling and fouling deposits. The formation of air bubbles during AC cleaning contributes to the overall cleaning efficiency of the process. In the long-term operation, in the reduction electrode, hydrogen is generated while oxygen is produced in the oxidation electrode. However, in the case of DC, changes in the pH of the solution can adversely affect the process. On the other hand, AC

is advantageous for practical use as it can minimize this negative impact since ECM can be utilized for both the cathode and anode. Additionally, in the case of DC, the water flow on the membrane surface is relatively low, and the scaling layer can clog the membrane surface, resulting in poor bubble production and cleaning efficiency. Conversely, AC has a more turbulent water flow on the surface, allowing better contact between water and the membrane, resulting in smooth bubble production and making removing the scaling layer on the membrane surface easier. Furthermore, this mechanism improves as the applied voltage increases, making it essential to optimize the applied voltage.

In summary, the cleaning mechanism and efficiency of inorganic scaling can differ between DC and AC cleaning methods in ECMD. While DC can help to prevent fouling and scaling by sweeping away particles and impurities in the feed solution, AC can induce joule heating and acoustic cavitation to more effectively remove scaling and fouling deposits that have already formed on the membrane surface. The behavior of water and the generation of air bubbles can also contribute to the cleaning efficiency of AC, making it a promising method for inorganic scaling cleaning in ECMD. AC not only helps with simple scaling removal but also contributes to the improvement of overall

cleaning efficiency by inducing the circulation of water on the membrane surface, which leads to increased efficiency of hydraulic flushing.

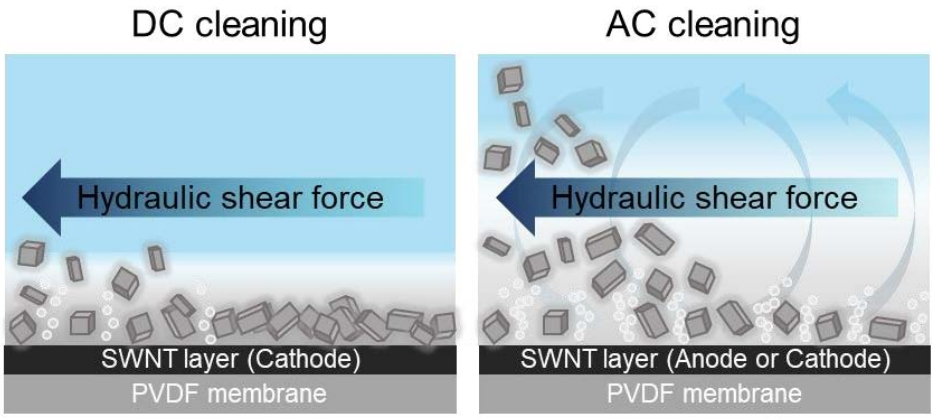

Figure 6-5 Inorganic scaling cleaning mechanism (DC, AC) by EC

6.4. Conclusions

In this study, the effect of electrochemical cleaning (EC) was investigated for controlling inorganic scaling in MD processes. The cleaning efficiency of EC was systematically evaluated under DC, AC, and various applied voltage conditions. Optimal conditions and the inorganic scaling cleaning mechanism were identified through quantitative comparisons of the FDR values for each condition. The key findings of this study are as follows:

- Conventional hydraulic flushing for inorganic scaling cleaning showed a rapid decrease in efficiency for scaling stages 2 and 3,

and although cleaning efficiency was good for stage 1, its practical application in the process is limited when considering cleaning cycles.

- EC could achieve stage 3 cleaning, and AC was more effective than DC, with higher voltages leading to better and more stable long-term MD performance without a decrease in cleaning efficiency with increasing cycles.
- The mechanism of EC involves scaling removal due to bubble generation on the membrane surface and increased hydraulic flushing due to the generation of turbulence. Additional research is required for reducing energy consumption and optimization module development through related operational condition optimization for practical application.

7. Conclusions and recommendations

7.1. Conclusions

This study aims to improve fouling mitigation performance under high recovery conditions and ultimately achieve ZLD by applying effective ECM technology to MD operations. In terms of the perspective of the study, fundamental and detailed mechanisms for inorganic scaling phenomena in MD processes were investigated. Based on this, the feasibility of ECM technology was evaluated through operational optimization and water production performance assessment for scaling control and membrane cleaning purposes.

In Chapter 3, a thorough literature review was conducted on the current status and limitations of ECM technology for fouling control. Fundamental mechanisms such as electrochemical oxidation and reduction, electrostatic interaction, and microbubble by electrolysis were suggested. Through an analysis of ECM application cases for each membrane process, the current performance trends and limitations of fouling control through process-specific ECM were confirmed. This led to the derivation and presentation of future directions for ECM technology, including understanding feedwater composition from an ECM perspective, selection of appropriate modification materials, and effective and optimized low-energy operation.

In Chapter 4, to understand and identify the fundamental mechanisms for inorganic scaling in MD processes, synthetic solutions of ion mixtures were used to evaluate inorganic scaling in actual MD processes. Scaling stages were confirmed, and optimal MD operation conditions were suggested for each stage.

In Chapter 5, ECM operation for scaling control was theoretically and experimentally evaluated. Additionally, ECMD AC operation was applied as a new scaling control mode, which showed excellent performance (88% of FDR decrease and 27% of CF increase), and the effects of each operating parameter on scaling control performance were evaluated and optimized for low-energy consumption (34 kWh/m^3). Based on these findings, the scaling control mechanism for ECMD AC operation was first suggested.

In Chapter 6, a new application of ECM, the EC concept, was presented and experimentally evaluated. The superiority of EC AC operation was demonstrated, and the ECM scaling cleaning mechanism was presented. As a result, excellent membrane cleaning efficiency was achieved through EC AC (2.6 times higher than conventional cleaning methods), and the value of ECM technology as a new scaling cleaning method was confirmed.

In conclusion, this study thoroughly and systematically evaluated the use of ECM technology for scaling control and confirmed the limitations of the current technology. By applying ECM technology to MD scaling control, more than twice the water productivity compared to conventional technology was achieved. Furthermore, it is expected that the maturity of ECM technology will be enhanced by establishing and optimizing customized fouling control operation strategies such as AC operation and ECMD. Additionally, based on this study, future directions have been proposed to enhance the applicability of ECM technology. Therefore, it is expected that ECMD will contribute to overcoming the global water resource shortage crisis as a valuable concentration technology in the future.

7.2. Recommendations

Despite the excellent scalability potential of ECMD technology in various fields utilizing electrochemical phenomena, its research maturity remains relatively low as it is still in the fundamental research stage. Therefore, various studies must be conducted to enhance its practical applicability, extending beyond mere inorganic scaling mitigation to encompass ion behavior control in processes using electrolytes. Based on the content of this study, future directions to increase the feasibility

of ECMD technology include (1) a thorough review of expanded application areas, and (2) evaluation and selection of optimal ECM materials and operating modes (Fig. 7-1).

A thorough review of expanded application areas: The inorganic scaling mitigation of ECMD is based on the electrical interaction between the ECM surface and ions present within the solution. This mechanism can be applied not only to simple attraction and repulsion between the ECM and ions, but also to fields that require inducing or restricting ion movement. Firstly, it can be applied to the conventional electrochemical field of batteries. In lithium-ion batteries, charging and discharging are determined by the movement of lithium ions within the electrolyte, which is controlled using a semi-permeable membrane. The introduction of ECM technology could potentially enhance charging and discharging performance as well as overall battery life by increasing ion mobility. Recently, the emerging fields of green hydrogen production and carbon neutrality, which focus on improving sustainability, have also gained attention as promising application areas for ECM. Green hydrogen production is achieved through water electrolysis. Large-scale water electrolysis requires significant amounts of pure water and energy. Recently, direct seawater electrolysis has been actively researched to conserve water resources and energy consumption. Although catalyst

research for enhancing electrolysis efficiency is active, long-term efficiency declines rapidly due to scaling phenomena caused by the ionic components of seawater. These issues can be addressed by applying ECM technology and developing a new electrolysis cell configuration. Through this new configuration, the control of ion behavior in seawater can reduce the ion concentration in the electrolyte and block access to the electrode surface. Finally, it can be applied to carbon capture, utilization, and storage (CCUS) technology. In CCUS, carbon capture prevents the release of carbon dioxide into the air, while carbon conversion is carried out to utilize captured carbon. Processes such as membrane contactors are employed at this stage. Applying ECM technology to carbon capture and conversion can improve energy efficiency compared to conventional separation processes that require high thermal energy, and the catalytic action during carbon conversion can result in more efficient material transformation.

Evaluation and selection of optimal ECM materials and operating modes: In ECM technology, materials play a crucial role as they directly impact ion behavior. Generally, desirable material properties include high electrical conductivity and hydrophobicity. However, additional characteristics may be required depending on the specific application. In particular, for processes targeting the removal

and treatment of specific substances, the electrochemical reactivity to the target material will be a key factor in material evaluation. As the purpose of this study was MD inorganic scaling mitigation, SWNT alone provided satisfactory results. Nevertheless, electrochemical reactivity may be more critical in previously mentioned expanded application areas. Consequently, metal-organic frameworks (MOFs) could be promising ECM material candidates. Depending on MOFs' type and fabrication method, the reaction selectivity for specific ions can be controlled. This allows for improvements in battery efficiency using lithium-ion-targeted MOFs and enhanced carbon capture and conversion process efficiency using MOFs targeting carbon dioxide in the solution. Once the expanded application areas have been determined, it will be possible to evaluate and select the optimal ECM materials suited to the characteristics of each field. Furthermore, the evaluation of operating modes is essential. In this study, two operating modes, AC operation and EC, were assessed. AC operation was suitable for fields with high scaling potential or requiring a high water recovery rate, where ion behavior control was always essential (resource recovery, ZLD), while EC was more appropriate for fields with relatively low ion concentrations (brackish water desalination). Therefore, following the selection of expanded application areas, evaluations from an energy consumption optimization perspective

must be carried out according to the characteristics of each field. Furthermore, developing an optimal ECM module should be carried out simultaneously. In particular, ensuring the flow of water inside the module and the electrical conductivity, including the ECM, is the most crucial factor. Safety during long-term operation, energy efficiency, and power density will also be important considerations.

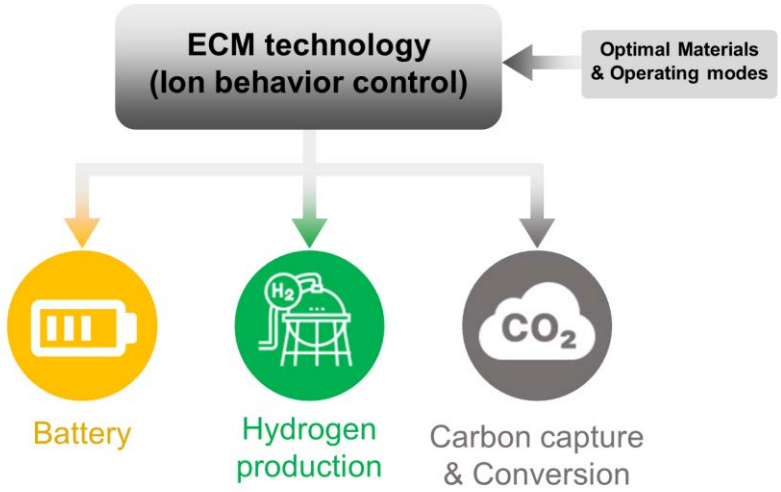

Figure 7-1 Expansion of applied fields of ECM technology and future research direction

REFERENCES

Abdel-Karim, A., Leaper, S., Skuse, C., Zaragoza, G., Gryta, M., & Gorgojo, P. (2021). Membrane cleaning and pretreatments in membrane distillation–a review. *Chemical Engineering Journal, 422*, 129696.

Abdulbaki, D., Al-Hindi, M., Yassine, A., & Abou Najm, M. (2017). An optimization model for the allocation of water resources. *Journal of Cleaner Production, 164*, 994-1006.

AbdulKadir, W. A. F. W., Ahmad, A. L., Seng, O. B., & Lah, N. F. C. (2020). Biomimetic hydrophobic membrane: A review of anti-wetting properties as a potential factor in membrane development for membrane distillation (MD). *Journal of Industrial and Engineering Chemistry, 91*, 15-36.

Adam, M. R., Othman, M. H. D., Kurniawan, T. A., Puteh, M. H., Ismail, A., Khongnakorn, W., Rahman, M. A., & Jaafar, J. (2022). Advances in adsorptive membrane technology for water treatment and resource recovery applications: A critical review. *Journal of Environmental Chemical Engineering*, 107633.

Aguila-Hernández, J., Trejo, A., & Gracia-Fadrique, J. (2001). Surface tension of aqueous solutions of alkanolamines: single amines, blended amines and systems with nonionic surfactants. *Fluid Phase Equilibria, 185*(1-2), 165-175.

Ahmad, A., Yasin, N. M., Derek, C., & Lim, J. (2013). Harvesting of microalgal biomass using MF membrane: Kinetic model, CDE model and extended DLVO theory. *Journal of membrane science, 446*, 341-349.

Ahmad, N., & Baddour, R. E. (2014). A review of sources, effects, disposal methods, and regulations of brine into marine environments. *Ocean & coastal management, 87*, 1-7.

Ahmed, F., Lalia, B. S., Kochkodan, V., Hilal, N., & Hashaikeh, R. (2016). Electrically conductive polymeric membranes for fouling prevention and detection: A review. *Desalination, 391*, 1-15.

Ahmed, F. E., Hashaikeh, R., & Hilal, N. (2019a). Fouling control in reverse osmosis membranes through modification with conductive carbon nanostructures. *Desalination, 470*, 114118.

Ahmed, F. E., Hashaikeh, R., & Hilal, N. (2019b). Solar powered desalination–Technology, energy and future outlook. *Desalination, 453*, 54-76.

Ahmed, F. E., Hilal, N., & Hashaikeh, R. (2018). Electrically conductive membranes for in situ fouling detection in membrane distillation

using impedance spectroscopy. *Journal of membrane science, 556*, 66-72.

Ahmed, F. E., Lalia, B. S., & Hashaikeh, R. (2017). Membrane-based detection of wetting phenomenon in direct contact membrane distillation. *Journal of membrane science, 535*, 89-93.

Ahmed, F. E., Lalia, B. S., Hashaikeh, R., & Hilal, N. (2022). Intermittent direct joule heating of membrane surface for seawater desalination by air gap membrane distillation. *Journal of membrane science, 648*, 120390.

Al-Abri, M., Al-Ghafri, B., Bora, T., Dobretsov, S., Dutta, J., Castelletto, S., Rosa, L., & Boretti, A. (2019). Chlorination disadvantages and alternative routes for biofouling control in reverse osmosis desalination. *NPJ Clean Water, 2*(1), 1-16.

Ali, A., Tufa, R. A., Macedonio, F., Curcio, E., & Drioli, E. (2018). Membrane technology in renewable-energy-driven desalination. *Renewable and Sustainable Energy Reviews, 81*, 1-21.

Alkhatib, A., Ayari, M. A., & Hawari, A. H. (2021). Fouling mitigation strategies for different foulants in membrane distillation. *Chemical Engineering and Processing-Process Intensification, 167*, 108517.

Alkhudhiri, A., Darwish, N., & Hilal, N. (2012). Membrane distillation: A comprehensive review. *Desalination, 287*, 2-18.

Alkhudhiri, A., & Hilal, N. (2017). Air gap membrane distillation: A detailed study of high saline solution. *Desalination, 403*, 179-186.

Alvarez, P. J., Chan, C. K., Elimelech, M., Halas, N. J., & Villagrán, D. (2018). Emerging opportunities for nanotechnology to enhance water security. *Nature Nanotechnology, 13*(8), 634-641.

Amirabedi, P., Akbari, A., & Yegani, R. (2019). Fabrication of hydrophobic PP/CH3SiO2 composite hollow fiber membrane for membrane contactor application. *Separation and Purification Technology, 228*, 115689.

Anis, S. F., Lalia, B. S., Hashaikeh, R., & Hilal, N. (2022). Titanium coating on ultrafiltration inorganic membranes for fouling control. *Separation and Purification Technology, 282*, 119997.

Anis, S. F., Lalia, B. S., Khair, M., Hashaikeh, R., & Hilal, N. (2021). Electro-ceramic self-cleaning membranes for biofouling control and prevention in water treatment. *Chemical Engineering Journal, 415*, 128395.

Anvari, A., Kekre, K. M., & Ronen, A. (2020). Scaling mitigation in radio-frequency induction heated membrane distillation. *Journal of membrane science, 600*, 117859.

Anvari, A., Yancheshme, A. A., Kekre, K. M., & Ronen, A. (2020). State-of-the-art methods for overcoming temperature polarization in membrane distillation process: A review. *Journal of membrane science, 616*, 118413.

Atchariyawut, S., Phattaranawik, J., Leiknes, T., & Jiraratananon, R. (2009). Application of ozonation membrane contacting system for dye wastewater treatment. *Separation and Purification Technology, 66*(1), 153-158.

Baker, R. W. (2012). *Membrane technology and applications*. John Wiley & Sons.

Bakeri, G., Ismail, A., Rana, D., & Matsuura, T. (2012). Development of high performance surface modified polyetherimide hollow fiber membrane for gas–liquid contacting processes. *Chemical Engineering Journal, 198*, 327-337.

Bakeri, G., Matsuura, T., Ismail, A., & Rana, D. (2012). A novel surface modified polyetherimide hollow fiber membrane for gas–liquid contacting processes. *Separation and Purification Technology, 89*, 160-170.

Bamperng, S., Suwannachart, T., Atchariyawut, S., & Jiraratananon, R. (2010). Ozonation of dye wastewater by membrane contactor using PVDF and PTFE membranes. *Separation and Purification Technology, 72*(2), 186-193.

Barbhuiya, N. H., Misra, U., & Singh, S. P. (2021). Synthesis, fabrication, and mechanism of action of electrically conductive membranes: a review. *Environmental Science: Water Research & Technology, 7*(4), 671-705.

Barrera-Díaz, C. E., Lugo-Lugo, V., & Bilyeu, B. (2012). A review of chemical, electrochemical and biological methods for aqueous Cr (VI) reduction. *Journal of hazardous materials, 223*, 1-12.

Beauregard, N., Al-Furaiji, M., Dias, G., Worthington, M., Suresh, A., Srivastava, R., Burkey, D. D., & McCutcheon, J. R. (2020). Enhancing iCVD modification of electrospun membranes for membrane distillation using a 3D printed Scaffold. *Polymers, 12*(9), 2074.

Bernhardsen, I. M., & Knuutila, H. K. (2017). A review of potential amine solvents for CO2 absorption process: Absorption capacity, cyclic capacity and pKa. *International Journal of Greenhouse Gas Control, 61*, 27-48.

Biniaz, P., Torabi Ardekani, N., Makarem, M. A., & Rahimpour, M. R. (2019). Water and wastewater treatment systems by novel

integrated membrane distillation (MD). *ChemEngineering, 3*(1), 8.

Bogler, A., & Bar-Zeev, E. (2018). Membrane distillation biofouling: Impact of feedwater temperature on biofilm characteristics and membrane performance. *Environmental Science & Technology, 52*(17), 10019-10029.

Boo, C., & Elimelech, M. (2017). Carbon nanotubes keep up the heat. *Nature Nanotechnology, 12*(6), 501-503.

Boo, C., Lee, J., & Elimelech, M. (2016). Omniphobic polyvinylidene fluoride (PVDF) membrane for desalination of shale gas produced water by membrane distillation. *Environmental Science & Technology, 50*(22), 12275-12282.

Boo, C., Wang, Y., Zucker, I., Choo, Y., Osuji, C. O., & Elimelech, M. (2018). High performance nanofiltration membrane for effective removal of perfluoroalkyl substances at high water recovery. *Environmental science & technology, 52*(13), 7279-7288.

Boussouga, Y.-A., Frey, H., & Schäfer, A. I. (2021). Removal of arsenic (V) by nanofiltration: Impact of water salinity, pH and organic matter. *Journal of membrane science, 618*, 118631.

Brant, J. A., & Childress, A. E. (2002). Assessing short-range membrane–colloid interactions using surface energetics. *Journal of membrane science, 203*(1-2), 257-273.

Bush, J. A., Vanneste, J., & Cath, T. Y. (2016). Membrane distillation for concentration of hypersaline brines from the Great Salt Lake: Effects of scaling and fouling on performance, efficiency, and salt rejection. *Separation and Purification Technology, 170*, 78-91. https://doi.org/https://doi.org/10.1016/j.seppur.2016.06.028

Cai, J., & Guo, F. (2017). Study of mass transfer coefficient in membrane desalination. *Desalination, 407*, 46-51.

Cai, J., Yin, H., & Guo, F. (2020). Transport analysis of material gap membrane distillation desalination processes. *Desalination, 481*, 114361.

Caldera, U., Bogdanov, D., & Breyer, C. (2016). Local cost of seawater RO desalination based on solar PV and wind energy: A global estimate. *Desalination, 385*, 207-216.

Castillo, E. H. C., Thomas, N., Al-Ketan, O., Rowshan, R., Al-Rub, R. K. A., Nghiem, L. D., Vigneswaran, S., Arafat, H. A., & Naidu, G. (2019). 3D printed spacers for organic fouling mitigation in membrane distillation. *Journal of membrane science, 581*, 331-343.

Cha, M., Boo, C., & Park, C. (2022). Simultaneous retention of organic and inorganic contaminants by a ceramic nanofiltration membrane for the treatment of semiconductor wastewater. *Process Safety and Environmental Protection, 159*, 525-533.

Chagas, V. B., Chaffe, P. L., & Blöschl, G. (2022). Climate and land management accelerate the Brazilian water cycle. *Nature communications, 13*(1), 1-10.

Chamani, H., Woloszyn, J., Matsuura, T., Rana, D., & Lan, C. Q. (2021). Pore wetting in membrane distillation: A comprehensive review. *Progress in Materials Science, 122*, 100843.

Chang, H., Liu, B., Zhang, Z., Pawar, R., Yan, Z., Crittenden, J. C., & Vidic, R. D. (2020). A critical review of membrane wettability in membrane distillation from the perspective of interfacial interactions. *Environmental Science & Technology, 55*(3), 1395-1418.

Chang, Y., Ooi, B., Ahmad, A., Leo, C., & Low, S. (2021). Vacuum membrane distillation for desalination: Scaling phenomena of brackish water at elevated temperature. *Separation and Purification Technology, 254*, 117572.

Chen, L., Qian, Y., Wang, Y., He, F., & Zhang, X. (2022). An insight into the performance of CNT-based membrane with the application of electric field for distillation process. *Desalination, 528*, 115613.

Chen, S., Perathoner, S., Ampelli, C., Mebrahtu, C., Su, D., & Centi, G. (2017). Electrocatalytic synthesis of ammonia at room temperature and atmospheric pressure from water and nitrogen on a carbon-nanotube-based electrocatalyst. *Angewandte Chemie, 129*(10), 2743-2747.

Chen, W., Chen, S., Liang, T., Zhang, Q., Fan, Z., Yin, H., Huang, K.-W., Zhang, X., Lai, Z., & Sheng, P. (2018). High-flux water desalination with interfacial salt sieving effect in nanoporous carbon composite membranes. *Nature Nanotechnology, 13*(4), 345-350.

Chen, X., & Yip, N. Y. (2018). Unlocking high-salinity desalination with cascading osmotically mediated reverse osmosis: Energy and operating pressure analysis. *Environmental Science & Technology, 52*(4), 2242-2250.

Cheng, X., Liang, H., Ding, A., Qu, F., Shao, S., Liu, B., Wang, H., Wu, D., & Li, G. (2016). Effects of pre-ozonation on the ultrafiltration of different natural organic matter (NOM) fractions: membrane

fouling mitigation, prediction and mechanism. *Journal of membrane science, 505*, 15-25.

Chiao, Y.-H., Cao, Y., Ang, M. B. M. Y., Sengupta, A., & Wickramasinghe, S. R. (2022). Application of superomniphobic electrospun membrane for treatment of real produced water through membrane distillation. *Desalination, 528*, 115602.

Cho, H., Choi, Y., & Lee, S. (2018). Effect of pretreatment and operating conditions on the performance of membrane distillation for the treatment of shale gas wastewater. *Desalination, 437*, 195-209.

Choudhury, M. R., Anwar, N., Jassby, D., & Rahaman, M. S. (2019). Fouling and wetting in the membrane distillation driven wastewater reclamation process–A review. *Advances in colloid and interface science, 269*, 370-399.

Cosgrove, W. J., & Loucks, D. P. (2015). Water management: Current and future challenges and research directions. *Water Resources Research, 51*(6), 4823-4839.

Costa, F. C., Ricci, B. C., Teodoro, B., Koch, K., Drewes, J. E., & Amaral, M. C. (2021). Biofouling in membrane distillation applications-a review. *Desalination, 516*, 115241.

Cruz-Tato, P., Rivera-Fuentes, N., Flynn, M., & Nicolau, E. (2019). Anti-fouling electroconductive forward osmosis membranes: Electrochemical and chemical properties. *ACS Applied Polymer Materials, 1*(5), 1061-1070.

Dagan-Jaldety, C., Fridman-Bishop, N., & Gendel, Y. (2020). Nitrate hydrogenation by microtubular CNT-made catalytic membrane contactor. *Chemical Engineering Journal, 401*, 126142.

Darbari, Z. M., Mungray, A. A. J. D., & Treatment, W. (2016). Synthesis of an electrically cleanable forward osmosis membrane. *57*(4), 1634-1646.

DashtArzhandi, M. R., Ismail, A., & Matsuura, T. (2015). Carbon dioxide stripping through water by porous PVDF/montmorillonite hollow fiber mixed matrix membranes in a membrane contactor. *Rsc Advances, 5*(28), 21916-21924.

Davey, C., Luqmani, B., Thomas, N., & McAdam, E. J. (2022). Transforming wastewater ammonia to carbon free energy: Integrating fuel cell technology with ammonia stripping for direct power production. *Separation and Purification Technology, 289*, 120755.

de Lannoy, C.-F., Jassby, D., Gloe, K., Gordon, A. D., & Wiesner, M. R. (2013). Aquatic biofouling prevention by electrically charged

nanocomposite polymer thin film membranes. *Environmental science & technology, 47*(6), 2760-2768.

Deka, B. J., Guo, J., Wong, P. W., Khanzada, N. K., Kharraz, J. A., Tsang, C.-W., & An, A. K. (2021). A Conductive Hydrophobic Polyaniline Sandwiched Polyvinylidene Fluoride Membrane for Early Detection of Surfactant-Induced Wetting in Membrane Distillation Using Impedance. *ACS Applied Polymer Materials, 3*(2), 679-690.

Deshmukh, A., Boo, C., Karanikola, V., Lin, S., Straub, A. P., Tong, T., Warsinger, D. M., & Elimelech, M. (2018). Membrane distillation at the water-energy nexus: limits, opportunities, and challenges. *Energy & environmental science, 11*(5), 1177-1196.

Donaldson Jr, S. H., Røyne, A., Kristiansen, K., Rapp, M. V., Das, S., Gebbie, M. A., Lee, D. W., Stock, P., Valtiner, M., & Israelachvili, J. (2015). Developing a general interaction potential for hydrophobic and hydrophilic interactions. *Langmuir, 31*(7), 2051-2064.

Dong, Y., Dai, X., Zhao, L., Gao, L., Xie, Z., & Zhang, J. (2021). Review of transport phenomena and popular modelling approaches in membrane distillation. *Membranes, 11*(2), 122.

Du, L., Quan, X., Fan, X., Wei, G., & Chen, S. (2020). Conductive CNT/nanofiber composite hollow fiber membranes with electrospun support layer for water purification. *Journal of membrane science, 596*, 117613.

Duan, W., Chen, G., Chen, C., Sanghvi, R., Iddya, A., Walker, S., Liu, H., Ronen, A., & Jassby, D. (2017). Electrochemical removal of hexavalent chromium using electrically conducting carbon nanotube/polymer composite ultrafiltration membranes. *Journal of membrane science, 531*, 160-171.

Duan, W., Ronen, A., Walker, S., & Jassby, D. (2016). Polyaniline-coated carbon nanotube ultrafiltration membranes: enhanced anodic stability for in situ cleaning and electro-oxidation processes. *ACS applied materials & interfaces, 8*(34), 22574-22584.

Duca, M., & Koper, M. T. (2012). Powering denitrification: the perspectives of electrocatalytic nitrate reduction. *Energy & Environmental Science, 5*(12), 9726-9742.

Dudchenko, A. V., Chen, C., Cardenas, A., Rolf, J., & Jassby, D. (2017). Frequency-dependent stability of CNT Joule heaters in ionizable media and desalination processes. *Nature Nanotechnology, 12*(6), 557-563.

Dudchenko, A. V., Rolf, J., Russell, K., Duan, W., & Jassby, D. (2014). Organic fouling inhibition on electrically conducting carbon nanotube–polyvinyl alcohol composite ultrafiltration membranes. *Journal of membrane science, 468*, 1-10.

Duong, H. C., Duke, M., Gray, S., Cooper, P., & Nghiem, L. D. (2016). Membrane scaling and prevention techniques during seawater desalination by air gap membrane distillation. *Desalination, 397*, 92-100.

El-Bourawi, M. S., Ding, Z., Ma, R., & Khayet, M. (2006). A framework for better understanding membrane distillation separation process. *Journal of Membrane Science, 285*(1), 4-29. https://doi.org/https://doi.org/10.1016/j.memsci.2006.08.002

El Hadri, N., Quang, D. V., Goetheer, E. L., & Zahra, M. R. A. (2017). Aqueous amine solution characterization for post-combustion CO2 capture process. *Applied Energy, 185*, 1433-1449.

Elcik, H., Fortunato, L., Alpatova, A., Soukane, S., Orfi, J., Ali, E., AlAnsary, H., Leiknes, T., & Ghaffour, N. (2020). Multi-effect distillation brine treatment by membrane distillation: Effect of antiscalant and antifoaming agents on membrane performance and scaling control. *Desalination, 493*, 114653.

ElHadidy, A. M., Peldszus, S., & Van Dyke, M. I. (2013). Development of a pore construction data analysis technique for investigating pore size distribution of ultrafiltration membranes by atomic force microscopy. *Journal of membrane science, 429*, 373-383.

Eykens, L., De Sitter, K., Dotremont, C., Pinoy, L., & Van der Bruggen, B. (2016). How to optimize the membrane properties for membrane distillation: a review. *Industrial & Engineering Chemistry Research, 55*(35), 9333-9343.

Fan, X., Zhao, H., Quan, X., Liu, Y., & Chen, S. (2016). Nanocarbon-based membrane filtration integrated with electric field driving for effective membrane fouling mitigation. *Water Research, 88*, 285-292.

Francis, L., Ahmed, F. E., & Hilal, N. (2022). Electrospun membranes for membrane distillation: The state of play and recent advances. *Desalination, 526*, 115511.

Franken, A. C. M., Nolten, J. A. M., Mulder, M. H. V., Bargeman, D., & Smolders, C. A. (1987). Wetting criteria for the applicability of membrane distillation. *Journal of Membrane Science, 33*(3), 315-328. https://doi.org/https://doi.org/10.1016/S0376-7388(00)80288-4

Fuzil, N. S., Othman, N. H., Alias, N. H., Marpani, F., Othman, M. H. D., Ismail, A. F., Lau, W. J., Li, K., Kusworo, T. D., & Ichinose, I. (2021). A review on photothermal material and its usage in the development of photothermal membrane for sustainable clean water production. *Desalination, 517*, 115259.

Gao, L., Zhang, J., & Gray, S. (2019). Modelling mass and heat transfers of Permeate Gap Membrane Distillation using hollow fibre membrane. *Desalination, 467*, 196-209.

Gao, W., Liang, H., Ma, J., Han, M., Chen, Z.-l., Han, Z.-s., & Li, G.-b. (2011). Membrane fouling control in ultrafiltration technology for drinking water production: A review. *Desalination, 272*(1-3), 1-8.

Gao, Y., Qin, J., Wang, Z., & Østerhus, S. W. (2019). Backpulsing technology applied in MF and UF processes for membrane fouling mitigation: A review. *Journal of membrane science, 587*, 117136.

Goh, P., Matsuura, T., Ismail, A., & Hilal, N. (2016). Recent trends in membranes and membrane processes for desalination. *Desalination, 391*, 43-60.

González, D., Amigo, J., & Suárez, F. (2017). Membrane distillation: Perspectives for sustainable and improved desalination. *Renewable and Sustainable Energy Reviews, 80*, 238-259.

Gray, G. T., McCutcheon, J. R., & Elimelech, M. (2006). Internal concentration polarization in forward osmosis: role of membrane orientation. *Desalination, 197*(1-3), 1-8.

Gryta, M. (2008). Fouling in direct contact membrane distillation process. *Journal of Membrane Science, 325*(1), 383-394. https://doi.org/https://doi.org/10.1016/j.memsci.2008.08.001

Gryta, M. (2009). Calcium sulphate scaling in membrane distillation process. *Chemical Papers, 63*(2), 146-151. https://doi.org/10.2478/s11696-008-0095-y

Gryta, M. (2011). The influence of magnetic water treatment on CaCO3 scale formation in membrane distillation process. *Separation and Purification Technology, 80*(2), 293-299. https://doi.org/https://doi.org/10.1016/j.seppur.2011.05.008

Gude, V. G. (2015). Energy storage for desalination processes powered by renewable energy and waste heat sources. *Applied Energy, 137*, 877-898.

Gude, V. G. (2017). Desalination and water reuse to address global water scarcity. *Reviews in Environmental Science and Bio/Technology, 16*(4), 591-609.

Gunasekaran, P., Veawab, A., & Aroonwilas, A. (2013). Corrosivity of single and blended amines in CO2 capture process. *Energy Procedia, 37*, 2094-2099.

Guo, J., Zhu, L., Sun, N., & Lan, Y. (2017). Degradation of nitrobenzene by sodium persulfate activated with zero-valent zinc in the presence of low frequency ultrasound. *Journal of the Taiwan Institute of Chemical Engineers, 78*, 137-143.

Guo, W., Ngo, H.-H., & Li, J. (2012). A mini-review on membrane fouling. *Bioresource technology, 122*, 27-34.

Gwak, G., Kim, D. I., & Hong, S. J. J. o. M. S. (2018). New industrial application of forward osmosis (FO): Precious metal recovery from printed circuit board (PCB) plant wastewater. *552*, 234-242.

Hamad, E. M., Al-Gharabli, S., & Kujawa, J. (2022). Tunable hydrophobicity and roughness on PVDF surface by grafting to mode–Approach to enhance membrane performance in membrane distillation process. *Separation and Purification Technology, 291*, 120935.

Han, F., Mao, J., & Wang, K. (2022). Enhance the anti-scaling performance of conductive heating vacuum membrane distillation by carbon nanotube-based electroactive membrane. *Journal of Environmental Chemical Engineering, 10*(6), 108722.

Han, M., Wang, Y., Yao, J., Liu, C., Chew, J. W., Wang, Y., Dong, Y., & Han, L. (2021). Electrically conductive hydrophobic membrane cathode for membrane distillation with super anti-oil-fouling capability: Performance and mechanism. *Desalination, 516*, 115199.

Hardikar, M., Marquez, I., & Achilli, A. (2020). Emerging investigator series: membrane distillation and high salinity: analysis and implications. *Environmental Science: Water Research & Technology, 6*(6), 1538-1552.

Hashaikeh, R., Lalia, B. S., Kochkodan, V., & Hilal, N. (2014). A novel in situ membrane cleaning method using periodic electrolysis. *Journal of membrane science, 471*, 149-154.

Hasson, D., & Semiat, R. (2006). Scale control in saline and wastewater desalination. *Israel journal of chemistry, 46*(1), 97-104.

He, F., Sirkar, K. K., & Gilron, J. (2009). Studies on scaling of membranes in desalination by direct contact membrane distillation: CaCO3 and mixed CaCO3/CaSO4 systems. *Chemical Engineering Science, 64*(8), 1844-1859. https://doi.org/https://doi.org/10.1016/j.ces.2008.12.036

Hong, S., & Elimelech, M. (1997). Chemical and physical aspects of natural organic matter (NOM) fouling of nanofiltration membranes. *Journal of membrane science, 132*(2), 159-181.

Hong, S. K., Kim, H., Lee, H., Lim, G., & Cho, S. J. (2022). A pore-size tunable superhydrophobic membrane for high-flux membrane distillation. *Journal of membrane science, 641*, 119862.

Hou, D., Iddya, A., Chen, X., Wang, M., Zhang, W., Ding, Y., Jassby, D., & Ren, Z. J. (2018). Nickel-based membrane electrodes enable high-rate electrochemical ammonia recovery. *Environmental science & technology, 52*(15), 8930-8938.

Howe, K. J., & Clark, M. M. (2002). Fouling of microfiltration and ultrafiltration membranes by natural waters. *Environmental science & technology, 36*(16), 3571-3576.

Huang, K., & Peng, H.-L. (2017). Solubilities of Carbon Dioxide in 1-Ethyl-3-methylimidazolium Thiocyanate, 1-Ethyl-3-methylimidazolium Dicyanamide, and 1-Ethyl-3-methylimidazolium Tricyanomethanide at (298.2 to 373.2) K and (0 to 300.0) kPa. *Journal of Chemical & Engineering Data, 62*(12), 4108-4116.

Huang, Q., Liu, H., Wang, Y., & Xiao, C. (2018). A hybrid electric field assisted vacuum membrane distillation method to mitigate membrane fouling. *Rsc Advances, 8*(32), 18084-18092.

Huang, R., Zhang, T., Wang, Q., Gu, H., Zhou, Z., Wu, Z., & Wang, Z. (2023). New insights into the cleaning mechanisms of conductive membrane by NaClO and electric field in terms of protein and polysaccharide degradation. *Chemical Engineering Journal, 453*, 139891.

Im, S.-J., Jeong, S., & Jang, A. (2021). Forward osmosis (FO)-reverse osmosis (RO) hybrid process incorporated with hollow fiber FO. *npj Clean Water, 4*(1), 1-10.

Jamil, M. A., & Zubair, S. M. (2017). Design and analysis of a forward feed multi-effect mechanical vapor compression desalination system: An exergo-economic approach. *Energy, 140*, 1107-1120.

Jang, Y., Somanna, Y., & Kim, H. (2016). Source, distribution, toxicity and remediation of arsenic in the environment–a review. *Int J Appl Environ Sci, 11*(2), 559-581.

Jansen, R., De Rijk, J., Zwijnenburg, A., Mulder, M., & Wessling, M. (2005). Hollow fiber membrane contactors—A means to study the reaction kinetics of humic substance ozonation. *Journal of membrane science, 257*(1-2), 48-59.

Ji, B., Asif, M. B., & Zhang, Z. (2023). Photothermally-activated peroxymonosulfate (PMS) pretreatment for fouling alleviation of membrane distillation of surface water: Performance and mechanism. *Separation and Purification Technology, 309*, 123043.

Jiang, L., Chen, L., & Zhu, L. (2019). Electrically conductive membranes for anti-biofouling in membrane distillation with two novel operation modes: Capacitor mode and resistor mode. *Water Research, 161*, 297-307.

Jiang, L., Chen, L., & Zhu, L. (2021). In-situ electric-enhanced membrane distillation for simultaneous flux-increasing and anti-wetting. *Journal of membrane science, 630*, 119305.

Jin, Z., Meng, F., Gong, H., Wang, C., & Wang, K. (2017). Improved low-carbon-consuming fouling control in long-term membrane-based sewage pre-concentration: The role of enhanced coagulation process and air backflushing in sustainable sewage treatment. *Journal of membrane science, 529*, 252-262.

Jing, Y., Guo, L., & Chaplin, B. P. (2016). Electrochemical impedance spectroscopy study of membrane fouling and electrochemical regeneration at a sub-stoichiometric TiO2 reactive electrochemical membrane. *Journal of membrane science, 510*, 510-523.

Jung, B., Ma, S., Khor, C. M., Khanzada, N. K., Anvari, A., Wang, X., Im, S., Wu, J., Rao, U., & An, A. K. (2023). Impact of polarity reversal on inorganic scaling on carbon nanotube-based electrically-conducting nanofiltration membranes. *Chemical Engineering Journal, 452*, 139216.

Kalla, S. (2021). Use of membrane distillation for oily wastewater treatment–a review. *Journal of Environmental Chemical Engineering, 9*(1), 104641.

Kamranvand, F., Davey, C. J., Williams, L., Parker, A., Jiang, Y., Tyrrel, S., & McAdam, E. J. (2020). Ultrafiltration pretreatment enhances membrane distillation flux, resilience and permeate quality during water recovery from concentrated blackwater (urine/faeces). *Separation and Purification Technology, 253*, 117547. https://doi.org/https://doi.org/10.1016/j.seppur.2020.117547

Kang, K. H. (2002). How electrostatic fields change contact angle in electrowetting. *Langmuir, 18*(26), 10318-10322.

Karanikola, V., Boo, C., Rolf, J., & Elimelech, M. (2018). Engineered slippery surface to mitigate gypsum scaling in membrane

distillation for treatment of hypersaline industrial wastewaters. *Environmental Science & Technology, 52*(24), 14362-14370.

Karkooti, A., Rastgar, M., Nazemifard, N., & Sadrzadeh, M. (2020). Graphene-based electro-conductive anti-fouling membranes for the treatment of oil sands produced water. *Science of the Total Environment, 704*, 135365.

Kaspar, P., Sobola, D., Částková, K., Dallaev, R., Šťastná, E., Sedlák, P., Knápek, A., Trčka, T., & Holcman, V. (2021). Case study of polyvinylidene fluoride doping by carbon nanotubes. *Materials, 14*(6), 1428.

Kaspar, P., Sobola, D., Částková, K., Knápek, A., Burda, D., Orudzhev, F., Dallaev, R., Tofel, P., Trčka, T., & Grmela, L. (2020). Characterization of polyvinylidene fluoride (PVDF) electrospun fibers doped by carbon flakes. *Polymers, 12*(12), 2766.

Khaisri, S., deMontigny, D., Tontiwachwuthikul, P., & Jiraratananon, R. (2011). CO2 stripping from monoethanolamine using a membrane contactor. *Journal of membrane science, 376*(1-2), 110-118.

Khanzada, N. K., Jassby, D., & An, A. K. (2022). Conductive reverse osmosis membrane for electrochemical chlorine reduction and sustainable brackish water treatment. *Chemical Engineering Journal, 435*, 134858.

Kharraz, J. A., Farid, M. U., Khanzada, N. K., Deka, B. J., Arafat, H. A., & An, A. K. (2020). Macro-corrugated and nano-patterned hierarchically structured superomniphobic membrane for treatment of low surface tension oily wastewater by membrane distillation. *Water Research, 174*, 115600.

Kim, G. S., Cao, T., & Hwang, Y. (2021). Thermoeconomic investigation for a multi-stage solar-thermal vacuum membrane distillation system for coastal cities. *Desalination, 498*, 114797.

Kim, H.-W., Yun, T., Kang, P. K., Hong, S., Jeong, S., & Lee, S. (2019). Evaluation of a real-time visualization system for scaling detection during DCMD, and its correlation with wetting. *Desalination, 454*, 59-70.

Kim, J., Kim, H.-W., Tijing, L. D., Shon, H. K., & Hong, S. (2022). Elucidation of physicochemical scaling mechanisms in membrane distillation (MD): Implication to the control of inorganic fouling. *Desalination, 527*, 115573.

Kim, J., Kim, J., & Hong, S. (2018a). Recovery of water and minerals from shale gas produced water by membrane distillation crystallization. *Water Research, 129*, 447-459.

Kim, J., Kim, J., & Hong, S. J. W. r. (2018b). Recovery of water and minerals from shale gas produced water by membrane distillation crystallization. *Water Research, 129*, 447-459.

Kim, J., Kim, J., Lim, J., Lee, S., Lee, C., & Hong, S. (2019). Cold-cathode X-ray irradiation pre-treatment for fouling control of reverse osmosis (RO) in shale gas produced water (SGPW) treatment. *Chemical Engineering Journal, 374*, 49-58.

Kim, J., Kwon, H., Lee, S., Lee, S., & Hong, S. (2017a). Membrane distillation (MD) integrated with crystallization (MDC) for shale gas produced water (SGPW) treatment. *Desalination, 403*, 172-178.

Kim, J., Kwon, H., Lee, S., Lee, S., & Hong, S. J. D. (2017b). Membrane distillation (MD) integrated with crystallization (MDC) for shale gas produced water (SGPW) treatment. *Desalination, 403*, 172-178.

Kim, J., Yun, E.-T., Tijing, L., Shon, H. K., & Hong, S. (2022). Mitigation of fouling and wetting in membrane distillation by electrical repulsion using a multi-layered single-wall carbon nanotube/polyvinylidene fluoride membrane. *Journal of membrane science, 653*, 120519.

Kim, S., Scholes, C. A., Heath, D. E., & Kentish, S. E. (2021). Gas-liquid membrane contactors for carbon dioxide separation: A review. *Chemical Engineering Journal, 411*, 128468.

Kinidi, L., Tan, I. A. W., Abdul Wahab, N. B., Tamrin, K. F. B., Hipolito, C. N., & Salleh, S. F. (2018). Recent development in ammonia stripping process for industrial wastewater treatment. *International Journal of Chemical Engineering, 2018*.

Kiss, A. A., & Kattan Readi, O. M. (2018). An industrial perspective on membrane distillation processes. *Journal of Chemical Technology & Biotechnology, 93*(8), 2047-2055.

Korminouri, F., Rahbari-Sisakht, M., Rana, D., Matsuura, T., & Ismail, A. (2014). Study on the effect of air–gap length on properties and performance of surface modified PVDF hollow fiber membrane contactor for carbon dioxide absorption. *Separation and Purification Technology, 132*, 601-609.

Kumar, R., & Ismail, A. (2015). Fouling control on microfiltration/ultrafiltration membranes: Effects of morphology, hydrophilicity, and charge. *Journal of Applied Polymer Science, 132*(21).

Lampreia, I. M., Santos, Â. F., Barbas, M. J. A., Santos, F. J., & Matos Lopes, M. L. (2007). Changes in aggregation patterns detected

by diffusion, viscosity, and surface tension in water+ 2-(diethylamino) ethanol mixtures at different temperatures. *Journal of Chemical & Engineering Data, 52*(6), 2388-2394.

Laqbaqbi, M., García-Payo, M., Khayet, M., El Kharraz, J., & Chaouch, M. (2019). Application of direct contact membrane distillation for textile wastewater treatment and fouling study. *Separation and Purification Technology, 209*, 815-825.

Lee, E.-J., An, A. K., He, T., Woo, Y. C., & Shon, H. K. (2016). Electrospun nanofiber membranes incorporating fluorosilane-coated TiO2 nanocomposite for direct contact membrane distillation. *Journal of membrane science, 520*, 145-154.

Lee, J. H., Yun, E.-T., Ham, S.-Y., Kim, H.-S., Sun, P.-F., & Park, H.-D. (2022). Electrically conductive carbon nanotube/graphene composite membrane for self-cleaning of biofouling via bubble generation. *Desalination, 535*, 115841.

Lee, S., Boo, C., Elimelech, M., & Hong, S. (2010a). Comparison of fouling behavior in forward osmosis (FO) and reverse osmosis (RO). *Journal of membrane science, 365*(1-2), 34-39.

Lee, S., Boo, C., Elimelech, M., & Hong, S. J. J. o. m. s. (2010b). Comparison of fouling behavior in forward osmosis (FO) and reverse osmosis (RO). *365*(1-2), 34-39.

Lee, S., Kim, J., Lee, E., & Hong, S. (2022). Improving the performance of membrane contactors for carbon dioxide stripping from water: Experimental and theoretical analysis. *Journal of membrane science, 654*, 120552.

Lee, S., Shon, H. K., & Hong, S. (2017). Dewatering of activated sludge by forward osmosis (FO) with ultrasound for fouling control. *Desalination, 421*, 79-88.

Lee, W. J., Ng, Z. C., Hubadillah, S. K., Goh, P. S., Lau, W. J., Othman, M., Ismail, A. F., & Hilal, N. (2020). Fouling mitigation in forward osmosis and membrane distillation for desalination. *Desalination, 480*, 114338.

Li, K., Xu, L., Zhang, Y., Cao, A., Wang, Y., Huang, H., & Wang, J. (2019). A novel electro-catalytic membrane contactor for improving the efficiency of ozone on wastewater treatment. *Applied Catalysis B: Environmental, 249*, 316-321.

Li, K., Zhang, Y., Xu, L., Liu, L., Wang, Z., Hou, D., Wang, Y., & Wang, J. (2020). Mass transfer and interfacial reaction mechanisms in a novel electro-catalytic membrane contactor for wastewater treatment by O3. *Applied Catalysis B: Environmental, 264*, 118512.

Li, L., Liu, X.-p., & Li, H.-q. (2017). A review of forward osmosis membrane fouling: Types, research methods and future prospects. *Environmental technology reviews, 6*(1), 26-46.

Li, N., Wang, W., Ma, C., Zhu, L., Chen, X., Zhang, B., & Zhong, C. (2022). A novel conductive rGO/ZnO/PSF membrane with superior water flux for electrocatalytic degradation of organic pollutants. *Journal of membrane science, 641*, 119901.

Li, R., Wu, Y., Shen, L., Chen, J., Lin, H. J. J. o. c., & science, i. (2018). A novel strategy to develop antifouling and antibacterial conductive Cu/polydopamine/polyvinylidene fluoride membranes for water treatment. *531*, 493-501.

Li, X., Ma, F., Li, Y., Zhang, H., Min, J., Zhang, X., & Yao, H. (2020). Enhanced mechanisms of electrocatalytic-ozonation of ibuprofen using a TiO2 nanoflower-coated porous titanium gas diffuser anode: Role of TiO2 catalysts and electrochemical action in reactive oxygen species formation. *Chemical Engineering Journal, 389*, 124411.

Li, X., Mo, Y., Qing, W., Shao, S., Tang, C. Y., & Li, J. (2019). Membrane-based technologies for lithium recovery from water lithium resources: A review. *Journal of membrane science, 591*, 117317.

Lian, B., Wang, Y., Le-Clech, P., Chen, V., & Leslie, G. (2016). A numerical approach to module design for crossflow vacuum membrane distillation systems. *Journal of membrane science, 510*, 489-496.

Liao, X., Chou, S., Gu, C., Zhang, X., Shi, M., You, X., Liao, Y., & Razaqpur, A. G. (2023). Engineering omniphobic corrugated membranes for scaling mitigation in membrane distillation. *Journal of membrane science, 665*, 121130.

Liao, Y., Bokhary, A., Maleki, E., & Liao, B. (2018). A review of membrane fouling and its control in algal-related membrane processes. *Bioresource technology, 264*, 343-358.

Lin, B., & Malmali, M. (2023). Energy and exergy analysis of multi-stage vacuum membrane distillation integrated with mechanical vapor compression. *Separation and Purification Technology, 306*, 122568.

Lin, J., Peng, Z., Liu, Y., Ruiz-Zepeda, F., Ye, R., Samuel, E. L., Yacaman, M. J., Yakobson, B. I., & Tour, J. M. (2014). Laser-induced porous graphene films from commercial polymers. *Nature communications, 5*(1), 1-8.

Lin, Y., Xu, Y., Loh, C. H., & Wang, R. (2018). Development of robust fluorinated TiO2/PVDF composite hollow fiber membrane for CO2 capture in gas-liquid membrane contactor. *Applied Surface Science, 436*, 670-681.

Lin, Y. F., Chen, C. H., Tung, K. L., Wei, T. Y., Lu, S. Y., & Chang, K. S. (2013). Mesoporous Fluorocarbon-Modified Silica Aerogel Membranes Enabling Long-Term Continuous CO2 Capture with Large Absorption Flux Enhancements. *ChemSusChem, 6*(3), 437-442.

Liu, C., Chen, L., & Zhu, L. (2018). Fouling mechanism of hydrophobic polytetrafluoroethylene (PTFE) membrane by differently charged organics during direct contact membrane distillation (DCMD) process: An especial interest in the feed properties. *Journal of membrane science, 548*, 125-135.

Liu, C., Zhu, L., Ji, R., & Tang, S. (2022). Application of a hybrid ultrasonic stripping-membrane distillation (US-MD) system for the treatment of mariculture wastewater. *Desalination, 544*, 116115.

Liu, G., Li, L., Qiu, L., Yu, S., Liu, P., Zhu, Y., Hu, J., Liu, Z., Zhao, D., & Yang, H. (2018). Chemical cleaning of ultrafiltration membranes for polymer-flooding wastewater treatment: Efficiency and molecular mechanisms. *Journal of membrane science, 545*, 348-357.

Liu, H., Zhang, G., Zhao, C., Liu, J., & Yang, F. (2015a). Hydraulic power and electric field combined antifouling effect of a novel conductive poly (aminoanthraquinone)/reduced graphene oxide nanohybrid blended PVDF ultrafiltration membrane. *Journal of Materials Chemistry A, 3*(40), 20277-20287.

Liu, H., Zhang, G., Zhao, C., Liu, J., & Yang, F. J. J. o. M. C. A. (2015b). Hydraulic power and electric field combined antifouling effect of a novel conductive poly (aminoanthraquinone)/reduced graphene oxide nanohybrid blended PVDF ultrafiltration membrane. *3*(40), 20277-20287.

Liu, J., Wang, Q., Shan, H., Guo, H., & Li, B. (2019). Surface hydrophobicity based heat and mass transfer mechanism in membrane distillation. *Journal of membrane science, 580*, 275-288.

Liu, J., Wang, Y., Li, Z., Liu, X., & Li, W. (2021). Flux decline induced by scaling of calcium sulfate in membrane distillation: Theoretical analysis on the role of different mechanisms. *Journal of Membrane Science, 628*, 119257.

Liu, L., He, H., Wang, Y., Tong, T., Li, X., Zhang, Y., & He, T. (2021). Mitigation of gypsum and silica scaling in membrane distillation by pulse flow operation. *Journal of Membrane Science, 624*, 119107.

Liu, L., Xu, Y., Wang, K., Li, K., Xu, L., Wang, J., & Wang, J. (2019). Fabrication of a novel conductive ultrafiltration membrane and its application for electrochemical removal of hexavalent chromium. *Journal of Membrane Science, 584*, 191-201.

Liu, M., Wang, D., Chen, X., Chen, Y., Gao, L., & Deng, H. (2022). Impacts of climate variability and land use on the blue and green water resources in a subtropical basin of China. *Scientific Reports, 12*(1), 1-11.

Liu, Q., Qiu, G., Zhou, Z., Li, J., Amy, G. L., Xie, J., & Lee, J. Y. (2016). An effective design of electrically conducting thin-film composite (TFC) membranes for bio and organic fouling control in forward osmosis (FO). *Environmental science & technology, 50*(19), 10596-10605.

Liu, Q., Xu, G.-R., & Das, R. (2019). Inorganic scaling in reverse osmosis (RO) desalination: Mechanisms, monitoring, and inhibition strategies. *Desalination, 468*, 114065. https://doi.org/https://doi.org/10.1016/j.desal.2019.07.005

Liu, R., Sui, Y., & Wang, X. (2019). Metal–organic framework-based ultrafiltration membrane separation with capacitive-type for enhanced phosphate removal. *Chemical Engineering Journal, 371*, 903-913.

Liu, X., Dai, J., Ng, T.-L., & Chen, G. (2019). Evaluation of potential environmental benefits from seawater toilet flushing. *Water Research, 162*, 505-515.

Lohaus, T., Beck, J., Harhues, T., de Wit, P., Benes, N. E., & Wessling, M. (2020). Direct membrane heating for temperature induced fouling prevention. *Journal of membrane science, 612*, 118431.

Lou, M., Zhu, X., Fang, X., Liu, Y., & Li, F. (2022). Interception of volatile organic compounds through CNT electrochemistry of electrified membrane surface during membrane distillation. *Separation and Purification Technology*, 121380.

Lu, J.-G., Zheng, Y.-F., & Cheng, M.-D. (2008). Wetting mechanism in mass transfer process of hydrophobic membrane gas absorption. *Journal of membrane science, 308*(1-2), 180-190.

Lu, K. J., Chen, Y., & Chung, T.-S. (2019). Design of omniphobic interfaces for membrane distillation–a review. *Water Research, 162*, 64-77.

Ma, Q., Xu, Z., & Wang, R. (2021). Distributed solar desalination with membrane distillation: current status and future perspectives. *Water research*, 117154.

Ma, S., Yang, F., Chen, X., Khor, C. M., Jung, B., Iddya, A., Sant, G., & Jassby, D. (2021). Removal of As (III) by Electrically Conducting Ultrafiltration Membranes. *Water Research, 204*, 117592.

Ma, W., Lu, X., Guan, Y.-F., & Elimelech, M. (2021). Joule-heated layered double hydroxide sponge for rapid removal of silica from water. *Environmental Science & Technology, 55*(23), 16130-16142.

Madalosso, H. B., Machado, R., Hotza, D., & Marangoni, C. (2021). Membrane surface modification by electrospinning, coating, and plasma for membrane distillation applications: a state-of-the-art review. *Advanced Engineering Materials, 23*(6), 2001456.

Mansourizadeh, A., Aslmahdavi, Z., Ismail, A., & Matsuura, T. (2014). Blend polyvinylidene fluoride/surface modifying macromolecule hollow fiber membrane contactors for CO2 absorption. *International Journal of Greenhouse Gas Control, 26*, 83-92.

Mantel, T., Benne, P., & Ernst, M. (2021). Electrically conducting duplex-coated gold-PES-UF membrane for capacitive organic fouling mitigation and rejection enhancement. *Journal of membrane science, 620*, 118831.

Mantel, T., Benne, P., Parsin, S., & Ernst, M. (2018). Electro-conductive composite gold-polyethersulfone-ultrafiltration-membrane: Characterization of membrane and natural organic matter (NOM) filtration performance at different in-situ applied surface potentials. *Membranes, 8*(3), 64.

Mao, H., Qiu, M., Zhang, T., Chen, X., Da, X., Jing, W., & Fan, Y. (2019). Robust CNT-based conductive ultrafiltration membrane with tunable surface potential for in situ fouling mitigation. *Applied Surface Science, 497*, 143786.

McCutcheon, J. R., & Elimelech, M. (2006). Influence of concentrative and dilutive internal concentration polarization on flux behavior in forward osmosis. *Journal of Membrane Science, 284*(1-2), 237-247.

McGaughey, A., Gustafson, R., & Childress, A. (2017). Effect of long-term operation on membrane surface characteristics and performance in membrane distillation. *Journal of membrane science, 543*, 143-150.

Melo, R. P. F., Neto, E. B., Nunes, S., Dantas, T. C., & Neto, A. D. (2018). Removal of Reactive Blue 14 dye using micellar solubilization followed by ionic flocculation of surfactants. *Separation and Purification Technology, 191*, 161-166.

Meng, F., Zhang, S., Oh, Y., Zhou, Z., Shin, H.-S., & Chae, S.-R. (2017). Fouling in membrane bioreactors: An updated review. *Water Research, 114*, 151-180.

Mi, B., & Elimelech, M. J. J. o. m. s. (2008). Chemical and physical aspects of organic fouling of forward osmosis membranes. *320*(1-2), 292-302.

Miao, R., Wang, L., Zhu, M., Deng, D., Li, S., Wang, J., Liu, T., Lv, Y. J. E. S., & Technology. (2017). Effect of hydration forces on protein fouling of ultrafiltration membranes: the role of protein charge, hydrated ion species, and membrane hydrophilicity. *51*(1), 167-174.

Miklos, D. B., Remy, C., Jekel, M., Linden, K. G., Drewes, J. E., & Hübner, U. (2018). Evaluation of advanced oxidation processes for water and wastewater treatment–A critical review. *Water Research, 139*, 118-131.

Mo, Y., Tiraferri, A., Yip, N. Y., Adout, A., Huang, X., Elimelech, M. J. E. s., & technology. (2012). Improved antifouling properties of polyamide nanofiltration membranes by reducing the density of surface carboxyl groups. *46*(24), 13253-13261.

Mo, Y., Zhang, L., Zhao, X., Li, J., & Wang, L. (2022). A Critical Review on Classifications, Characteristics, and Applications of Electrically Conductive Membranes for Toxic Pollutant Removal From Water: Comparison Between Composite and Inorganic Electrically Conductive Membranes. *Journal of Hazardous Materials*, 129162.

Mohammad, A. W., Ng, C. Y., Lim, Y. P., & Ng, G. H. (2012). Ultrafiltration in food processing industry: review on application, membrane fouling, and fouling control. *Food and bioprocess technology, 5*(4), 1143-1156.

Morlanés, N., Katikaneni, S. P., Paglieri, S. N., Harale, A., Solami, B., Sarathy, S. M., & Gascon, J. (2021). A technological roadmap to the ammonia energy economy: Current state and missing technologies. *Chemical Engineering Journal, 408*, 127310.

Mosadegh-Sedghi, S., Rodrigue, D., Brisson, J., & Iliuta, M. C. (2014). Wetting phenomenon in membrane contactors–causes and prevention. *Journal of membrane science, 452*, 332-353.

Mpala, T. J., Etale, A., Richards, H., & Nthunya, L. N. (2023). Biofouling phenomena in membrane distillation: mechanisms and mitigation strategies. *Environmental Science: Advances, 2*(1), 39-54.

Naidu, G., Jeong, S., Kim, S.-J., Kim, I. S., & Vigneswaran, S. (2014). Organic fouling behavior in direct contact membrane distillation. *Desalination, 347*, 230-239.

Naidu, G., Jeong, S., & Vigneswaran, S. (2015). Interaction of humic substances on fouling in membrane distillation for seawater desalination. *Chemical Engineering Journal, 262*, 946-957.

Naji, O., Al-Juboori, R. A., Bowtell, L., Alpatova, A., & Ghaffour, N. (2020). Direct contact ultrasound for fouling control and flux enhancement in air-gap membrane distillation. *Ultrasonics sonochemistry, 61*, 104816.

Nghiem, L. D., & Cath, T. (2011). A scaling mitigation approach during direct contact membrane distillation. *Separation and Purification Technology, 80*(2), 315-322. https://doi.org/https://doi.org/10.1016/j.seppur.2011.05.013

Omi, F. R., Choudhury, M. R., Anwar, N., Bakr, A. R., & Rahaman, M. S. (2017). Highly conductive ultrafiltration membrane via vacuum filtration assisted layer-by-layer deposition of functionalized carbon nanotubes. *Industrial & Engineering Chemistry Research, 56*(30), 8474-8484.

Omi, F. R., Choudhury, M. R., Anwar, N., Bakr, A. R., Rahaman, M. S. J. I., & Research, E. C. (2017). Highly conductive ultrafiltration membrane via vacuum filtration assisted layer-by-layer deposition of functionalized carbon nanotubes. *56*(30), 8474-8484.

Onsekizoglu, P. (2012). Membrane distillation: principle, advances, limitations and future prospects in food industry. *Distillation-advances from modeling to applications, 282*.

Pan, Z., Yu, F., Li, L., Liu, M., Song, C., Yang, J., Li, H., Wang, C., Pan, Y., & Wang, T. (2020). Low-cost electrochemical filtration carbon membrane prepared from coal via self-bonding. *Chemical Engineering Journal, 385*, 123928.

Panagopoulos, A. (2021). Study and evaluation of the characteristics of saline wastewater (brine) produced by desalination and industrial plants. *Environmental Science and Pollution Research*, 1-14.

Phattaranawik, J., Leiknes, T., & Pronk, W. (2005). Mass transfer studies in flat-sheet membrane contactor with ozonation. *Journal of membrane science, 247*(1-2), 153-167.

Pistocchi, A., Bleninger, T., Breyer, C., Caldera, U., Dorati, C., Ganora, D., Millán, M., Paton, C., Poullis, D., & Herrero, F. S. (2020). Can seawater desalination be a win-win fix to our water cycle? *Water Research, 182*, 115906.

Politano, A., Di Profio, G., Fontananova, E., Sanna, V., Cupolillo, A., & Curcio, E. (2019). Overcoming temperature polarization in membrane distillation by thermoplasmonic effects activated by Ag nanofillers in polymeric membranes. *Desalination, 451*, 192-199.

Presson, L. K., Felix, V., Hardikar, M., Achilli, A., & Hickenbottom, K. L. (2023). Fouling characterization and treatment of water reuse concentrate with membrane distillation: Do organics really matter. *Desalination, 553*, 116443.

Qi, B., He, X., Zeng, G., Pan, Y., Li, G., Liu, G., Zhang, Y., Chen, W., & Sun, Y. (2017). Strict molecular sieving over electrodeposited 2D-interspacing-narrowed graphene oxide membranes. *Nature communications, 8*(1), 1-10.

Qiao, J., Jiao, W., & Liu, Y. (2021). Degradation of nitrobenzene-containing wastewater by sequential nanoscale zero valent iron-persulfate process. *Green Energy & Environment, 6*(6), 910-919.

Qtaishat, M., Matsuura, T., Kruczek, B., & Khayet, M. (2008). Heat and mass transfer analysis in direct contact membrane distillation. *Desalination, 219*(1), 272-292. https://doi.org/https://doi.org/10.1016/j.desal.2007.05.019

Qu, F., Yan, Z., Yu, H., Fan, G., Pang, H., Rong, H., & He, J. (2020). Effect of residual commercial antiscalants on gypsum scaling and membrane wetting during direct contact membrane distillation. *Desalination, 486*, 114493.

Rabuni, M., Sulaiman, N. N., Aroua, M. K., Chee, C. Y., & Hashim, N. A. (2015). Impact of in situ physical and chemical cleaning on PVDF membrane properties and performances. *Chemical Engineering Science, 122*, 426-435.

Rácz, G., Kerker, S., Schmitz, O., Schnabel, B., Kovacs, Z., Vatai, G., Ebrahimi, M., & Czermak, P. (2015). Experimental determination of liquid entry pressure (LEP) in vacuum membrane distillation for oily wastewaters. *Membr. Water Treat, 6*(3), 237-249.

Rahbari-Sisakht, M., Ismail, A., Rana, D., & Matsuura, T. (2012a). Effect of novel surface modifying macromolecules on morphology and performance of Polysulfone hollow fiber

membrane contactor for CO2 absorption. *Separation and Purification Technology, 99*, 61-68.

Rahbari-Sisakht, M., Ismail, A., Rana, D., & Matsuura, T. (2012b). A novel surface modified polyvinylidene fluoride hollow fiber membrane contactor for CO2 absorption. *Journal of membrane science, 415*, 221-228.

Rahbari-Sisakht, M., Ismail, A., Rana, D., Matsuura, T., & Emadzadeh, D. (2013). Effect of SMM concentration on morphology and performance of surface modified PVDF hollow fiber membrane contactor for CO2 absorption. *Separation and Purification Technology, 116*, 67-72.

Rao, U., Iddya, A., Jung, B., Khor, C. M., Hendren, Z., Turchi, C., Cath, T., Hoek, E. M., Ramon, G. Z., & Jassby, D. (2020). Mineral scale prevention on electrically conducting membrane distillation membranes using induced electrophoretic mixing. *Environmental Science & Technology, 54*(6), 3678-3690.

Rastgar, M., Bozorg, A., Shakeri, A., & Sadrzadeh, M. (2019). Substantially improved antifouling properties in electro-oxidative graphene laminate forward osmosis membrane. *Chemical Engineering Research and Design, 141*, 413-424.

Rezaei-DashtArzhandi, M., Ismail, A., Goh, P., Wan Azelee, I., Abbasgholipourghadim, M., Ur Rehman, G., & Matsuura, T. (2016). Zeolite ZSM5-filled PVDF hollow fiber mixed matrix membranes for efficient carbon dioxide removal via membrane contactor. *Industrial & engineering chemistry research, 55*(49), 12632-12643.

Rezaei, M., Ismail, A., Hashemifard, S., Bakeri, G., & Matsuura, T. (2014). Experimental study on the performance and long-term stability of PVDF/montmorillonite hollow fiber mixed matrix membranes for CO2 separation process. *International Journal of Greenhouse Gas Control, 26*, 147-157.

Rezaei, M., Warsinger, D. M., Duke, M. C., Matsuura, T., & Samhaber, W. M. (2018). Wetting phenomena in membrane distillation: Mechanisms, reversal, and prevention. *Water Research, 139*, 329-352.

Rodriguez-Blanco, J. D., Shaw, S., & Benning, L. G. (2011). The kinetics and mechanisms of amorphous calcium carbonate (ACC) crystallization to calcite, via vaterite. *Nanoscale, 3*(1), 265-271.

Rodriguez-Narvaez, O. M., Peralta-Hernandez, J. M., Goonetilleke, A., & Bandala, E. R. (2017). Treatment technologies for emerging

contaminants in water: A review. *Chemical Engineering Journal, 323*, 361-380.

Rolf, J., Cao, T., Huang, X., Boo, C., Li, Q., & Elimelech, M. (2022). Inorganic scaling in membrane desalination: models, mechanisms, and characterization methods. *Environmental Science & Technology, 56*(12), 7484-7511.

Ronen, A., Duan, W., Wheeldon, I., Walker, S., & Jassby, D. (2015). Microbial attachment inhibition through low-voltage electrochemical reactions on electrically conducting membranes. *Environmental Science & Technology, 49*(21), 12741-12750.

Samanta, A., Zhao, A., Shimizu, G. K., Sarkar, P., & Gupta, R. (2012). Post-combustion CO2 capture using solid sorbents: a review. *Industrial & engineering chemistry research, 51*(4), 1438-1463.

Schantz, A. B., Xiong, B., Dees, E., Moore, D. R., Yang, X., & Kumar, M. (2018). Emerging investigators series: prospects and challenges for high-pressure reverse osmosis in minimizing concentrated waste streams. *Environmental Science: Water Research & Technology, 4*(7), 894-908.

Schmitt, A., Mendret, J., Roustan, M., & Brosillon, S. (2020). Ozonation using hollow fiber contactor technology and its perspectives for micropollutants removal in water: A review. *Science of the Total Environment, 729*, 138664.

Seo, D. H., Pineda, S., Woo, Y. C., Xie, M., Murdock, A. T., Ang, E. Y., Jiao, Y., Park, M. J., Lim, S. I., & Lawn, M. (2018). Anti-fouling graphene-based membranes for effective water desalination. *Nature communications, 9*(1), 1-12.

Shah, K. M., Billinge, I. H., Chen, X., Fan, H., Huang, Y., Winton, R. K., & Yip, N. Y. (2022). Drivers, challenges, and emerging technologies for desalination of high-salinity brines: A critical review. *Desalination, 538*, 115827.

Shakeri, A., Salehi, H., & Rastgar, M. (2019). Antifouling electrically conductive membrane for forward osmosis prepared by polyaniline/graphene nanocomposite. *Journal of Water Process Engineering, 32*, 100932.

Shalaby, S., Kabeel, A., Abosheiasha, H., Elfakharany, M., El-Bialy, E., Shama, A., & Vidic, R. D. (2022). Membrane distillation driven by solar energy: a review. *Journal of Cleaner Production*, 132949.

Shaulsky, E., Nejati, S., Boo, C., Perreault, F., Osuji, C. O., & Elimelech, M. (2017). Post-fabrication modification of electrospun

nanofiber mats with polymer coating for membrane distillation applications. *Journal of membrane science, 530*, 158-165.

Shenvi, S. S., Isloor, A. M., & Ismail, A. (2015). A review on RO membrane technology: Developments and challenges. *Desalination, 368*, 10-26.

Shin, Y.-U., Yun, E.-T., Kim, J., Lee, H., Hong, S., & Lee, J. (2020). Electrochemical oxidation–membrane distillation hybrid process: utilizing electric resistance heating for distillation and membrane defouling through thermal activation of anodically formed persulfate. *Environmental Science & Technology, 54*(3), 1867-1877.

Singh, R., Singh, S., Parihar, P., Singh, V. P., & Prasad, S. M. (2015). Arsenic contamination, consequences and remediation techniques: a review. *Ecotoxicology and environmental safety, 112*, 247-270.

Sirés, I., Brillas, E., Oturan, M. A., Rodrigo, M. A., & Panizza, M. (2014). Electrochemical advanced oxidation processes: today and tomorrow. A review. *Environmental Science and Pollution Research, 21*(14), 8336-8367.

Soukane, S., & Ghaffour, N. (2021). Showerhead feed distribution for optimized performance of large scale membrane distillation modules. *Journal of membrane science, 618*, 118664.

Stenzel, F., Greve, P., Lucht, W., Tramberend, S., Wada, Y., & Gerten, D. (2021). Irrigation of biomass plantations may globally increase water stress more than climate change. *Nature communications, 12*(1), 1-9.

Suen, N.-T., Hung, S.-F., Quan, Q., Zhang, N., Xu, Y.-J., & Chen, H. M. (2017). Electrocatalysis for the oxygen evolution reaction: recent development and future perspectives. *Chemical Society Reviews, 46*(2), 337-365.

Sun, H., Liu, H., Wang, S., Cheng, F., & Liu, Y. (2018). Ceramic membrane fouling by dissolved organic matter generated during on-line chemical cleaning with ozone in MBR. *Water Research, 146*, 328-336.

Sun, J., Wang, G., Zhang, H., Zhang, B., & Hu, C. (2021). Facile fabrication of a conductive polypyrrole membrane for anti-fouling enhancement by electrical repulsion and in situ oxidation. *Chemosphere, 270*, 129416.

Sun, M., Wang, X., Winter, L. R., Zhao, Y., Ma, W., Hedtke, T., Kim, J.-H., & Elimelech, M. (2021). Electrified membranes for water treatment applications. *ACS ES&T Engineering, 1*(4), 725-752.

Sun, Y., Karaki, T., Fujii, T., & Yamashita, Y. J. (2022). Spurious-mode vibrations caused by alternating current poling and their solution process for Pb (Mg1/3Nb2/3) O3-PbTiO3 single crystals. *Journal of Materiomics, 8*(1), 96-103.

Sun, Y., Tian, J., Song, L., Gao, S., Shi, W., & Cui, F. (2018). Dynamic changes of the fouling layer in forward osmosis based membrane processes for municipal wastewater treatment. *Journal of membrane science, 549*, 523-532.

Surwade, S. P., Smirnov, S. N., Vlassiouk, I. V., Unocic, R. R., Veith, G. M., Dai, S., & Mahurin, S. M. (2015). Water desalination using nanoporous single-layer graphene. *Nature Nanotechnology, 10*(5), 459-464.

Swaminathan, J., Chung, H. W., & Warsinger, D. M. (2018). Energy efficiency of membrane distillation up to high salinity: Evaluating critical system size and optimal membrane thickness. *Applied Energy, 211*, 715-734.

Swaminathan, J., Chung, H. W., Warsinger, D. M., AlMarzooqi, F. A., & Arafat, H. A. (2016). Energy efficiency of permeate gap and novel conductive gap membrane distillation. *Journal of membrane science, 502*, 171-178.

Tabassian, R., Oh, J.-H., Kim, S., Kim, D., Ryu, S., Cho, S.-M., Koratkar, N., & Oh, I.-K. (2016). Graphene-coated meshes for electroactive flow control devices utilizing two antagonistic functions of repellency and permeability. *Nature communications, 7*(1), 1-9.

Talavari, A., Ghanavati, B., Azimi, A., & Sayyahi, S. (2020). Preparation and characterization of PVDF-filled MWCNT hollow fiber mixed matrix membranes for gas absorption by Al2O3 nanofluid absorbent via gas–liquid membrane contactor. *Chemical Engineering Research and Design, 156*, 478-494.

Tang, C. Y., Reinhard, M., & Leckie, J. O. (2012). Effects of hypochlorous acid exposure on the rejection of salt, polyethylene glycols, boron and arsenic (V) by nanofiltration and reverse osmosis membranes. *Water Research, 46*(16), 5217-5223.

Tang, L., Iddya, A., Zhu, X., Dudchenko, A. V., Duan, W., Turchi, C., Vanneste, J., Cath, T. Y., & Jassby, D. (2017). Enhanced flux and electrochemical cleaning of silicate scaling on carbon nanotube-coated membrane distillation membranes treating geothermal brines. *ACS applied materials & interfaces, 9*(44), 38594-38605.

Tanudjaja, H. J., & Chew, J. W. (2018). Assessment of oil fouling by oil-membrane interaction energy analysis. *Journal of membrane science, 560*, 21-29.

Thakur, A. K., Singh, S. P., Kleinberg, M. N., Gupta, A., Arnusch, C. J. J. A. a. m., & interfaces. (2019). Laser-induced graphene–PVA composites as robust electrically conductive water treatment membranes. *11*(11), 10914-10921.

Thakur, A. K., Singh, S. P., Thamaraiselvan, C., Kleinberg, M. N., & Arnusch, C. J. J. J. o. M. S. (2019). Graphene oxide on laser-induced graphene filters for antifouling, electrically conductive ultrafiltration membranes. *591*, 117322.

Thamaraiselvan, C., Ronen, A., Lerman, S., Balaish, M., Ein-Eli, Y., & Dosoretz, C. G. (2018). Low voltage electric potential as a driving force to hinder biofouling in self-supporting carbon nanotube membranes. *Water Research, 129*, 143-153.

Tian, J.-y., Ernst, M., Cui, F., & Jekel, M. (2013). Effect of particle size and concentration on the synergistic UF membrane fouling by particles and NOM fractions. *Journal of membrane science, 446*, 1-9.

Tijing, L. D., Woo, Y. C., Choi, J.-S., Lee, S., Kim, S.-H., & Shon, H. K. (2015). Fouling and its control in membrane distillation—A review. *Journal of Membrane Science, 475*, 215-244. https://doi.org/https://doi.org/10.1016/j.memsci.2014.09.042

Trellu, C., Coetsier, C., Rouch, J.-C., Esmilaire, R., Rivallin, M., Cretin, M., & Causserand, C. (2018). Mineralization of organic pollutants by anodic oxidation using reactive electrochemical membrane synthesized from carbothermal reduction of TiO2. *Water Research, 131*, 310-319.

Varcoe, J. R., Atanassov, P., Dekel, D. R., Herring, A. M., Hickner, M. A., Kohl, P. A., Kucernak, A. R., Mustain, W. E., Nijmeijer, K., & Scott, K. (2014). Anion-exchange membranes in electrochemical energy systems. *Energy & environmental science, 7*(10), 3135-3191.

Vázquez, G., Alvarez, E., Navaza, J. M., Rendo, R., & Romero, E. (1997). Surface tension of binary mixtures of water+ monoethanolamine and water+ 2-amino-2-methyl-1-propanol and tertiary mixtures of these amines with water from 25 C to 50 C. *Journal of Chemical & Engineering Data, 42*(1), 57-59.

Vázquez, G., Alvarez, E., Rendo, R., Romero, E., & Navaza, J. M. (1996). Surface tension of aqueous solutions of diethanolamine

and triethanolamine from 25° C to 50° C. *Journal of Chemical & Engineering Data, 41*(4), 806-808.

Veawab, A., Tontiwachwuthikul, P., & Chakma, A. (1999). Corrosion behavior of carbon steel in the CO2 absorption process using aqueous amine solutions. *Industrial & engineering chemistry research, 38*(10), 3917-3924.

Velasco, P., Jegatheesan, V., Thangavadivel, K., Othman, M., & Zhang, Y. (2021). A focused review on membrane contactors for the recovery of dissolved methane from anaerobic membrane bioreactor (AnMBR) effluents. *Chemosphere, 278*, 130448.

Velazquez-Pena, S., Barrera-Diaz, C., Linares-Hernandez, I., Bilyeu, B., & Martínez-Delgadillo, S. (2012). An effective electrochemical Cr (VI) removal contained in electroplating industry wastewater and the chemical characterization of the sludge produced. *Industrial & engineering chemistry research, 51*(17), 5905-5910.

Wang, G., Feng, H., Hu, L., Jin, W., Hao, Q., Gao, A., Peng, X., Li, W., Wong, K.-Y., & Wang, H. (2018). An antibacterial platform based on capacitive carbon-doped TiO2 nanotubes after direct or alternating current charging. *Nature communications, 9*(1), 1-12.

Wang, J.-W., Li, L., Zhang, J.-W., Xu, X., & Chen, C.-S. (2016). β-Sialon ceramic hollow fiber membranes with high strength and low thermal conductivity for membrane distillation. *Journal of the European Ceramic Society, 36*(1), 59-65.

Wang, J., Gao, X., Xu, Y., Wang, Q., Zhang, Y., Wang, X., & Gao, C. (2016). Ultrasonic-assisted acid cleaning of nanofiltration membranes fouled by inorganic scales in arsenic-rich brackish water. *Desalination, 377*, 172-177.

Wang, L., Miao, R., Wang, X., Lv, Y., Meng, X., Yang, Y., Huang, D., Feng, L., Liu, Z., & Ju, K. (2013). Fouling behavior of typical organic foulants in polyvinylidene fluoride ultrafiltration membranes: characterization from microforces. *Environmental science & technology, 47*(8), 3708-3714.

Wang, M., Cao, B., Hu, Y., & Rodrigues, D. F. (2021). Mineral Scaling on Reverse Osmosis Membranes: Role of Mass, Orientation, and Crystallinity on Permeability. *Environmental Science & Technology, 55*(23), 16110-16119.

Wang, W., Xie, C., Zhu, L., Shan, B., Liu, C., & Cui, F. (2019). A novel 3-dimensional graphene-based membrane with superior water flux and electrocatalytic properties for organic pollutant degradation. *Journal of Materials Chemistry A, 7*(1), 172-187.

Wang, X., Chang, V. W., & Tang, C. Y. (2016). Osmotic membrane bioreactor (OMBR) technology for wastewater treatment and reclamation: Advances, challenges, and prospects for the future. *Journal of membrane science, 504*, 113-132.

Wang, Y.-J., Huang, L., Fang, Z., Wang, X.-M., Gao, M., Liu, H.-Q., Li, W.-W., & Huang, T.-Y. (2022a). Electrochemically self-cleanable carbon nanotube interlayered membrane for enhanced forward osmosis in wastewater treatment. *Journal of Environmental Chemical Engineering, 10*(3), 107399.

Wang, Y.-J., Huang, L., Fang, Z., Wang, X.-M., Gao, M., Liu, H.-Q., Li, W.-W., & Huang, T.-Y. J. J. o. E. C. E. (2022b). Electrochemically self-cleanable carbon nanotube interlayered membrane for enhanced forward osmosis in wastewater treatment. *10*(3), 107399.

Wang, Z., Chu, J., & Zhang, X. (2007). Study of a cake model during stirred dead-end microfiltration. *Desalination, 217*(1-3), 127-138.

Warsinger, D. M., Swaminathan, J., Guillen-Burrieza, E., & Arafat, H. A. (2015). Scaling and fouling in membrane distillation for desalination applications: a review. *Desalination, 356*, 294-313.

Wei, K., Cui, T., Huang, F., Zhang, Y., & Han, W. (2020). Membrane separation coupled with electrochemical advanced oxidation processes for organic wastewater treatment: a short review. *Membranes, 10*(11), 337.

Wu, C., Huang, L., Xue, S.-G., Pan, W.-S., Zou, Q., Hartley, W., & Wong, M.-H. (2017). Oxic and anoxic conditions affect arsenic (As) accumulation and arsenite transporter expression in rice. *Chemosphere, 168*, 969-975.

Wu, X., Zhao, B., Wang, L., Zhang, Z., Zhang, H., Zhao, X., & Guo, X. (2016). Hydrophobic PVDF/graphene hybrid membrane for CO2 absorption in membrane contactor. *Journal of membrane science, 520*, 120-129.

Wu, Z.-Y., Karamad, M., Yong, X., Huang, Q., Cullen, D. A., Zhu, P., Xia, C., Xiao, Q., Shakouri, M., & Chen, F.-Y. (2021). Electrochemical ammonia synthesis via nitrate reduction on Fe single atom catalyst. *Nature communications, 12*(1), 1-10.

Xiao, Z., Li, Z., Guo, H., Liu, Y., Wang, Y., Yin, H., Li, X., Song, J., Nghiem, L. D., & He, T. (2019). Scaling mitigation in membrane distillation: From superhydrophobic to slippery. *Desalination, 466*, 36-43.

Xie, J., Zhang, C., & Waite, T. D. (2022). Hydroxyl radicals in anodic oxidation systems: generation, identification and quantification. *Water Research*, 118425.

Xie, S., Wong, N. H., Sunarso, J., Guo, Q., Hou, C., Pang, Z., & Peng, Y. (2023). Cleaning mechanism of gypsum scaling in hydrophobic porous membranes. *Desalination, 547*, 116237.

Xie, T., Jing, Z., Hu, J., Yuan, P., Liu, Y., & Cao, S. (2018). Degradation of nitrobenzene-containing wastewater by a microbial-fuel-cell-coupled constructed wetland. *Ecological Engineering, 112*, 65-71.

Xie, W., Tang, P., Wu, Q., Chen, C., Song, Z., Li, T., Bai, Y., Lin, S., Tiraferri, A., & Liu, B. (2022). Solar-driven desalination and resource recovery of shale gas wastewater by on-site interfacial evaporation. *Chemical Engineering Journal, 428*, 132624.

Xu, D., Zhu, Z., Tan, G., Xue, X., & Li, J. (2022). Mechanism insight into gypsum scaling of differently wettable membrane surfaces with antiscalants in membrane distillation. *Journal of membrane science, 652*, 120499.

Xu, L., Graham, N. J., Wei, C., Zhang, L., & Yu, W. J. W. R. (2020). Abatement of the membrane biofouling: Performance of an in-situ integrated bioelectrochemical-ultrafiltration system. *179*, 115892.

Xu, L. L., Liu, L., Wang, K. P., Zhao, S. Y., Liu, Q. Y., Zhang, Y., & Wang, J. (2021). Development of a novel electrocoagulation membrane reactor with electrically conductive membranes as cathode to mitigate membrane fouling. *Journal of membrane science, 618*, 118713.

Xu, L. L., Xu, Y., Liu, L., Wang, K. P., Patterson, D. A., & Wang, J. (2019). Electrically responsive ultrafiltration polyaniline membrane to solve fouling under applied potential. *Journal of membrane science, 572*, 442-452.

Xu, M., Zhao, P., Tang, C. Y., Yi, X., & Wang, X. (2022). Preparation of electrically enhanced forward osmosis (FO) membrane by two-dimensional MXenes for organic fouling mitigation. *Chinese Chemical Letters, 33*(8), 3818-3822.

Xu, X., Zhang, H., Gao, T., & Teng, J. J. S. o. T. T. E. (2021). Impacts of applied voltage on forward osmosis process harvesting microalgae: Filtration behaviors and lipid extraction efficiency. *773*, 145678.

Xu, X., Zhang, H., Gao, T., Wang, Y., Teng, J., & Lu, M. J. S. o. t. T. E. (2020). Customized thin and loose cake layer to mitigate

membrane fouling in an electro-assisted anaerobic forward osmosis membrane bioreactor (AnOMEBR). *729*, 138663.

Xu, X., Zhang, H., Yu, M., Wang, Y., Gao, T., & Yang, F. (2019). Conductive thin film nanocomposite forward osmosis membrane (TFN-FO) blended with carbon nanoparticles for membrane fouling control. *Science of the Total Environment, 697*, 134050.

Xu, Y., Goh, K., Wang, R., & Bae, T.-H. (2019). A review on polymer-based membranes for gas-liquid membrane contacting processes: Current challenges and future direction. *Separation and Purification Technology, 229*, 115791.

Yan, K.-K., Jiao, L., Lin, S., Ji, X., Lu, Y., & Zhang, L. (2018). Superhydrophobic electrospun nanofiber membrane coated by carbon nanotubes network for membrane distillation. *Desalination, 437*, 26-33.

Yan, Z., Lu, Z., Chen, X., Jiang, Y., Huang, Z., Liu, L., Fan, G., Chang, H., Qu, F., & Liang, H. (2022). Membrane distillation treatment of landfill leachate: Characteristics and mechanism of membrane fouling. *Separation and Purification Technology, 289*, 120787.

Yan, Z., Qu, F., Liang, H., Yu, H., Pang, H., Rong, H., Fan, G., & Van der Bruggen, B. (2021). Effect of biopolymers and humic substances on gypsum scaling and membrane wetting during membrane distillation. *Journal of membrane science, 617*, 118638.

Yang, M.-Y., Wang, J.-W., Li, L., Dong, B.-B., Xin, X., & Agathopoulos, S. (2019). Fabrication of low thermal conductivity yttrium silicate ceramic flat membrane for membrane distillation. *Journal of the European Ceramic Society, 39*(2-3), 442-448.

Yang, S., Jasim, S. A., Bokov, D., Chupradit, S., Nakhjiri, A. T., & El-Shafay, A. (2022). Membrane distillation technology for molecular separation: a review on the fouling, wetting and transport phenomena. *Journal of Molecular Liquids, 349*, 118115.

Yao, M., Tijing, L. D., Naidu, G., Kim, S.-H., Matsuyama, H., Fane, A. G., & Shon, H. K. (2020). A review of membrane wettability for the treatment of saline water deploying membrane distillation. *Desalination, 479*, 114312.

Ye, Q., Xu, J.-M., Zhang, Y.-J., Chen, S.-H., Zhan, X.-Q., Ni, W., Tsai, L.-C., Jiang, T., Ma, N., & Tsai, F.-C. (2022). Metal-organic framework modified hydrophilic polyvinylidene fluoride porous membrane for efficient degerming selective oil/water emulsion separation. *npj Clean Water, 5*(1), 1-9.

Ye, Y., Yu, S., Liu, B., Xia, Q., Liu, G., & Li, P. (2019). Microbubble aeration enhances performance of vacuum membrane distillation desalination by alleviating membrane scaling. *Water Research, 149*, 588-595.

Yi, Y., Tornow, J., Willinger, E., Willinger, M. G., Ranjan, C., & Schlögl, R. (2015). Electrochemical degradation of multiwall carbon nanotubes at high anodic potential for oxygen evolution in acidic media. *ChemElectroChem, 2*(12), 1929-1937.

Yin, Y., Jeong, N., Minjarez, R., Robbins, C. A., Carlson, K. H., & Tong, T. (2021). Contrasting behaviors between gypsum and silica scaling in the presence of antiscalants during membrane distillation. *Environmental Science & Technology, 55*(8), 5335-5346.

Younker, J. M., & Walsh, M. E. (2015). Impact of salinity and dispersed oil on adsorption of dissolved aromatic hydrocarbons by activated carbon and organoclay. *Journal of Hazardous Materials, 299*, 562-569.

Yu, W., Liu, Y., Xu, Y., Li, R., Chen, J., Liao, B.-Q., Shen, L., & Lin, H. (2019). A conductive PVDF-Ni membrane with superior rejection, permeance and antifouling ability via electric assisted in-situ aeration for dye separation. *Journal of membrane science, 581*, 401-412.

Yu, X., An, L., Yang, J., Tu, S.-T., & Yan, J. (2015). CO2 capture using a superhydrophobic ceramic membrane contactor. *Journal of membrane science, 496*, 1-12.

Zaky, A. M., & Chaplin, B. P. (2013). Porous substoichiometric TiO2 anodes as reactive electrochemical membranes for water treatment. *Environmental science & technology, 47*(12), 6554-6563.

Zhang, B., Wong, P. W., Guo, J., Zhou, Y., Wang, Y., Sun, J., Jiang, M., Wang, Z., & An, A. K. (2022). Transforming Ti3C2Tx MXene's intrinsic hydrophilicity into superhydrophobicity for efficient photothermal membrane desalination. *Nature communications, 13*(1), 1-10.

Zhang, C., Shi, Y., Shi, L., Li, H., Li, R., Hong, S., Zhuo, S., Zhang, T., & Wang, P. (2021). Designing a next generation solar crystallizer for real seawater brine treatment with zero liquid discharge. *Nature communications, 12*(1), 1-10.

Zhang, H., Quan, X., Fan, X., Yi, G., Chen, S., Yu, H., & Chen, Y. (2018). Improving ion rejection of conductive nanofiltration membrane

through electrically enhanced surface charge density. *Environmental science & technology, 53*(2), 868-877.

Zhang, L., Lee, Y.-W., & Jahng, D. (2012). Ammonia stripping for enhanced biomethanization of piggery wastewater. *Journal of hazardous materials, 199*, 36-42.

Zhang, P., Knötig, P., Gray, S., & Duke, M. (2015). Scale reduction and cleaning techniques during direct contact membrane distillation of seawater reverse osmosis brine. *Desalination, 374*, 20-30.

Zhang, Q.-Q., Ying, G.-G., Pan, C.-G., Liu, Y.-S., & Zhao, J.-L. (2015). Comprehensive evaluation of antibiotics emission and fate in the river basins of China: source analysis, multimedia modeling, and linkage to bacterial resistance. *Environmental science & technology, 49*(11), 6772-6782.

Zhang, Q., Arribas, P., Remillard, E. M., Garcia-Payo, M. C., Khayet, M., & Vecitis, C. D. (2017). Interlaced CNT electrodes for bacterial fouling reduction of microfiltration membranes. *Environmental Science & Technology, 51*(16), 9176-9183.

Zhang, Q., & Vecitis, C. D. (2014). Conductive CNT-PVDF membrane for capacitive organic fouling reduction. *Journal of membrane science, 459*, 143-156.

Zhang, W., Yu, S., Zhao, H., Ji, X., & Ning, R. (2022). Vacuum membrane distillation for seawater concentrate treatment coupled with microbubble aeration cleaning to alleviate membrane fouling. *Separation and Purification Technology, 290*, 120864.

Zhang, Y., & Wang, R. (2013). Fabrication of novel polyetherimide-fluorinated silica organic–inorganic composite hollow fiber membranes intended for membrane contactor application. *Journal of membrane science, 443*, 170-180.

Zhang, Y., Wang, R., Yi, S., Setiawan, L., Hu, X., & Fane, A. G. (2011). Novel chemical surface modification to enhance hydrophobicity of polyamide-imide (PAI) hollow fiber membranes. *Journal of membrane science, 380*(1-2), 241-250.

Zhang, Y., Wang, T., Meng, J., Lei, J., Zheng, X., Wang, Y., Zhang, J., Cao, X., Li, X., & Qiu, X. (2021). A novel conductive composite membrane with polypyrrole (PPy) and stainless-steel mesh: Fabrication, performance, and anti-fouling mechanism. *Journal of membrane science, 621*, 118937.

Zhang, Z., Huang, G., Li, Y., Chen, X., Yao, Y., Ren, S., Li, M., Wu, Y., & An, C. (2022). Electrically conductive inorganic membranes:

A review on principles, characteristics and applications. *Chemical Engineering Journal, 427*, 131987.

Zhao, S., Jiang, C., Fan, J., Hong, S., Mei, P., Yao, R., Liu, Y., Zhang, S., Li, H., & Zhang, H. (2021). Hydrophilicity gradient in covalent organic frameworks for membrane distillation. *Nature Materials, 20*(11), 1551-1558.

Zhong, L., Wang, Y., Liu, D., Zhu, Z., & Wang, W. (2021). Recent advances in membrane distillation using electrospun membranes: advantages, challenges, and outlook. *Environmental Science: Water Research & Technology, 7*(6), 1002-1019.

Zhong, L., Zhang, X., Ma, J., Liu, D., Liu, D., Wang, Y., Cui, F., & Wang, W. (2022). Synergy of feed-side aeration and super slippery interface in membrane distillation for enhanced water flux and scaling mitigation. *Water Research, 215*, 118246.

Zhou, Y., Maharubin, S., Tran, P., Reid, T., & Tan, G. Z. (2018). Anti-biofilm AgNP-polyaniline-polysulfone composite membrane activated by low intensity direct/alternating current. *Environmental Science: Water Research & Technology, 4*(10), 1511-1521.

Zhu, X., & Jassby, D. (2019). Electroactive membranes for water treatment: Enhanced treatment functionalities, energy considerations, and future challenges. *Accounts of chemical research, 52*(5), 1177-1186.

Zhu, Z., Wang, K., Lei, M., Li, X., Li, X., Jiang, L., Gao, X., Li, S., & Liang, J. (2022). Identification of priority areas for water ecosystem services by a techno-economic, social and climate change modeling framework. *Water Research, 221*, 118766.

Zuo, K., Wang, W., Deshmukh, A., Jia, S., Guo, H., Xin, R., Elimelech, M., Ajayan, P. M., Lou, J., & Li, Q. (2020). Multifunctional nanocoated membranes for high-rate electrothermal desalination of hypersaline waters. *Nature Nanotechnology, 15*(12), 1025-1032.